Analysis and Mapping of Post-Fire Hydrologic Hazards for the 2002 Hayman, Coal Seam, and Missionary Ridge Wildfires, Colorado

By J.G. Elliott, M.E. Smith, M.J. Friedel, M.R. Stevens, C.R. Bossong, D.W. Litke, R.S. Parker, C. Costello, J. Wagner, S.J. Char, M.A. Bauer, and S.R. Wilds

Prepared in cooperation with the
Federal Emergency Management Agency

Scientific Investigations Report 2004–5300

U.S. Department of the Interior
U.S. Geological Survey

U.S. Department of the Interior
Gale A. Norton, Secretary

U.S. Geological Survey
Charles G. Groat, Director

U.S. Geological Survey, Reston, Virginia: 2005

For sale by U.S. Geological Survey, Information Services
Box 25286, Denver Federal Center
Denver, CO 80225

For more information about the USGS and its products:
Telephone: 1-888-ASK-USGS
World Wide Web: http://www.usgs.gov/

Suggested citation:
Elliott, J.G., Smith, M.E., Friedel, M.J., Stevens, M.R., Bossong, C.R., Litke, D.W., Parker, R.S., Costello, C., Wagner, J., Char, S.J., Bauer, M.A., and Wilds, S.R., 2005, Analysis and mapping of post-fire hydrologic hazards for the 2002 Hayman, Coal Seam, and Missionary Ridge wildfires, Colorado: U.S. Geological Survey Scientific Investigations Report 2004–5300, 104 p.

Contents

Figures

Tables

Appendix Figure

Appendix Tables

Conversion Factors, Abbreviations, and Datums

Multiply	By	To obtain
millimeter (mm)	0.03937	inch
meter (m)	3.281	foot (ft)
kilogram per square meter (kg/m^2)	0.2048	pound per square foot (lb/ft^2)
newton per square meter (N/m^2)	0.02088	pound per square foot (lb/ft^2)
newton per cubic meter (N/m^3)	0.006365	pound per cubic foot (lb/ft^3)
foot (ft)	0.3048	meter (m)
mile (mi)	1.609	kilometer (km)
acre	4,047	square meter (m^2)
square mile (mi^2)	2.590	square kilometer (km^2)
foot per second (ft/s)	0.3048	meter per second (m/s)
cubic foot per second (ft^3/s)	0.02832	cubic meter per second (m^3/s)
acre-foot (acre-ft)	1,233	cubic meter (m^3)
ton, short	0.9072	megagram (Mg)

Vertical coordinate information is referenced to the *North Geodetic Vertical Datum of 1929 (NGVD 29)* and to the *North American Vertical Datum of 1988 (NAV 88).*

Horizontal coordinate information is referenced to the *North American Datum of 1983 (NAD 83).*

Analysis and Mapping of Post-Fire Hydrologic Hazards for the 2002 Hayman, Coal Seam, and Missionary Ridge Wildfires, Colorado

By J.G. Elliott, M.E. Smith, M.J. Friedel, M.R. Stevens, C.R. Bossong, D.W. Litke, R.S. Parker, C. Costello, J. Wagner, S.J. Char, M.A. Bauer, and S.R. Wilds

Abstract

Wildfires caused extreme changes in the hydrologic, hydraulic, and geomorphologic characteristics of many Colorado drainage basins in the summer of 2002. Detailed assessments were made of the short-term effects of three wildfires on burned and adjacent unburned parts of drainage basins. These were the Hayman, Coal Seam, and Missionary Ridge wildfires. Longer term runoff characteristics that reflect post-fire drainage basin recovery expected to develop over a period of several years also were analyzed for two affected stream reaches: the South Platte River between Deckers and Trumbull, and Mitchell Creek in Glenwood Springs. The 10-, 50-, 100-, and 500-year flood-plain boundaries and water-surface profiles were computed in a detailed hydraulic study of the Deckers-to-Trumbull reach.

The Hayman wildfire burned approximately 138,000 acres (216 square miles) in granitic terrain near Denver, and the predominant potential hazard in this area is flooding by sediment-laden water along the large tributaries to and the main stem of the South Platte River. The Coal Seam wildfire burned approximately 12,200 acres (19.1 square miles) near Glenwood Springs, and the Missionary Ridge wildfire burned approximately 70,500 acres (110 square miles) near Durango, both in areas underlain by marine shales where the predominant potential hazard is debris-flow inundation of low-lying areas.

Hydrographs and peak discharges for pre-burn and post-burn scenarios were computed for each drainage basin and tributary subbasin by using rainfall-runoff models because streamflow data for most tributary subbasins were not available. An objective rainfall-runoff model calibration method based on nonlinear regression and referred to as the "objective calibration method" was developed and applied to rainfall-runoff models for three burned areas. The HEC–1 rainfall-runoff model was used to simulate the pre-burn rainfall-runoff processes in response to the 100-year storm, and HEC-HMS was used for runoff hydrograph generation.

Post-burn rainfall-runoff parameters were determined by adjusting the runoff-curve numbers on the basis of a weighting procedure derived from the U.S. Soil Conservation Service (now the National Resources Conservation Service) equation for precipitation excess and the effect of burn severity. This weighting procedure was determined to be more appropriate than simple area weighting because of the potentially marked effect of even small burned areas on the runoff hydrograph in individual drainage basins. Computed water-peak discharges from HEC-HMS models were increased volumetrically to account for increased sediment concentrations that are expected as a result of accelerated erosion after burning. Peak discharge estimates for potential floods in the South Platte River were increased by a factor that assumed a volumetric sediment concentration (C_v) of 20 percent. Flood hydrographs for the South Platte River and Mitchell Creek were routed down main-stem channels using watershed-routing algorithms included in the HEC-HMS rainfall-runoff model.

In areas subject to debris flows in the Coal Seam and Missionary Ridge burned areas, debris-flow discharges were simulated by 100-year rainfall events, and the inflow hydrographs at tributary mouths were simulated by using the objective calibration method. Sediment concentrations (C_v) used in debris-flow simulations were varied through the event, and were initial C_v 20 percent, mean C_v approximately 31 percent, maximum C_v 48 percent, C_v 43 percent at the time of the water hydrograph peak, and C_v 20 percent for the duration of the event. The FLO-2D flood- and debris-flow routing model was used to delineate the area of unconfined debris-flow inundation on selected alluvial fan and valley floor areas.

A method was developed to objectively determine the post-fire recovery period for the Hayman and Coal Seam burned areas using runoff-curve numbers (RCN) for all drainage basins for a 50-year period. A time assumed to be the recovery period was determined when the rate of change in the estimated 100-year flood peak became less than 5 percent per year. The method was based on a limited amount of historical data collected in drainage basins that were monitored during the post-fire recovery process.

The simulated post-burn 100-year peak discharges for 19 subbasins, routed to the point of confluence with the South Platte River, are expected to increase 3 to 90 times the pre-burn peaks in the short term. Among subbasins with greater than 50 percent moderately to severely burned areas, post-burn peak discharges are expected to be 28 to 91 times greater than pre-burn peaks. Post-fire recovery-time estimates are estimated to be 6 years for the Platte River upstream and downstream from Cheesman Reservoir.

Potential post-fire hazards in the Coal Seam burned area are waterflooding in Mitchell Creek and debris flows from smaller tributaries. Post-burn, sediment-bulked 100-year peak water flows for Mitchell Creek tributaries are expected to increase 2 to 21 times the pre-burn peaks. Post-burn peak discharges for points along the main stem of Mitchell Creek are expected to increase 3 to 4 times over the pre-burn peaks. Debris-flow analysis was done for 26 tributaries with drainage areas that ranged from 0.01 to 0.75 square mile. Estimates of the increase in 100-year discharge resulting from post-fire debris flows, relative to unburned conditions, range from 8 to 14 times in the Red Mountain area, 2 to 9 times in the West Glenwood Springs area, and 8 to 14 times for selected tributaries of Mitchell Creek. Post-fire recovery-time estimates were not made for the smaller subbasins burned by the Coal Seam wildfire; however, the estimated recovery time for Mitchell Creek is about 4 years.

Short-term effects of 100-year storm-generated debris flows in 25 tributaries in the Missionary Ridge burned area with drainage areas that range from 0.07 to 9.78 square miles were evaluated. The largest increase from estimated pre-burn discharge to post-burn debris flow 100-year discharge is expected to occur in Coon Creek where peak discharges could increase by a factor of greater than 240. Increases range from 9 to 38 times in other Animas River tributaries. In the Florida River area, increases range from 22 to 31 times, and in the Vallecito Reservoir and Los Pinos River areas, from 9 to 30 times.

Introduction

Drought conditions in Colorado made the 2002 wildfire season unusually active. At least 16 wildfires were burning or had burned as of July 2, 2002 (fig. 1). These wildfires caused extreme changes in the hydrologic, hydraulic, and geomorphologic characteristics of the affected drainage basins. Post-fire basin conditions increase the risk of flood and debris-flow damage to homes, roads, bridges, and other infrastructure. In cooperation with the Federal Emergency Management Agency (FEMA), a team of scientists from the U.S. Geological Survey (USGS) and the Bureau of Reclamation (BOR): (1) assessed and ranked the 16 existing Colorado wildfires (as of July 2, 2002) in terms of relative hazard to population centers and infrastructure; (2) conducted detailed assessments of the hydrologic, hydraulic, and geomorphologic effects of selected, high-priority wildfires on burned and adjacent unburned parts of the drainage basins; and (3) summarized hydrologic information for use by water managers about the effects of wildfire on runoff and sediment from burned drainage basins. Additional wildfires in 2002 started after early July (fig. 1); however, these wildfires were not evaluated in this study.

The technical assessment focused on population centers and infrastructure affected by the wildfires. Pre-fire National Flood Insurance Program (NFIP) maps (where they exist) needed to be revised to reflect post-fire drainage-basin conditions. The technical response team, consisting of experts in hydrology, hydraulics, sediment transport, geomorphology, and geographical information system (GIS) mapping, used NFIP study data to evaluate post-fire changes to flood-inundation maps where these data existed.

Purpose and Scope

The purpose of this report is to document analyses and mapping of post-fire hydrologic hazards for the 2002 Hayman, Coal Seam, and Missionary Ridge wildfires in Colorado. The wildfires in Colorado caused extreme changes in the hydrologic, hydraulic, and geomorphologic characteristics of the affected drainage basins. A rapid technical assessment of these changes was needed to evaluate their effects on flood plains, population centers, infrastructure, and transportation systems within and downstream from the burned areas. Accordingly, a three-phase hydrologic analysis was undertaken for the areas affected by the 16 Colorado wildfires that had burned or were burning as of July 2, 2002.

Phase 1.—Post-wildfire reconnaissance-hazard maps were created for analysis of the 16 Colorado wildfires identified as of July 2, 2002. Each map was produced at 1:24,000 scale, and fire perimeter, fire intensity (if available), and other types of readily available information were depicted. These maps then were used to rank the relative priority of each of the wildfires in terms of anticipated hydrologic hazard (category 1 = high; category 2 = moderate; category 3 = low). These maps were developed for reconnaissance purposes only and are not included in this report. Category 1 wildfires were selected for detailed hydrologic analysis under Phase 2 of the study.

Phase 2.—Detailed hydrologic studies were conducted for the Category 1 wildfires, leading to the production of post-fire flood- or debris-flow hazard maps for areas with existing National Flood Insurance Program (NFIP) maps and for other flood-prone areas where post-fire flooding could threaten downstream population centers or infrastructure.

Phase 3.—Phase 3 studies include analysis of long-term runoff characteristics that reflect post-fire drainage-basin recovery and stabilizing hydrologic conditions expected to develop over a period of several years after the wildfire. Past studies of post-fire hydrology indicate that a drainage-basin recovery period of about 5 years may be typical (Moody and Martin, 2001a; USDA Forest Service, 2002a). The long-term 100-year flood elevations from Phase 3 studies will be used by the FEMA for regulatory purposes.

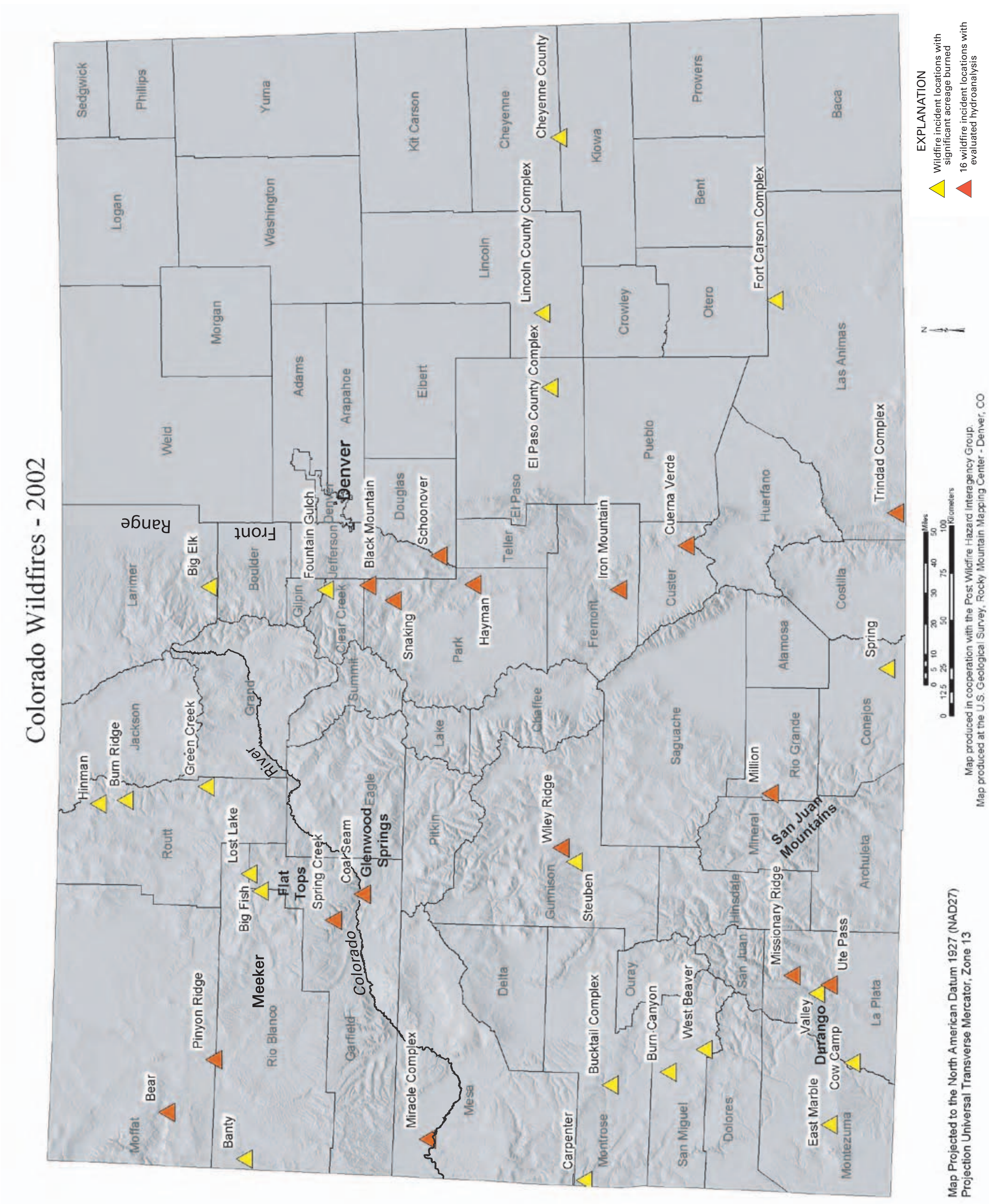

Figure 1. Location of Colorado wildfires, 2002.

Two specific study reaches were identified in which followup studies would be conducted to develop detailed 10-, 50-, 100-, and 500-year flood-plain maps. These reaches are the South Platte River between Deckers and Trumbull, and Mitchell Creek in Glenwood Springs. Results from the study of the South Platte River between Deckers and Trumbull are included in this report. Hydraulic modeling and flood-plain mapping of Mitchell Creek are being completed as part of a separate project and are not covered by this report.

Acknowledgments

This study was conducted with interagency and interdisciplinary USGS collaboration and was authorized under Presidential Disaster Declaration FEMA_DR–1421, Colorado (a wildland fire disaster declared on June 19, 2002) due to extreme post-fire hazards and changes in flood plains and affected areas (*http://www.fema.gov/news/dfrn.fema?id=712*, accessed October 1, 2004). Because the study is being done to meet FEMA standards for flood-plain mapping, the data also will be used in the long term for National Flood Insurance Program mapping under the National Flood Insurance Act of 1968 and the Flood Disaster Protection Act of 1973. The funding for this study was provided by the President's Disaster Relief Fund and under the authority of FEMA Region VIII. FEMA Region VIII staff provided the guidance and direction for this study.

The authors thank John Liou, FEMA project officer, for his assistance in this project; Ben Glass, Mickey Messer, Greg Smith, Dick Orr, and Bob Stull (USGS) for their help with onsite surveys and measurements used in the hydrologic and hydraulic analyses; and Sue Cannon and John Michael (USGS) for providing drainage-basin characteristics and preliminary estimates of potential debris-flow discharge magnitudes from severely burned areas. Jon Major (USGS) provided many helpful comments on the analysis of debris-flow hazards. Alexis Ellis and Jennifer Stefanacci (USGS) assisted with preparation of the overview and hazard mitigation maps. Technical reviews of an early draft of this report were made by Kathy Chase and Chuck Parrett.

Study Areas

The initial (Phase 1) study area included most of the mountainous and forested regions of Colorado. The 16 wildfires that had burned or were burning as of July 2, 2002, ranged from the Trinidad Complex Fire in south-central Colorado, to the Pinyon Ridge Fire near Meeker in northwestern Colorado, to the Missionary Ridge Fire near Durango in southwestern Colorado (fig. 1). Three wildfires were determined to be Category 1 wildfires with high anticipated hazard and potential threat to infrastructure and life and were selected for additional, more detailed hydrologic assessments in Phase 2. Category 1 wildfires were the Hayman wildfire in the Colorado Front Range mountains southwest of Denver, the Coal Seam wildfire at the southern edge of the Flat Tops region and along the Colorado River near Glenwood Springs, and the Missionary Ridge wildfire in the southern San Juan Mountains near Durango. Each Category 1 wildfire is treated in a separate section that follows in this report.

Reconnaissance of 2002 Wildfires—Phase 1

Major 2002 Colorado Wildfires through July 2, 2002

The 16 wildfires that had burned or were burning as of July 2, 2002, (fig. 1) listed in no particular order, are the following:

1. Hayman (137,760 acres)
2. Coal Seam (12,209 acres)
3. Missionary Ridge (70,485 acres)
4. Iron Mountain (4,439 acres)
5. Million (9,346 acres)
6. Spring Creek (13,493 acres)
7. Trinidad Complex (33,000 acres)
8. Bear (4,800 acres)
9. Black Mountain (200 acres)
10. Cuerna Verde (500 acres)
11. Dietrich/Miracle Complex (3,951 acres)
12. Pinyon Ridge (2,400 acres)
13. Schoonover (3,852 acres)
14. Snaking (2,590 acres)
15. Ute Pass (60 acres)
16. Wiley Ridge (1,084 acres)

The existing Colorado wildfires (as of July 2, 2002) were assessed during this study on the basis of areal extent and intensity of the wildfire, mapped infrastructure and inhabited areas, terrain, drainage networks, geology, and other information, when available. "Fire intensity," used in the reconnaissance phase of the study, is contrasted with "burn severity," used in the subsequent detailed hydrologic analyses. Fire intensity is related to fire behavior and the fire effect on overstory vegetation. Early estimates of fire intensity for the 16 wildfires were made on the basis of remotely sensed (satellite imagery) vegetation changes. Burn severity is specifically related to the effects of fire on soil conditions and hydrologic function, such as the amount of surface litter and duff, ash depth, soil structure and erodibility, hydrophobicity, and residual fuels (USDA Forest Service, 2002b, p. 109). Burn severities were estimated by the Burned Area Emergency Rehabilitation (BAER) teams, interagency groups formed to evaluate each wildfire.

Fire-intensity mapping was an integral layer on the reconnaissance hazard maps. Fire intensity was derived using remotely sensed Landsat Thematic Mapper (TM) and Enhanced Thematic Mapper Plus (ETM+) data and a technique called the Normalized Burn Ratio (NBR). NBR was developed for post-fire assessment by remote sensing on National Park Service lands by determining the difference between NBR data sets to enhance contrast and detection of wildfires through a scale of change from before fire (pre-burn) to after fire (post-burn) (Key and Benson, 2002). Pre- and post-fire Landsat images are used to calculate the NBR, an estimate of fire intensity ranging from low to high. Areas that are not affected by wildfire also are interpreted.

Potential hazards were associated with each burned area; however, 9 of the 16 wildfires were determined to have a lesser associated potential risk to infrastructure and life than the others and were excluded from additional evaluation in this study. These were the Bear, Black Mountain, Cuerna Verde, Dietrich/Miracle Complex, Pinyon Ridge, Schoonover, Snaking, Ute Pass, and Wiley Ridge wildfires. Three wildfires received additional scrutiny after the initial assessment but also were found to have a lesser associated risk: the Iron Mountain, Spring Creek, and Trinidad Complex wildfires.

High-Priority Wildfires Selected for Detailed Hydrologic Analyses

Three wildfires were determined to have substantially greater potential hazards than the others, and areas affected by these wildfires were selected for additional Phase 2 analyses described in separate sections in this report. Detailed assessments of the hydrologic, hydraulic, and geomorphologic effects of these high-priority wildfires on burned and adjacent unburned parts of the drainage basins were made, and the effects of wildfire on runoff and sediment from burned drainage basins were analyzed. These were the Hayman (figs. 4, 5, 8–14), Coal Seam (figs. 17–19), and Missionary Ridge wildfires (figs. 20–22). Because of its proximity to the Hayman wildfire, the area burned by the Schoonover wildfire was combined with that of the Hayman wildfire in subsequent hydrologic analyses. A fourth wildfire, the Million wildfire, also was determined to have a greater potential flood hazard. Hydrologic assessment of the Million wildfire is being done in another USGS study and is not addressed in this report.

Hayman Wildfire Area

The Hayman wildfire (fig. 4) started in June 2002 near Lake George in the South Platte River Basin and burned approximately 138,000 acres (216 mi^2). Elevations in the burned area ranged from 6,289 to more than 11,000 ft (USDA Forest Service, 2002a). The drainage area of the South Platte River just upstream from the confluence with the North Fork of the South Platte is about 2,580 mi^2. The South Platte River flows from southwest to the northeast through the interior of the burned area. Perennial tributaries affected by the wildfire include Horse Creek, Fourmile Creek, Goose Creek, Wigwam Creek, West Creek, and Turkey Creek.

Cheesman Reservoir is a major impoundment on the South Platte River and is located near the center of the burned area. Strontia Springs Reservoir is another important impoundment on the South Platte River and is located downstream from the burned area. These reservoirs, owned and operated by the Denver Water Board, are important water-supply facilities for the Denver metropolitan area. Approximately 44 percent of the burned area drains into the South Platte River downstream from Cheesman Reservoir Dam, whereas about 56 percent of the burned area drains either directly into Cheesman Reservoir or into the South Platte River upstream from Cheesman Reservoir.

Most of the burned area is composed of shallow, easily eroded, weathered granitic soils from the Precambrian Pikes Peak batholith. The landscape is highly dissected in the upland forested part of the burned area. Annual precipitation is composed of snowfall during the winter and high intensity rainstorms during the summer. There are several roads, trails, and forest recreation sites within the burned area as well as a summer camp, recreation residences, and year-round residences (USDA Forest Service, 2002a).

Coal Seam Wildfire Area

The Coal Seam wildfire (fig. 17) started on June 8, 2002, near Glenwood Springs, Colorado, and burned approximately 12,200 acres (19.1 mi^2) and several homes. Elevations in the burned area ranged from 5,800 to 10,500 ft (USDA Forest Service, 2002b). Abundant, fine-grained sediment is available for debris-flow entrainment in the Coal Seam area. The sediment originates from tributaries underlain by weathered Paleozoic sedimentary rocks of the Maroon and other formations (Cannon, Michael, and Gartner, 2003; USDA Forest Service, 2002a). Infrastructure that survived the wildfire, including homes, businesses, the Municipal Operations Center, roads, bridges, and a railroad, is potentially threatened by subsequent flooding and debris flows. Flooding in Mitchell Creek, a major tributary entering the Glenwood Springs area from the north, is another potential hazard in the Coal Seam area. Approximately 25 percent of Mitchell Creek's 11.9-mi^2 drainage area was burned by the Coal Seam wildfire.

Missionary Ridge Wildfire Area

The Missionary Ridge wildfire (fig. 20) burned from June 9 to July 14, 2002, and affected approximately 70,500 acres (110 mi^2) of Federal, State, and private land in La Plata County, Colorado. Elevations in the burned area ranged from approximately 6,500 to 11,400 ft (USDA Forest Service, 2002c). The wildfire destroyed several homes and other structures in three major drainage basins near Durango: the Animas, Florida, and Los Pinos River drainage basins. Approximately 61 percent of the area was burned with a moderate or high severity (USDA Forest Service, 2002c). Most of the area affected by the wildfire is underlain by sedimentary rocks including the Paleozoic Cutler and Hermosa Formations and the Mesozoic Morrison Formation, which are known sources of debris-flow sediments (USDA Forest Service, 2002c). Infrastructure that survived the wildfire, including homes, businesses, several major roads, bridges, and the dams at Lemon and Vallecito Reservoirs, is potentially threatened by subsequent flooding and debris flows.

Dominant Post-Fire Hazard Processes

Low-relief areas, valley floors, and alluvial fans in the Colorado mountains are subject to periodic flooding and debris flows; these processes become more severe after wildfires have devegetated the upland drainage basins, consumed organic litter, and changed the infiltration characteristics of the soil (Moody and Martin, 2001b). Stratigraphic evidence indicates that prehistoric forest fires in the Colorado Front Range and elsewhere have been followed by transport and deposition of large amounts of sediment in tributary and main-stem channels (Elliott and Parker, 2001).

The predominant potential hazard process in the Hayman wildfire area is flooding by sediment-laden water in the large tributaries to, and in the main stem of, the South Platte River. Although much sediment is available for erosion and transport by storm runoff in the Hayman area, there is little potential for debris-flow activity because the amount of silt- and clay-size material derived from the weathered parent rock is relatively small (S.H. Cannon, U.S. Geological Survey, oral commun., July 2002). The area is underlain by granitic material of the Pikes Peak batholith, a lithology whose weathering products are not associated with debris flows.

The other two high-priority burned areas are subject to debris-flow activity that could adversely affect life and infrastructure. The Coal Seam and Missionary Ridge wildfires burned in forests over geologic materials similar to those exposed by the 1994 South Canyon wildfire near Glenwood Springs. Debris flows that occurred after a summer thunderstorm soon after the South Canyon wildfire in 1994 blocked a 1.2-mile length of Interstate 70 near Glenwood Springs. These debris flows were generated from basins adjacent to those burned in the 2002 Coal Seam wildfire (Cannon and others, 1998, 2001). The marine shales exposed in formations within the Coal Seam and Missionary Ridge burned areas weather into fine-grain sediments including clays that are essential to the mobility and transport competence of debris flows (Griffiths and others, 1996).

Methods for Post-Fire Flood Hazard Analysis—Phase 2

The following section describes methods used to analyze potential hazards caused from flooding in perennial and ephemeral streams by sediment-laden water originating in burned areas. Methods used to analyze potential hazards from debris flows are described in a subsequent section of the report, “Methods for Post-Fire Debris-Flow Hazard Analysis—Phase 2.”

Short-Term Post-Fire Effects and Long-Term Recovery

Hydrologic responses are greatest immediately after a wildfire and persist for several years. As vegetation becomes reestablished, hydrophobic soil conditions change, organic litter accumulates on the land surface, and hydrologic conditions return to near pre-fire conditions. Both short-term hydrologic responses and long-term recovery hydrologic responses are evaluated in this study.

Short-term hydrologic responses have been defined on the basis of burned area and severity, and long-term hydrologic responses during the post-fire recovery period have been characterized on the basis of the pre-fire and post-fire conditions and streamflow data from two burned basins in New Mexico (Veenhuis, 2002).

Preparation of Digital Elevation Data

Many rainfall-runoff model parameters are extracted from the topography captured in digital elevation models (DEMs). Ten- or 30-m digital elevation model (DEM) data and Interferometric Synthetic Aperture Radar (IFSAR) 2.5-m data were prepared for this study. The source material for preparing 10-m DEM data is elevation contour lines (hypsography) from standard USGS 1:24,000-scale topographic maps. The USGS uses a software program named LT4X to process the digitally scanned source material (Infotek, 1993); this software calculates elevations for 10-m-square grid cells overlain on the hypsography map. Research has shown that a 10-m cell size is sufficient to capture all of the elevation information present on a 1:24,000-scale map (D.W. Litke, U.S. Geological Survey, oral commun., 2002). Elevations at cells located between contour lines are estimated using bilateral interpolation. The accuracy of the 10-m DEM elevation data is the same as the original hypsography data, which is plus or minus one-half of a contour interval. Contour intervals on maps in the study area generally are 40 ft in mountainous areas and 20 ft in flatter areas; therefore, the corresponding accuracy of an elevation value in the 10-m DEM is plus or minus 20 ft in mountainous areas and plus or minus 10 ft in flatter areas. The ground condition represented in the elevation data is that of the original orthophotography used to produce each 1:24,000 quadrangle map. In general, orthophotography for the study area was made from flights between 1950 and 1980.

IFSAR data provided by Intermap Technologies for the Hayman burned area were used to develop a more accurate DEM. IFSAR is an aircraft-mounted sensor designed to measure surface elevation, which is used to produce topographic imagery. The sensor sends radar pulses to the Earth, which are received by two antennas that record elevations (z) at specific ground coordinates (x, y). The ground coordinates are determined by Global Positioning System (GPS) technology. The 2.5-m DEMs were then used to generate 10-ft contours of the study area for delineation of the 100-year flood plain. Shaded-relief imagery also was generated from the IFSAR DEMs to provide a visual base layer for various hazard-map products.

Rainfall-Runoff Model Calibration and Simulation

Measured streamflow information for most drainage basins and subbasins affected by the Hayman, Coal Seam, and Missionary Ridge wildfires were not available; therefore, hydrographs and peak discharges for pre- and post-burn conditions were simulated using a rainfall-runoff model. The ability of a rainfall-runoff model to provide reliable simulations depends on the adequacy of the conceptual model and model parameterization. Assuming that the conceptual model is adequate, model parameterization typically proceeds by assigning values to parameters that control the rate exchange of fluxes within the drainage basins and subbasins. Whereas parameters might be determined by relating them to observable characteristics of the drainage basin or subbasin, most model parameters are abstract conceptual representations of nonmeasurable characteristics that must be estimated through a calibration process.

Pre-Burn Model Calibration

Two model-calibration approaches were used to estimate the pre-burn parameter values in the course of this study: manual calibration and objective calibration based on nonlinear regression. Manual calibration of the Hayman rainfall-runoff model involved trial-and-error estimation of parameter values for all contributing basins and subbasins. The manual calibration approach was used in the initial Hayman modeling study (U.S. Geological Survey, written commun., 2003) and is described in Appendix 2.

Because two of the three basin parameter values being estimated are functions of a third unknown parameter value, the estimation problem is intrinsically nonlinear and difficult to solve using the manual approach. More problematic is that there is no way to ensure the optimal estimation of parameter values or to quantify the degree of uniqueness and(or) uncertainty associated with the estimated parameter values. For this reason, a second approach based on nonlinear regression (Doherty, 1998, 2001) was used to recalibrate the Hayman rainfall-runoff model; this approach is termed the objective calibration method. The objective calibration method was used exclusively to calibrate rainfall-runoff models for the Coal Seam and Missionary Ridge burned areas.

The objective calibration method was used to estimate pre-burn parameter values that minimized a predefined objective function. The predefined objective function was based on a least-squares formulation defined by the following equation:

$$\Phi_m = \sum_{i=1}^{N} w_i [Q_{ri}(t, x, y) - Q_{si}(p)]^2 \qquad (1)$$

where Φ_m is a measurement objective function that is composed of the sum of weighted squared differences between regional and simulated estimates of peak discharge values Q; p is the vector of parameter values being estimated; r and s are subscripts indicating regional and simulated values; N is the number of peak flood discharge measurements; and i is an index. The weights t, x, and y were chosen to be unity so that all measurements had the same influence on the estimation process. The actual number of measurement objective function terms used during the model calibration process is dependent on the number of measurements used to condition the inverse procedure.

Whereas the regional peak discharge values were determined using regional peak discharge equations (Vaill, 2000), the simulated peak discharge values were computed using the HEC–1 rainfall-runoff model (U.S. Army Corps of Engineers, 1998). The HEC–1 model components were based on simple mathematical relations that were intended to represent the meteorologic, hydrologic, and hydraulic processes constituting the rainfall-runoff processes in the drainage basins. Meteorological input to the model was based on the 100-year recurrent rainfall defined by amount, duration, and cumulative density function; these data were available from the National Oceanic and Atmospheric Administration (NOAA) atlas (Miller, and others, 1973). By characterizing rainfall in this way, the rainfall was assumed to represent a basin or subbasin average; that is, the rainfall was assumed to be uniformly distributed over each basin or subbasin.

Various basin and subbasin characteristics and model parameter values are required as input to the HEC–1 model to compute the hydrologic processes. Basin and subbasin characteristics were derived using GIS and included drainage area, length, and slope. Model parameter values that require estimation through a model calibration process—such as runoff-curve number, initial abstraction (an adjustment to precipitation that describes the amount of precipitation not expected to run off due to interception, surface-depression storage, evaporation, and other factors), and lag time—were defined by the equations (Soil Conservation Service, 1985):

$$T_{lag} = L^{0.8}\left\{\frac{(S+1)^{0.7}}{1,900\ Y^{0.5}}\right\} \quad (2)$$

$$IA = S * 0.2 \quad (3)$$

$$S = \left\{\frac{1,000}{RCN}\right\} - 10 \quad (4)$$

where

- T_{lag} is the SCS lag time;
- L is the hydraulic length of drainage basin, in feet;
- S is the maximum retention in the drainage basin, in inches;
- Y is the drainage basin slope, in percent;
- IA is the initial abstraction;

and

- RCN is the runoff-curve number for the drainage basin as defined by the SCS curve-number loss method.

On the basis of equations 1 to 4, sets of optimal pre-burn model parameters were estimated through an iterative process that minimized the measurement objective function (eq. 1) and simulated the resultant (calibrated) rainfall-runoff relation using HEC–1.

Post-Burn Adjustment of Model Parameters

The post-burn rainfall-runoff parameter values are determined by adjusting the runoff-curve numbers according to the observed burn conditions in each basin or subbasin. Typically this is done using a simple area-weighting procedure. However, because the relation between runoff-curve number and precipitation excess is nonlinear, area weighting tends to incorrectly account for small, severely burned areas (high RCN) within a basin or subbasin. In this study, the weighting procedure was based on the SCS equation for precipitation excess (Soil Conservation Service, 1985) and was designed to account for the combined effects of unburned, low burn, and medium-high burn areas within a basin or subbasin. The SCS equation for precipitation excess has the form:

$$P_e = \frac{\left(P - 0.2\left(\frac{1,000}{RCN} - 10\right)\right)^2}{P + 0.8\left(\frac{1,000}{RCN} - 10\right)} \quad (5)$$

where

- P_e is the precipitation excess, in inches;
- P is the 100-year precipitation depth, in inches;

and

- RCN is the runoff-curve number.

For basins or subbasins that included both burned (low, moderate, or high burn severity) and unburned areas, the post-burn precipitation excess was computed assuming a linear-weighted combination of runoff associated with burned and unburned conditions given by:

$$P_{e,subbasin} = (P_{e,u}\ DA_u) + (P_{e,l}\ DA_l) + (P_{e,mh}\ DA_{mh}) \quad (6)$$

where

- $P_{e,subbasin}$ is post-burn basin or subbasin precipitation excess, in inches;
- $P_{e,u}$ is precipitation excess for unburned area, in inches;
- DA_u is percentage of basin or subbasin drainage area unburned;
- $P_{e,l}$ is precipitation excess for low-severity burned areas;
- DA_l is percentage of basin or subbasin drainage area burned at low severity;
- $P_{e,mh}$ is precipitation excess for moderate- and high-severity burned areas;

and

- DA_{mh} is percentage of basin or subbasin area burned at moderate and high severity.

Initial abstraction values generally decrease as a result of moderate to severe burned conditions (URS Corporation, 2000). In the SCS method, initial abstraction is a function of RCN. An RCN value of 95 produced an initial abstraction of 0.11 inch; an RCN value of 98 produced an initial abstraction of 0.04 inch. Runoff data and field observations made by the USGS (Robert Jarrett, U.S. Geological Survey, oral commun., 2002) indicate that runoff in burned areas of the 1996 Buffalo Creek wildfire and 2002 Hayman wildfire (as well as other wildfires in the Western United States) can occur with as little as 0.1 inch of rainfall, indicating that initial abstractions (especially where burned soils may be hydrophobic) may be less than 0.1 inch. In view of these observations, a lower limit (conservative) abstraction value of 0.04 inch was used for areas of moderate-to-high burn severity (based on an assumed RCN of 98). An RCN of 85 was assumed for areas of low-burn severity, and the pre-burn RCN (estimated by the pre-burn calibration process) was used for unburned areas. The assigned moderate-to-high burn and low-burn RCN values were based on BAER team reports (USDA Forest Service, 2002a, 2002b, 2002c) and consensus among experts from FEMA and State and local agencies (John Liou, Federal Emergency Management Agency; Tom Browning, Colorado Water Conservation Board; Garth Englund, Douglas County, Colorado; oral communs., 2003). The values of precipitation excess for moderate- and high-severity burned areas, low-severity burned areas, and unburned areas were computed using equation 5.

Weighted, post-burn RCN values for individual basins and subbasins were computed by setting equations 5 and 6 equal and solving iteratively for values of RCN. Using the post-burn RCN values, the associated initial abstraction and lag-time values were computed using equations 2, 3, and 4 for use in post-burn rainfall-runoff simulations. After the weighting and computation process was complete, the post-burn subbasin parameter values and associated GIS information were used as input to the HEC-HMS rainfall-runoff model for hydrograph generation (U.S. Army Corps of Engineers, 2001b). HEC-HMS is a widely accepted, public-domain rainfall-runoff model commonly used by FEMA to conduct detailed rainfall-runoff analyses.

Sediment Bulking of Estimated Discharge

Studies of post-fire hydrology in the Western United States have shown that sediment loads can increase substantially during flooding in burned drainage basins (O'Brien and Fullerton, 1989; Moody and Martin, 2001a). The physical behavior of combined water-and-sediment flows depends on the concentration of sediment. Several investigators have identified a sediment-concentration limit of 20 percent by volume, up to which a water-sediment mixture has the characteristics of purely water flow. At volumetric concentrations greater than 20 percent, the mixture has the characteristics of a hyperconcentrated flow (mud flood) or a debris flow (mudflow) (Pierson and Costa, 1987; Costa, 1988; O'Brien, 2001).

Computed water-peak discharges from the HEC-HMS modeling were bulked, or increased volumetrically, to account for increased sediment concentrations that are expected to occur as a result of accelerated erosion after burning. Bulking analyses and computations were based on previous studies of post-fire runoff in other areas of the Western United States, and on published research documenting the physical behavior of combined water and sediment flows (Pierson and Costa, 1987; Costa, 1988; O'Brien, 2001). The amount of sediment bulking varied in the study, depending on whether predominantly water floods or debris flows were anticipated in response to the 100-year storm.

Water-Flow Routing and Computation of Flood Elevations

Hydrologic routing of flood hydrographs down main-stem channels was performed using routing algorithms included in the HEC-HMS rainfall-runoff model. Hydrologic routing methods used in each model (including Muskingum, Muskingum-Cunge, and Modified Puls reservoir routing) are discussed in greater detail in subsequent sections of the report covering the post-fire hydrologic hazards for the Hayman, Coal Seam, and Missionary Ridge wildfires.

Post-fire flood elevations were computed for bulked peak discharges at selected cross-section locations in each reach of the South Platte River, and the resulting flood plain was delineated on a topographic map. Flood boundaries between cross sections were interpolated by hydrologists and mapping experts. The accuracy of these interpolations depends on the available map scale and the cross-section spacing in each study area.

Delineation of the 100-Year Flood Plain

Delineation of the revised 100-year flood plain of the South Platte River (Phase 2 analysis) incorporated IFSAR elevation data and the simulated discharge values for the burned drainage basins and subbasins. The USGS surveyed and monumented representative cross sections through the study reach, spaced 1 to 2 mi apart. Post-fire, 100-year flood levels were computed for each cross section using the normal-depth computation method in the Quick-2 computer program (Federal Emergency Management Agency, written commun., 2003). Interpolation of the flood plain between surveyed cross sections was based on the contours generated from the 2.5-m IFSAR elevation data to generate the 100-year flood plain polygon using ArcGIS Spatial Analyst (Environmental Systems Research Institute, 2004).

Methods for Post-Fire Debris-Flow Hazard Analysis—Phase 2

The following section describes methods used to analyze potential hazards caused by debris flows originating in burned areas. Methods used to analyze potential flooding by sediment-laden water are described in the section "Methods for Post-Fire Flood Hazard Analysis—Phase 2."

Debris-Flow Mechanisms

Wildfire can have profound effects on a drainage basin through the consumption of the rainfall-intercepting canopy and the soil-mantling litter and duff and through the formation of water-repellent soils. These changes can result in decreased rainfall infiltration into the soil and, subsequently, a significant increase in overland flow and runoff in channels. Removal of obstructions by wildfire can enhance the erosive power of overland flow, resulting in accelerated erosion of material from hillslopes. Increased runoff also can erode substantial volumes of material from channels, the net result being the transport and deposition of large volumes of sediment both within and downstream from the burned area (Cannon, 2001).

Flow and fluid properties gradually begin to change with increasing sediment concentration. Sediment-particle fall velocity decreases, and fluid density and viscosity increase. The upper limit of sediment concentration, by volume, in a typical "water flood" is 20 percent (Costa, 1988). Volumetric sediment concentration in a "hyperconcentrated flow" ranges from 20 to 47 percent (Costa, 1988). Rapid runoff with extremely high concentrations of entrained sediment (47 to 77 percent, Costa, 1988) is known as a "mudflow" or "debris flow." Mudflows are runoff events with no more than 50 percent of the sediment coarser than gravel size (particle intermediate diameter greater than 2.0 mm, or 0.079 inch) (Varnes, 1978). Because most runoff events in rugged areas with a high sediment concentration transport sediment particles ranging in size from clay to boulders, the term "debris flow" is used in this study.

Debris flows are produced frequently in response to summer convective thunderstorm activity over drainage basins burned by wildfire (Cannon, 2001). Debris flows pose a hazard distinct from other sediment-laden flows because of their unique destructive power; debris flows can occur with little warning and can exert great impulsive loads on objects in their paths. Even small debris flows can strip vegetation, block drainageways, damage structures, and endanger human life (Cannon, Michael, and Gartner, 2003). Debris-flow peak velocities are dependent on flow depth and can range from 3 to 30 m/s (10 to 100 ft/s) (Hungr and others, 1984; Pierson and Costa, 1987).

Debris-flow behavior is dependent on the concentration and particle-size range of the entrained sediment (Costa and Jarrett, 1981) and on the relative proportion of inertial and viscous forces (Pierson and Costa, 1987). A relatively high proportion of clay-size particles (particle diameter less than 0.004 mm, or 0.0002 inch) in the transported sediment increases debris-flow matrix strength and helps maintain the high pore pressure necessary to support larger particles in the flow (Griffiths and others, 1996).

The volumetric sediment concentration (C_v) is difficult to measure precisely and varies during a debris-flow event. Several researchers have estimated or calculated concentration ranges for different periods during a debris flow. Pierson and Scott (1985) reported mean C_v greater than 57 percent in volcanic lahar-derived debris flows. Pierson and Scott also reported mean C_v of 30–35 percent and a maximum C_v of 37 percent in non-Newtonian hyperconcentrated flows. Pierson and Costa (1987) observed the range of mean C_v between 20 and 60 percent for hyperconcentrated flows. O'Brien (J.S. O'Brien, FLO Engineering, Inc., oral commun., December 2002) assumes a mean C_v of between 30 and 35 percent for debris flows, a maximum C_v of between 45 and 53 percent, and a C_v between 40 and 45 percent at the water hydrograph peak when calibrating the FLO-2D two-dimensional flood-routing model (FLO-2D; O'Brien, 1993, 2001) used for debris-flow analysis in this report.

Cannon and others (2003a and 2003b) categorized the potential debris-flow peak-discharge in the Coal Seam and Missionary Ridge burned areas on the basis of a regression equation developed from data measured in previously burned, mountainous areas (Cannon, 2001). These peak discharge categories, existing infrastructure, and input from local authorities were used to prioritize drainage basins for the further debris-flow analysis described in this report. This study includes a select group of tributaries to illustrate the potential for debris-flow inundation on existing alluvial fans and low-gradient features such as valley floors and flood plains. Other tributaries not included in this study also have the potential to produce floods and debris flows that could do great damage to other types of infrastructure, such as roads, bridges, railroads, utility lines, and isolated structures.

Post-Fire Debris-Flow Peak Discharge Estimates

Cannon (2001) developed a multiple regression model to define the range of potential peak discharges generated by post-fire debris flows. Cannon and others (2003) and Cannon, Michael, and Gartner (2003) revised the relation by using data measured from 49 burned drainage basins located throughout the Western United States; of these basins, 7 were in the Coal Seam burned area and 10 were in the Missionary Ridge burned area. The regression model relies on indirect peak discharge measurements (computed using either slope-area, critical flow, or super-elevation techniques from field surveys) and consists of a physical representation of peak discharge relative to average rainfall intensity (Q_p/I) as a function of basin gradient and burned extent where Q_p is the peak discharge (in cubic meters per second) and I is the average storm rainfall intensity (in meters per second). The slope-area method for determination of peak discharge generally is not assumed to be applicable for non-Newtonian debris flows; however, it does allow for at least a relative measure of the debris-flow response of burned drainage basins. For the steep basins and hillslopes from which Cannon's measurements were made, it generally was assumed that the discharges estimated using this approach are conservative in the context of engineering design (Cannon and others, 2003; Cannon, Michael, and Gartner, 2003).

All debris flows in Cannon's analysis were reported to be triggered by summer convective thunderstorms. Although the adjusted R^2 of 0.34 for Cannon's relation indicates significant scatter in the data used in the regression, and thus great uncertainty in the predicted values, Cannon and others (2003) and Cannon, Michael, and Gartner (2003) used the relation to estimate potential debris-flow peak discharges for several tributaries in the Coal Seam and Missionary Ridge burned areas on the basis of measured gradient extracted from 10-m

DEMs and estimated rainfall. The peak debris-flow discharge estimates were used in this study to help rank tributaries for additional analysis.

Debris-Flow Modeling in Colorado Wildfire Areas

A two-dimensional flood-routing model (FLO-2D; O'Brien, 1993, 2001) was used to delineate the area of unconfined debris-flow inundation on selected alluvial fan and valley floor areas in the Coal Seam and Missionary Ridge wildfire areas. FLO-2D was used in this analysis at the request of FEMA. The model uses a specified input hydrograph, volumetric sediment concentration, and existing topography to route a debris flow from the originating tributary to the depositional zone.

The HEC-HMS rainfall-runoff model (U.S. Army Corps of Engineers, 2001b) was used to generate the FLO-2D input hydrograph from burned drainage basins. Sediment concentration of the debris flow was estimated on the basis of results from previous studies (Pierson and Scott, 1985; Pierson and Costa, 1987; Costa, 1988; O'Brien, 2001). Topography of the debris-flow channel and alluvial fan area was extracted from 10-m DEMs prepared by the USGS. Model output is spatially and temporally varied and includes maximum depth and velocity.

Simulated flood and debris-flow discharges presented in this study were generated by 100-year rainfall events; however, the 25-year rainfall may be more representative of storms that generated debris flows in Cannon's regression equation (Susan H. Cannon, U.S. Geological Survey, oral commun., 2003). O'Brien (J.S. O'Brien, FLO Engineering, Inc., oral commun., 2002) notes that the 100-year storm may generate too much water relative to available sediment to produce debris flows, and that storms of less than a 25-year recurrence interval may not result in enough runoff to move a substantial volume of sediment from source areas to the alluvial fan.

Debris flows from some subbasins in this study were simulated with the 25-year storm for comparison to the 100-year storm. Simulated debris-flow inundations from the 25-year storms were nearly indistinguishable from 100-year storm debris-flow inundations. Consequently, runoff from the 100-year rainfall was used in this analysis for comparison to flood estimates from the Hayman and Mitchell Creek studies.

Debris-Flow Routing with FLO-2D

FLO-2D (O'Brien, 1993, 2001) was used to delineate the area of unconfined debris-flow inundation on selected alluvial fan and valley floor areas in the Coal Seam and Missionary Ridge areas. FLO-2D was used in several earlier studies to simulate debris flows in Telluride, Ouray, Aspen, Basalt, Glenwood Springs, and Colorado Springs, Colorado; Centerville, Utah; and along the north coast of Venezuela (O'Brien, 2001, p. 73–80).

As applied in this study, the FLO-2D model routes the water and sediment emanating from a burned tributary drainage basin onto an unconfined alluvial fan or flood-plain surface. FLO-2D conserves the hydrograph volume, predicts flood-wave attenuation, and predicts the area of inundation while routing the unconfined debris flow over nonuniform topography and roughness elements. The model uses either the diffusive-wave or the full dynamic-wave versions of the momentum equation. Model time steps are governed by wave celerity and are incremented according to flood-routing numerical stability criteria. Numerical stability is linked to flood-volume conservation. Model output is spatially and temporally varied. Maximum depth, velocity, and discharge can be reviewed numerically or graphically for the entire inundation surface or by the individual grid elements.

The FLO-2D model requires a representation of the potential flow-surface elevation in a square grid format; however, the USGS DEM map format is not directly readable by FLO-2D. Consequently, the 10-m DEMs were converted into an ArcGIS (Environmental Systems Research Institute, 2002) GRID format that is readable by FLO-2D. The GRID data sets were then subdivided into subsets for each area to be modeled using ArcGIS software. Output from the ArcGIS software included an ASCII point file of elevation data in the form of [x-location, y-location, z-elevation] and a georeferenced tagged image format (TIF) file of a portion of the USGS topographic map for each area to be modeled. These data sets were then loaded into the Grid Developer System (GDS) module of FLO-2D. The GDS was used to prepare the model grid files (CadPTS.DAT and FPlain.DAT) that are used in the FLO-2D model.

The inflow hydrograph at the alluvial fan head or tributary mouth was generated with the objective calibration method described in the section "Methods for Post-Fire Flood Hazard Analysis—Phase 2." The 100-year, 1-hour storm was used to simulate debris flows. For the Coal Seam area, the 100-year, 1-hour rainfall was 1.64 inches. For the Missionary Ridge area, the 100-year, 1-hour rainfall was 1.77 inches (Miller and others, 1973).

Drainage-basin geomorphic characteristics were derived with GIS methods by using the 10-m DEMs. Burned area and burn severity were taken from the BAER reports for the Coal Seam and Missionary Ridge areas (USDA Forest Service, 2002b and 2002c). An RCN for each delineated drainage basin was computed by area weighting the subbasin RCNs (percentage of area in each burn-severity category observed in the subbasin) and deriving a composite RCN from SCS equations 5 and 6.

The rheological properties (deformation and flow behavior) of debris flows are extremely sensitive to changes in sediment concentration (Major, 1993). Debris flows and hyperconcentrated flows are simulated in the FLO-2D model by assuming viscosity and yield-stress relations are a function of volumetric sediment concentration (C_v). Based on the post-fire assessments by Cannon (Cannon and others, 2003; Cannon, Michael, and Gartner, 2003), tributary subbasins were assumed to contain an abundant supply of sediment, and most of the sediment was assumed to originate from in- and near-channel erosion rather than from landsliding or mass failure into the flow path.

The sediment concentrations used in simulations at Coal Seam and Missionary Ridge are based on results from previous studies (Pierson and Scott, 1985; Pierson and Costa, 1987; Costa, 1988; O'Brien, 2001). Post-fire runoff was not bulked with sediment before being input into the FLO-2D as it was for the water floods described elsewhere in this report. The assumed volumetric concentrations for the input debris-flow hydrograph were varied through the event, and for this study, they were initial C_v 20 percent, mean C_v approximately 31 percent, maximum C_v 48 percent (preceding the input water hydrograph peak), C_v at the time of the input water hydrograph peak 43 percent, and C_v for the duration of the event 20 percent. Examples of runoff and sediment-concentration hydrographs used in the debris-flow simulations are presented in figure 2.

FLO-2D treats debris-flow composition as a temporally and spatially unvarying mixture; coarse material does not settle out during the simulation as it does in actual mud and debris flows. When the input sediment concentrations are decreased in FLO-2D, the debris-flow mixture travels a farther distance down a fan or valley; when concentrations are increased, the debris flow travels a shorter distance before stopping.

Interpretation of FLO-2D model output is limited by several factors. The FLO-2D model is a quasi-two-dimensional model and, although often used in unconfined flow situations, only routes flow in a downslope direction toward the nearest neighbor grid cell rather than in a truly lateral or transverse direction. Outflow from one square grid element into an adjacent square grid element is limited to eight possible directions (N, NE, E, SE, S, SW, W, NW). Model output is limited by the resolution of the topographic data supplied; in this study, 10-m digital elevation data. Most roughness elements less than 10 m, or 32.8 ft, in size are not accounted for. Also, the original topography remains static during a model run and is insensitive to large-scale channel scour or aggradation. Small-scale differences in grid-cell elevation values influence the direction of cell-to-cell flow propagation. Errors in the input elevation values or changes in elevation over time, such as from land use or subsequent debris-flow deposition, could render the existing model output inaccurate.

Inundation areas and depositional depths generated in these FLO-2D simulations reflect the median of predicted values. Minimum and maximum likelihood areas and depths are not presented in the model output, and there is large, unquantified variability in the expected outcome of the 100-year storm. Another limitation of the analyses is that estimated inundation areas and depths from the model output are not verifiable. No post-fire data exist at this time with which to compare the FLO-2D simulations; however, future debris flows from areas within the Missionary Ridge and Coal Seam burned areas where precipitation gages are operating may facilitate verification.

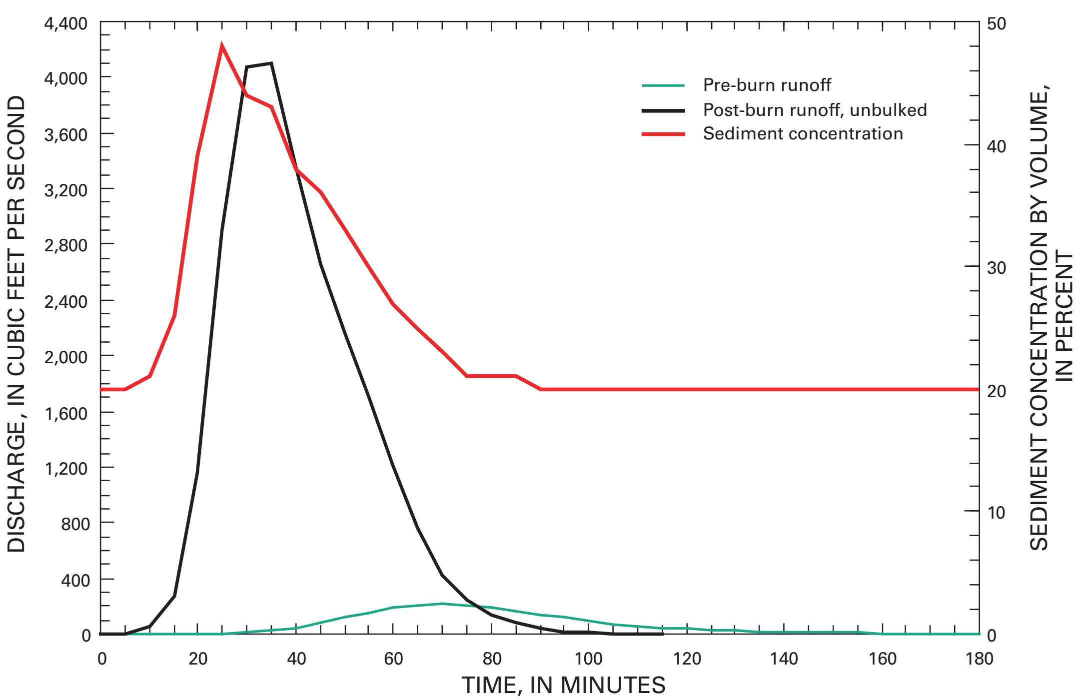

Figure 2. Example of pre- and post-burn runoff hydrographs and sediment-concentration hydrograph used in debris-flow modeling, 100-year, 1-hour storm.

Post-Fire Flood and Debris-Flow Hazard Maps

Various map products were created for the three burned areas determined to have high priority in the Phase 1 assessment—the Hayman, Coal Seam, and Missionary Ridge wildfires (see figs. 1, 4, 17, 20). The maps were compiled using the following raster data sources: 1-m imagery from the 133 Urban Area Initiative, USGS Digital Raster Graphics (DRG), 2.5-m IFSAR elevation data, USGS 30-m National Elevation Data (NED), and USGS 10-m DEMs. Vector data that complemented the raster data sets include the 100-year cross-section and flood-plain vectors, debris flow/alluvial fan data sets, fire perimeters, USGS transportation and hydrography data, and public-land survey reference data. The scale of the map determined the type of base layer imagery to be used in the map product. NED or USGS DRGs were used as background images on small-scale maps, depicting the entire extent of the wildfire (see figs. 4, 5, 17, 20). The large-scale maps used 1-m color imagery from the 133 Urban Area Initiative as the background layer (see figs. 12, 13, 14, 18, 19). At this scale the user can view potential structures at risk in the revised 100-year flood plain.

Method for Determination of Drainage Basin Recovery—Phase 3

Hydrologic responses during the post-fire recovery period are estimated in this report for the Hayman and Coal Seam burned areas based on the following assumptions:

1. A wildfire will raise the RCN in a burned drainage basin from a pre-fire RCN to a post-fire RCN as a function of burned area and severity.

2. During the recovery period, the value of the larger post-fire RCN will attenuate with time and eventually approach, or decay to, the value of the smaller pre-fire RCN.

3. Although it is recognized as a simplification, for the purposes of this report, recovery will be characterized as a decay function that reduces the post-fire RCN with time.

4. Initial decay will be the most rapid and will take place as a function of the magnitude of the pre-fire RCN and the difference between pre- and post-fire RCNs.

Pre- and post-fire RCNs were estimated for all subbasins in the Hayman and Coal Seam burned areas for use in the HEC-HMS model as described in the “Rainfall-Runoff Model Calibration and Simulation” section. Although very few systematic field data exist that characterize post-fire recovery, Veenhuis (2002) provides a nearly complete description of post-fire drainage-basin recovery in the Frijoles Canyon at Bandolier National Monument, New Mexico, on the basis of streamflow data collected in a burned area. The data indicate that the magnitude and frequency of post-fire flood peaks both decayed with time and that most of the decay occurred in 5 to 10 years; however, the report states that flood magnitudes remained above pre-fire levels 22 years after the wildfire. These results were used in the Hayman and Coal Seam wildfire recovery characterizations developed for this analysis as the general framework for a post-fire recovery equation that is a function of initial RCN, change in RCN (due to wildfire), and time. The equation has the form of an exponential decay equation:

$$CN_t = PCN + (DCN)\, e^{(-t/TC)} \qquad (7)$$

where

CN_t is RCN at time t in the recovery period,
PCN is pre-fire RCN number,
DCN is post-fire RCN minus PCN,
TC is a function of pre-fire RCN,

and

t is time, in years.

Equation 7 can be used to estimate an RCN at any point in the recovery process. In this analysis, equation 7 was used to develop estimates for parameters used in the HEC–1 and HEC-HMS models, and the models were then used to develop a time series of annual flood peaks of the 100-year design storm to characterize long-term recovery.

An example discussing the results from equation 7 is helpful to indicate how the equation was used in this analysis. Figure 3 indicates a family of curves generated with equation 7 that begin at the y-axis and intersect or closely approach the x-axis. These curves are RCN estimates for a recovery period beginning with post-fire conditions and continuing for 50 years in a hypothetical drainage basin with an assumed pre-fire RCN of 50, raised to post-fire RCNs of 55 to 100 in increments of 5. The first, or lowest, curve in figure 3 is for a drainage basin burned and raised to a post-fire curve number of 55. Likewise, the second curve shows the estimated response for a drainage basin burned and raised to a post-fire RCN of 60, and so on. In figure 3, the third curve from the top indicates RCN recovery for the hypothetical burned drainage basin having a post-fire RCN raised to 90. The curve intersects the y-axis at 90 and indicates that after 5 years it is estimated the RCN would recover from 90 to about 68, about a 55-percent reduction of the RCN increase attributed to this hypothetical wildfire.

In this report, “long-term recovery” is used to indicate an estimate of the period of time it takes for post-fire hydrologic responses to stabilize or reach a point where change occurs at a relatively slow and steady rate. In order to obtain an estimate of long-term recovery in each wildfire area, equation 7 was used to determine values for RCN for all subbasins for a period beginning with post-fire conditions and continuing through 50 years. For this exercise, pre-and post-fire RCNs in the Hayman and Coal Seam wildfire areas used in equation 7 were obtained using methods described in the “Rainfall-Runoff Model Calibration and Simulation” section. Initial abstractions were calculated on the basis of RCN by using equation 3, and lag times were calculated using equation 2.

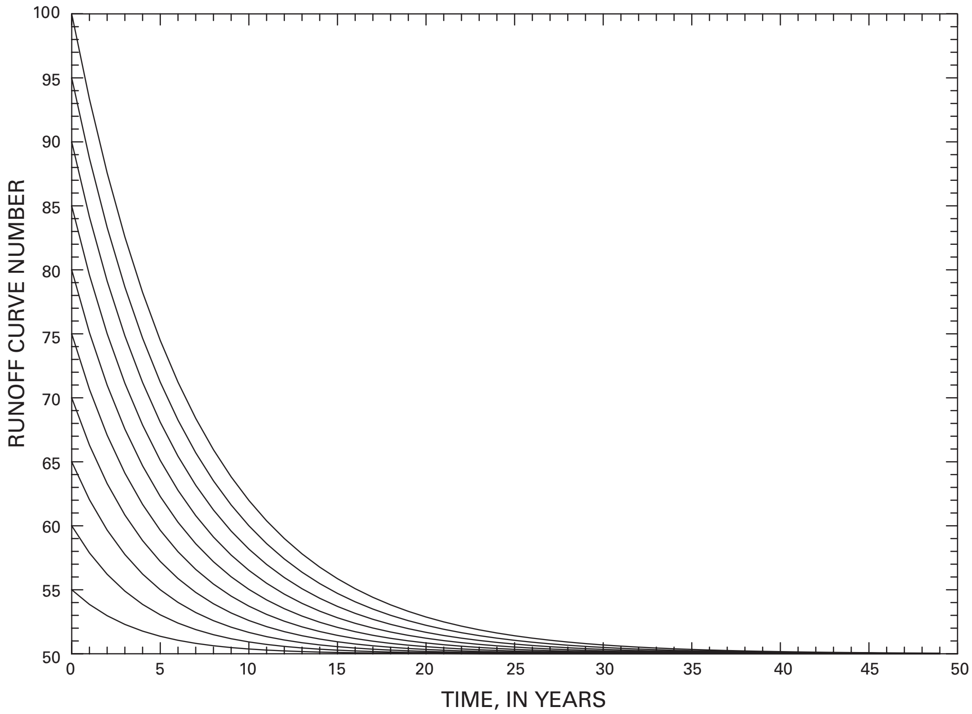

Figure 3. Estimated recovery curves for runoff-curve numbers in a drainage basin with a pre-burn runoff-curve number of 50. Plotted curves represent estimated post-burn response of runoff-curve numbers 55 through 100, incrementing by 5.

The calculated values for RCN, initial abstraction, and lag times were used to prepare batch input for the HEC–1 model and obtain a time series of 100-year storm flood-peak estimates, on the basis of the 100-year storm, in the Hayman and Coal Seam burned areas. The resultant time-series values were evaluated to identify a time in the recovery process when the change in estimated 100-year flood peak became less than 5 percent, per year, of the RCN change due to wildfire. Estimates were made for three locations: two represent outlets for the burned areas upstream and downstream from Cheesman Reservoir for the Hayman wildfire, and a third represents the burned area of Mitchell Creek for the Coal Seam wildfire. Although the times determined here do not represent the time to full recovery, they will be referred to, for convenience, as long-term recovery times. The long-term recovery times were rounded to the nearest whole year and used as the basis to prepare input for HEC-HMS to obtain estimates of the 100-year flood peak at the recovery time for the three outlet locations.

The estimated periods for long-term recovery are 6 years for the South Platte River upstream from Cheesman Reservoir, 6 years for the South Platte River downstream from Cheesman Reservoir, and 4 years for Mitchell Creek. Times in this range are consistent with BAER-team estimates of about 5 years to recovery due to the mitigating effects of vegetation reestablishment (USDA Forest Service, 2002a and b), and with field observations from the USGS National Research Program of about 3 to 7 years at drainage basins affected by other wildfires near the Hayman burned area (Robert Jarrett, U.S. Geological Survey, oral commun., February 2004). Additional details about the results of the HEC-HMS simulations are described in the sections “South Platte River Hydrology and Peak Flow Modeling for Long-Term Recovery—Phase 3” and “Mitchell Creek Hydrology and Peak Flow Modeling for Long-Term Recovery—Phase 3.” Finally, it is important to note, as suggested in the initial assumptions, that recovery is only generally a function of time. In reality, recovery is likely a complicated function of many variables such as storm characteristics (frequency, magnitude, and intensity), storm distribution, and vegetation reestablishment in the years following a wildfire.

Post-Fire Hydrologic Hazards for the Hayman Wildfire

South Platte River “Limited-Detail” Hydrologic Analysis—Phase 2

Post-fire hydrologic analyses were conducted to evaluate the effects of the 100-year peak flow on burned and adjacent unburned areas of the South Platte River Basin. Overview and index maps of the Hayman wildfire area are shown in figures 4 and 5, oversized maps that accompany this report. Analyses were designed to characterize increased runoff produced by rainstorms within and near the fire perimeter and to reflect drainage-basin conditions that are expected to exist during the next several years (before substantial regrowth of vegetation in the burned areas). The results of these analyses (known to FEMA as a "Limited Detail Analysis") were used to delineate a hazard-mitigation map for post-fire, 100-year flooding of the South Platte River. The map, shown in figures 12, 13, and 14, characterizes runoff conditions over the short term (approximately the first 6 years after the 2002 wildfire) and will not be used for regulatory purposes (John Liou, Federal Emergency Management Agency, oral commun., 2003).

Long-term hydrologic analysis reflecting more stable drainage-basin conditions (after a recovery period of approximately 6 years) and a more detailed hydraulic analysis (using step-backwater modeling routines) also have been made for the South Platte River Basin. Results of these analyses are presented in later sections of this report.

The approach to the post-fire "limited-detail" hydrologic analyses included the following steps and assumptions:

1. Inflow conditions were established for the South Platte River at the upstream boundary of the burned area and for the South Platte River downstream from Cheesman Dam.

2. A rainfall-runoff model was developed for pre-fire (unburned) conditions in the affected subbasins tributary to the South Platte River. Model parameters for runoff generated by the 100-year, 6-hour rainstorm (2.4 inches) were calibrated on the basis of regional estimates of computed 100-year peak discharge at selected stream-gage sites in the study area.

3. Peak discharges associated with the 100-year, 6-hour storm were simulated for post-fire conditions in burned subbasins tributary to the South Platte River. Hydrologic routing was used in the larger, multibasin drainages.

4. Peak discharges for burned subbasins were increased using a bulking factor to reflect the increased runoff volume due to large sediment loads.

5. Bulked peak discharges for selected reaches of the South Platte River (within and downstream from the burned area) were computed using a hydrograph routing algorithm.

Two rainfall-runoff calibration methods were used in the Hayman burned-area analysis: manual calibration and objective calibration. Initial model calibration was done using manual adjustment of drainage-basin parameters to produce a target 100-year peak discharge for each subbasin at the point of confluence with the South Platte River. Results of the manual calibration method, including the simulated 100-year peak discharges used to develop short-term (hazard-mitigation) flood maps, are described in Appendix 2.

The objective calibration method was used for the analysis of drainage basin-recovery (long term) conditions. The objective calibration method was developed subsequent to completion of the short-term flood-hazard assessment and is considered to be unbiased and more robust than the manual calibration method. Results from the objective calibration method are presented in this section.

South Platte River Inflow Conditions

The South Platte River within and downstream from the Hayman burned area is regulated by a series of reservoirs owned and operated by the Denver Water Board. In order to assess the effects of the 100-year storm and subsequent flooding on burned and adjacent unburned areas of the South Platte River Basin, boundary flow conditions were needed at the upstream edge of the fire perimeter and at the outflow from Cheesman Dam. Boundary flow conditions were established as follows.

Upstream Edge of Fire Perimeter.—Because of the large contributing drainage area of the South Platte River Basin upstream from the wildfire area (figs. 4 and 5) and the substantial regulation/storage capacity of upstream reservoirs, it is extremely unlikely that a 100-year flood would occur throughout the entire drainage basin during a single runoff event. To account for potential antecedent runoff and reservoir releases into the burned area, a 10-year peak discharge was selected as the boundary inflow condition. The 10-year peak discharge for streamflow-gaging station 06696000 (South Platte River near Lake George; drainage area 963 mi^2; period of record 1933–98 since completion of Elevenmile Canyon Reservoir) is 840 ft^3/s. Adjustment of discharge for contributing drainage area between the gage and the Hayman fire perimeter using a relation developed by Vaill (2000) resulted in a 10-year peak discharge of 940 ft^3/s. A similar analysis was used to compute the pre-burn discharge for Tarryall Creek, which also is regulated. The computed 10-year peak discharge was 715 ft^3/s (Tarryall Creek near Lake George). Tarryall Creek flows into the burned area of the Hayman wildfire and was treated as a boundary inflow point.

Outflow from Cheesman Dam.—Cheesman Reservoir is operated as a water-supply reservoir for the City of Denver. It is not designated for flood control, so hydrologic analysis of the 100-year flood assumes fill-and-spill operation of the dam. That is, the reservoir is allowed to fill to capacity, then freely spill excess over the spillway. Based on discussions with staff of the Denver Water Board (Robert Steger, Denver Water Board, oral commun., 2003), the following boundary conditions at Cheesman Dam were used:

1. Reservoir full, with uncontrolled flow over the spillway in response to upstream runoff.

2. Outlet works (release capacity 1,400 ft^3/s) closed.

3. Spillway (release capacity 22,370 ft^3/s) passes the entire flood (subject to peak attenuation by the reservoir).

4. Peak flow over the spillway is the inflow boundary condition for modeling of the South Platte River downstream from the dam. Outflow from Cheesman Dam is assumed to contain no sediment.

Cheesman Reservoir could be filled with water at any time after the 2002 wildfire in response to either operational considerations (Cheesman evaporation rates are smaller than upstream reservoirs on the South Platte River Basin) or natural runoff. As a result, both short-term (hazard-mitigation) and long-term modeling scenarios reflect a full-reservoir condition. The Modified Puls reservoir routing routine in HEC-HMS was used to route the computed flood hydrograph through Cheesman Reservoir and over the spillway to the downstream reach.

South Platte River Tributary Rainfall-Runoff Modeling

Because the study reach of the South Platte River is affected by flow regulation (Elevenmile Canyon and Cheesman Reservoirs), flood-frequency analyses of streamflow-gaging stations on the South Platte River were not used. Instead, rainfall-runoff modeling was used to develop post-fire hydrographs for 19 selected drainage basins (subbasins) tributary to the South Platte River within and downstream from the Hayman burned area. These 19 subbasins and an additional 22 minor contributing subbasins were delineated using a 30-m DEM. The U.S. Army Corps of Engineers (USACE) HEC-HMS computer model (U.S. Army Corps of Engineers, 2001b) was used for the analysis along with the 100-year, 6-hour storm (2.4 inches). The 100-year, 6-hour storm also was used by the USACE for hydrologic analysis of the 2000 Cerro Grande wildfire in New Mexico (URS Corporation, 2000).

Rainfall-Runoff Model Methodology for the Hayman Wildfire

Rainfall-runoff modeling was conducted in two steps to simulate (1) preburned or unburned conditions, and (2) burned conditions.

Step 1, Modeling of Unburned Conditions, South Platte River Tributaries

The runoff hydrograph for the 100-year peak discharge was developed for natural, unburned conditions of each subbasin. Because streamflow data for most subbasins were not available, a hydrograph and peak discharge for each tributary were computed using a rainfall-runoff model. Hydrographs were generated using the SCS curve-number loss method (Soil Conservation Service, 1985) as described in the “Rainfall-Runoff Model Calibration and Simulation” section of this report.

Calibration of simulated peak discharges by using regional regression equations developed from measured peak-flow data was desirable. However, a comparison of measured 100-year peak flows (Interagency Advisory Committee on Water Data, 1982) at five stream gages in the Goose and Tarryall Creek subbasins with the results of regional regression equations developed for mountain areas of Colorado (Vaill, 2000; Browning, 2001; Kircher and others, 1985) showed that the regional equations substantially overestimated the observed 100-year peaks (by a factor of 2 or more). It was apparent that existing regional equations do not fit this area of relatively low rainfall runoff (Jarrett and Costa, 1988). The landscape assessment for the Upper South Platte Watershed Protection and Restoration Project (Foster Wheeler Environmental Corporation, 1999) notes that the montane study area was heavily forested with ponderosa pine, Douglas fir, and lodgepole pine before the wildfire. The crown closure, which is the percentage of ground cover not visible from an aerial view looking straight down at the forest land, across most of the pre-fire study area was estimated to be 71 to 100 percent, and in four subbasins (Cheesman Reservoir, Horse Creek, Waterton/Deckers, and West Creek) was estimated to be greater than 90 percent. The presence of this protective canopy and a thick duff layer on the ground, coupled with historically low precipitation amounts (Hansen and others, 1978; Robert Jarrett, U.S. Geological Survey, oral commun., 2002), probably explains the anomalously low 100-year, gaged peak discharges as compared to those predicted by the regional regression equations.

As an alternative, the five streamflow gages in the Goose and Tarryall Creek subbasins were used to develop a local regional equation for the study area (table 1). The period of annual peak discharge at three of the sites (1978–86) is less than 10 years, which generally is considered the minimum required for flood-frequency analysis. In an effort to evaluate the 1978–86 period in terms of its hydro-climatic characteristics relative to long-term conditions, a flood-frequency analysis of peak discharges for 1978–84 at streamflow-gaging station 06700500 (Goose Creek above Cheesman Lake) was compared with that for the period of record (1924–84). Annual peaks for 1983 and 1984 at the Goose Creek gage were provided by the Colorado Division of Water Resources, subsequent to the completion of regional regression analysis; peaks for 1985 and 1986 were not available because the gage was discontinued. The 100-year peak discharge for 1978–84 was 857 ft^3/s, which lies within the 95-percent confidence interval for the analysis spanning the longer 1924–84 period. The 95-percent confidence interval for the long-term period of record was 546 to 884 ft^3/s.

In this comparison, peak discharges for 1978–84 generally can be considered representative of those for the period of record. Unfortunately, other acceptable comparison sites in the same general hydro-climatic region (and with appropriate periods of record) were not available. A review of available precipitation data for the Cheesman Reservoir precipitation gage indicates that the 1978–84 period generally is representative of long-term precipitation for the period 1949–99. The average annual precipitation for 1978–86 was 17.6 inches, and the long-term average was 17.1 inches. On the basis of the peak-flow comparison at the Goose Creek gage and the analysis of average annual precipitation for the study area, the short period of record (1978–86) used to develop the local regional equation is considered reasonable.

Table 1. Characteristics of streamflow-gaging stations used for calibration of 100-year peak discharge for pre-burn conditions, South Platte River drainage basin in Colorado.

[mi^2, square mile; ft, foot; ft/ft/, foot per foot; ft^3/s, cubic feet per second; Q_{100}, 100-year peak discharge]

Streamflow-gaging station	Period of record	Drainage area (mi^2)	Gage elevation above sea level (ft)	Subbasin slope (ft/ft)	Q_{100} at gage (ft^3/s)	Predicted Q_{100}, equation 8 (ft^3/s)	Predicted Q_{100}, Vaill[1] (ft^3/s)
Tarryall Creek at Upper Station near Como (06696980)	1978–86	23.7	9,935	0.316	236	192	569
Michigan Creek above Jefferson (06697450)	1978–86	23.1	9,503	0.246	196	188	513
Jefferson Creek near Jefferson (06698000)	1978–86	11.8	9,600	0.333	81	108	355
Tarryall Creek below Rock Creek, near Jefferson (06699005)	1983–97	236	9,020	0.182	1,050	1,270	2,390
Goose Creek above Cheesman Lake (06700500)	1924–84	86.6	6,910	0.317	646	559	1,410

[1]Vaill, 2000.

Table 1 gives a summary of the drainage-basin characteristics and the predicted 100-year peak discharges used to develop the relation (Interagency Advisory Committee on Water Data, 1982). The resulting peak discharges computed using the local regression model, along with those predicted by the Vaill regional equation (2000), are shown in table 1 for comparison. The sites generally are unaffected by regulation and are considered to reflect meteorological and hydrological characteristics representative of the burned and adjacent unburned subbasins affected by the wildfire. Because of the limited period of historical record for each gage, no mixed-population analyses (snowmelt and rainfall peaks) were done.

An ordinary-least-squares regression model to predict 100-year peak discharge, Q_{100}, as a function of drainage area, A, was developed using the streamflow-gaging station data shown in table 1. The resulting equation and regression statistics were:

	R squared	Standard error of estimate	
$Q_{100} = 14.21\ A^{0.823}$	0.995	28 percent	(8)

The regression coefficient (14.21) in the equation includes a bias correction factor to correct for bias introduced in the process of converting the results of log-space regression analysis back to rectangular coordinates (Duan, 1983).

Similar one-parameter models for Q_{100} have been developed by Browning (2001) and by Jarrett and Costa (1988). A plot of the new regression analysis showing the best-fit line defined by the equation is shown in figure 6; all five data points lie within the computed 95-percent confidence intervals (not shown) for the regression. The regression line generally plots lower and parallel to the equation defined by Jarrett and Costa (1988) (not shown) for a larger data set (basins below 8,000 ft elevation) developed for the South Platte River Basin.

The regression model was used as the basis for calibration of the pre-burn, 100-year peak discharge of subbasins simulated using HEC-HMS. The regression model is limited by the small number of streamflow gages available for analysis within the study area and by the relatively short period of record at each gage (which reduces the reliability of the peak-flow statistics).

The HEC-HMS rainfall-runoff model (U.S. Army Corps of Engineers, 2001b) was used to simulate the pre-burn rainfall-runoff processes in burned and adjacent unburned areas of the South Platte River Basin. The HEC-HMS model was composed of 19 selected drainage basins and consisted of subbasins and other single basins. Data for the basins and subbasins are provided in Appendix tables 3–1, 3–2, and 3–14. The name and basin identification number convention for basins and subbasins is explained in Appendix table 3–2.

The objective calibration method, described in the “Rainfall-Runoff Model Calibration and Simulation” section of this report, was used to calculate optimal pre-burn rainfall-runoff parameters. The objective calibration method used an optimization algorithm (Doherty, 1998, 2001), in conjunction with HEC-HMS, to estimate a set of drainage-basin parameters that minimized a predefined objective function. In this study, the objective function was defined as the sum of squared residuals between regional and simulated 100-year peak discharges; the regional peak discharges for pre-burn conditions were computed using equation 8. The objective calibration method resulted in a set of unbiased drainage-basin parameters (RCN, initial abstraction, and lag time) based on a robust, mathematical optimization procedure.

Five larger drainage basins were divided into smaller contributing subbasins that generally corresponded to basin delineations defined by the BAER team (USDA Forest Service, 2002a) in their post-fire analysis of the Hayman area. The SCS curve-number method was used to estimate drainage-basin losses in individual, smaller tributaries. Subbasin hydrographs were routed to the mouths of the larger, composite drainage

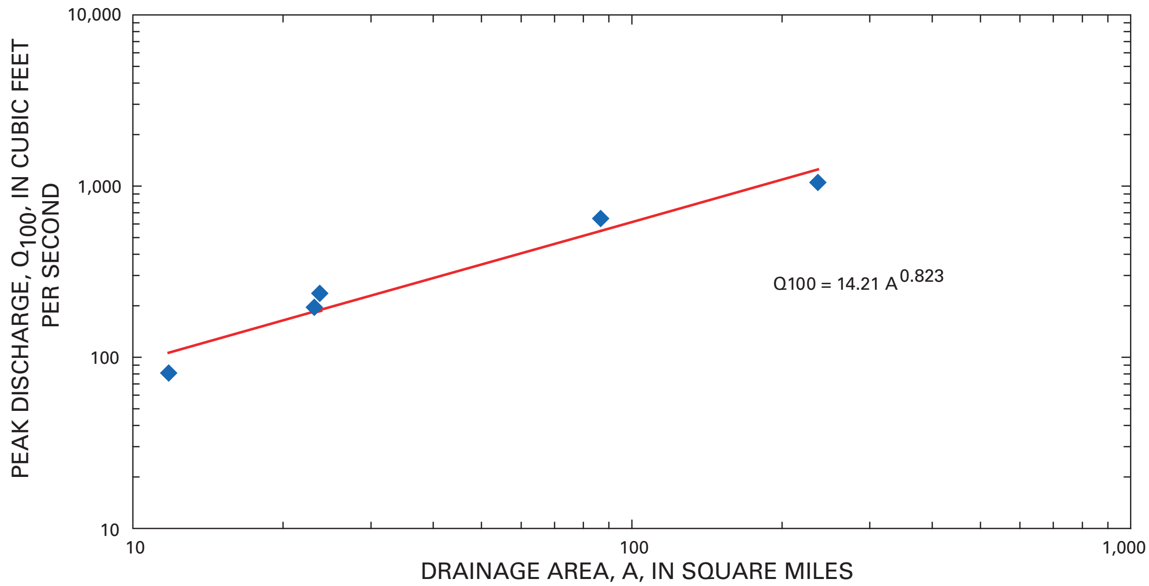

Figure 6. 100-Year flood peaks in relation to drainage area and the best-fit regression line using an ordinary-least-squares regression model.

basins. On the basis of existing reports that describe pre-fire drainage-basin conditions within the study area (Foster Wheeler Environmental Corporation, 1999; USDA Forest Service, 2002a) and assessment of aerial photography, pre-burn RCNs between 55 and 67 were selected for each subbasin (pre-burn RCNs used in this study are somewhat lower than those selected by the BAER team). In addition to subbasin RCN values, the initial abstraction (infiltration) and the percentage of impervious area were entered into the model. The pre-burn abstraction values were selected using default model computations based on pre-burn drainage-basin characteristics and are reflective of the weathered rock soils that dominate the area. Limited field observations from nearby areas appear to corroborate pre-burn abstraction values computed by the model (David Stannard, U.S. Geological Survey, oral commun., 2002). Impervious areas (rock outcrops, roads, and so forth) were mapped by the BAER team and were accounted for in the model by adjusting RCNs for those areas.

Flow routing within the five larger basins (table 2) was performed using the Muskingum method (McCuen, 1989). Because observed hydrograph or field data were not available for calibration of the routing parameters, values of Muskingum K (that defines the time of travel for a flood wave traversing the basin) and X (a weighting factor that describes the backwater storage effects of a channel) were selected within the range of commonly used values for channels in steep, upland drainage basins (or subbasins) (McCuen, 1989; John Liou, Federal Emergency Management Agency, oral commun., 2003):

- Muskingum K = 0.6 hour
- Muskingum X = 0.4, to reflect channels with little over-bank storage

A summary of pre-burn calibration data (RCN, abstraction, lag-time factors) for all principal and minor subbasins is provided in Appendix table 3–14.

Step 2, Modeling of Burned Conditions, South Platte River Tributaries

Adjustments of the calibrated, pre-burn drainage-basin parameters were made to reflect the burned conditions within each subbasin. Existing studies documenting the hydrologic response of burned drainage basins in other areas were used to guide the calibration for post-burn conditions. The BAER team's burned-area emergency stabilization and rehabilitation plan for the Hayman wildfire (USDA Forest Service, 2002a) was used to guide the selection of RCNs for post-burn conditions. Because of the detailed mapping of the post-burn subbasins (including burn severity, rock outcrops, unburned area, and water courses) conducted by the BAER team, and because of extensive USDA Forest Service experience with post-fire hydrology, the post-burn RCNs selected by the BAER team generally were adopted for this study. Exceptions were the use of lowered RCNs for some unburned areas, previously noted in the "Step 1, Modeling of Unburned Conditions, South Platte River Tributaries" section, and a slightly higher RCN for areas of moderate to high burn severity (explained herein).

- Rocky areas = 90
- Unburned forest = 55–60
- Low burn severity = 85
- Moderate and high burn severity = 98 (BAER team used 95)

Table 2. Subbasin characteristics, modeling parameters, and computed 100-year peak discharges for pre-burn, post-burn, and post-burn bulked floods for 19 selected subbasins affected by the Hayman wildfire, objective calibration method.

[mi^2, square miles; %, percent; in, inches; Q_{100}, 100-year discharge; ft^3/s, cubic feet per second; Q_u, pre-burn 100-year discharge; Q_b, post-burn 100-year discharge; Q_{bb}, post-burn bulked 100-year discharge; N/A, not applicable]

Subbasin name and number (downstream order)	Drainage area (mi^2)	Area of low burn (%)	Area of moderate to high burn (%)	Rainfall depth[1] (in)	Curve number*		100-Year peak discharge				Ratio Q_{bb}/Q_u
					Pre-burn	Post-burn (weighted)	Q_{100} Unburned (ft^3/s) Q_u	Q_{100} Burned (ft^3/s) Q_b	Q_{100} Post-burn bulked (ft^3/s) Q_{bb}	Q_{bb} (ft^3/s per mi^2)	
Vermillion Creek (1)	4.93	50.0	27.6	2.4	57	86	50.8	1,060	1,130	230	22.3
Crystal Creek (2)	5.27	46.4	29.0	2.4	57	86	52.8	1,120	1,200	228	22.8
Beaver Creek (3)	3.54	51.5	33.7	2.4	56	89	37.8	994	1,080	304	28.5
Hackett Gulch (4)	6.56	37.2	33.2	2.4	55	86	63.1	1,650	1,790	272	28.3
Tarryall Creek (5)	443	0.96	0.89	2.4	N/A	86	78.1	2,180	2,180	4.93	28.0
Longwater Gulch (6)	2.34	29.3	67.6	2.4	53	94	17.6	1,350	1,580	674	89.7
Corral Creek (7)	4.38	15.7	70.3	2.4	54	94	44.3	2,770	3,260	744	73.5
Northrup Gulch (8)	3.84	37.2	58.2	2.4	56	94	40.7	1,630	1,870	486	45.9
Turkey Creek (9)	28.2	32.4	50.6	2.4	55–60	82–98	224	5,380	6,060	215	27.1
Goose Creek (10)	95.2	5.29	15.1	2.4	57–58	55–97	471	7,100	7,370	77.4	15.6
Cheesman Reservoir											
Schoonover Gulch (11)	1.71	11.7	85.4	2.4	55	96	21.0	1,350	1,640	958	78.0
Sixmile/Wigwam Creek (12)	36.7	13.7	34.2	2.4	54–59	78–96	638	3,760	4,080	111	6.40
Fourmile Creek (13)	8.22	11.7	59.7	2.4	58	90	77.2	1,850	2,130	259	27.5
Horse Creek (14)	212	9.06	12.8	2.4	52–61	58–98	1,340	5,710	5,890	27.8	4.40
Lazy Gulch (15)	1.23	54.2	39.0	2.4	55	90	16.0	650	713	580	44.6
Brush Creek (16)	2.33	29.2	59.3	2.4	56	92	27.6	1,130	1,300	557	47.0
Unnamed drainage (17)	1.16	0.00	0.00	2.4	55	N/A	15.4	N/A	N/A	N/A	
Saloon Gulch (18)	1.26	39.7	46.6	2.4	55	90	16.6	619	691	548	41.6
Gunbarrel/Kelsey Creek (19)	10.2	8.00	2.00	2.4	55–56	55–62	103	276	277	27.2	2.69

*Runoff-curve numbers for the five larger subbasins are shown as a range of values determined for the subbasins within each drainage basin. Model data for the 19 selected subbasins, and other contributing subbasins in the Hayman burned area are in Appendix tables 3–1, 3–2, and 3–14.

[1]National Oceanic and Atmospheric Administration Atlas 2, Volume III—Colorado (Miller and others, 1973).

Removal of surface vegetation by wildfire can be expected to decrease the runoff lag time in an affected drainage basin (URS Corporation, 2000; U.S. Army Corps of Engineers, 2000). Adjustment of post-burn lag times was made according to the SCS lag-time equation (eq. 1), which is a function of the post-burn RCN. Post-burn lag times range from 24 to 93 percent of pre-burn lag times in South Platte River subbasins, depending on the amount of burned area in the subbasin. A summary of post-burn calibration data (RCNs, abstractions, lag-time factors) for all principal and minor subbasins is in Appendix table 3–14. Table 2 shows the 19 selected subbasins for which modeling was conducted and the results of the pre- and post-burn runoff calibrations. A rainfall depth of 2.4 inches (100-year, 6-hour storm) was applied uniformly over each subbasin, with no areal distribution of the storm (Miller and others, 1973).

Sediment Bulking of Discharge for Hayman Wildfire-Area Tributaries

Most of the Hayman wildfire area "is comprised of shallow, weathered soils from the Pikes Peak batholith" (USDA Forest Service, 2002a). This weathered granite is easily eroded and, although not expected to result in debris flows, can be expected to produce large sediment loads during flooding. To account for the potential sediment bulking of floodflows in burned subbasins, computed peak discharges were increased according to the assumption that sediment concentrations by volume (C_v) could reach the maximum water-flood limit of 20 percent (Costa, 1988). O'Brien and Fullerton (1989) computed the bulking factor (BF) applied to water discharge according to the equation:

$$BF = 1/(1 - C_v) \qquad (9)$$

For a C_v of 20 percent, the corresponding BF is 1.25. The BF was applied to peak water discharges computed by the HEC-HMS model for areas of moderate to high burn severity and was weighted according to relative burned area within each of the modeled subbasins. Studies indicate that sediment concentration in natural streams varies over the water-discharge hydrograph and, for most streams, tends to reach a maximum in advance of the water-discharge peak (Guy, 1970). Application of the BF to the peak discharge therefore may represent a conservative adjustment to the modeling results.

The reasonableness of the 1.25 BF was evaluated using the results of a study of the Buffalo Creek wildfire in Colorado (Moody and Martin, 2001a). Moody and Martin derived a regression equation from discharge, suspended-sediment, and bedload-sediment measurements at Spring Creek, a drainage basin severely burned by the 1996 Buffalo Creek wildfire. Like the Hayman burned area, weathered Pikes Peak batholith materials are exposed throughout the Spring Creek and Buffalo Creek drainage basins. The 1996 wildfire burned approximately 79 percent of the Spring Creek drainage basin, and 63 percent of the entire burned area (both drainage basins) was classified as severely burned. Data were collected at the mouth of Spring Creek from July 1997, one year after the Buffalo Creek wildfire, through the summer of 2000. Several floods were sampled; however, the initial large post-fire floods of 1996 and before July 1997 were not sampled.

Moody and Martin's (2001a) relation for total sediment transport (suspended and bedload) is:

$$Q_s = 23\ Q^{1.3} \qquad R^2 = 0.96 \qquad (10)$$

where

Q_s is sediment discharge, in kilograms per second;

Q is water discharge, in cubic meters per second;

and

R^2 is the coefficient of determination.

Post-fire, unbulked tributary peak discharges (Q_b in table 2) were converted to cubic meters per second and used in equation 10. The predicted sediment discharges were converted from kilograms per second to cubic feet per second by using a units conversion and an assumed sediment specific weight of 165.36 pounds per cubic foot. The estimated sediment volume was added to the post-fire tributary discharge to determine the post-fire bulked tributary discharge. Bulked Hayman tributary discharges estimated using Moody and Martin's (2001a) Spring Creek regression equation (eq. 10) were smaller than bulked discharges estimated with the 1.25 bulking factor (eq. 9) for most tributaries. Estimates from the two methods diverged as the percentage of the drainage-basin area moderately or severely burned increased (fig. 7). For Hayman subbasins with 0 to about 20 percent of the drainage basin moderately or severely burned, bulked discharge estimates using equation 10 were within about ±5 percent of estimates from the 1.25 bulking factor method. However, for subbasins with greater than 50 percent area moderately or severely burned, the difference was greater than 10 percent, with the two equations diverging steadily as the percentage of moderately and severely burned area increased.

One possible explanation for the difference in bulked discharges from the two methods could be that the 1.25 BF was applied only to the actual burned portion of each tributary subbasin, whereas equation 10 was applied to the total tributary drainage-basin area. Moody and Martin's (2001a) equation was derived from measurements at the mouth of the basin that integrated runoff and sediment from burned and unburned parts of the Spring Creek drainage basin and was applied in the same way to the Hayman subbasins.

Another explanation for the difference in bulked discharges could be that Moody and Martin's (2001a) transport equation did not fully reflect the high sediment-transport rates of the first, unsampled floods in 1996 and early 1997. Vegetation cover and soil conditions in the Spring Creek drainage basin were rapidly evolving in the first 5 years after the

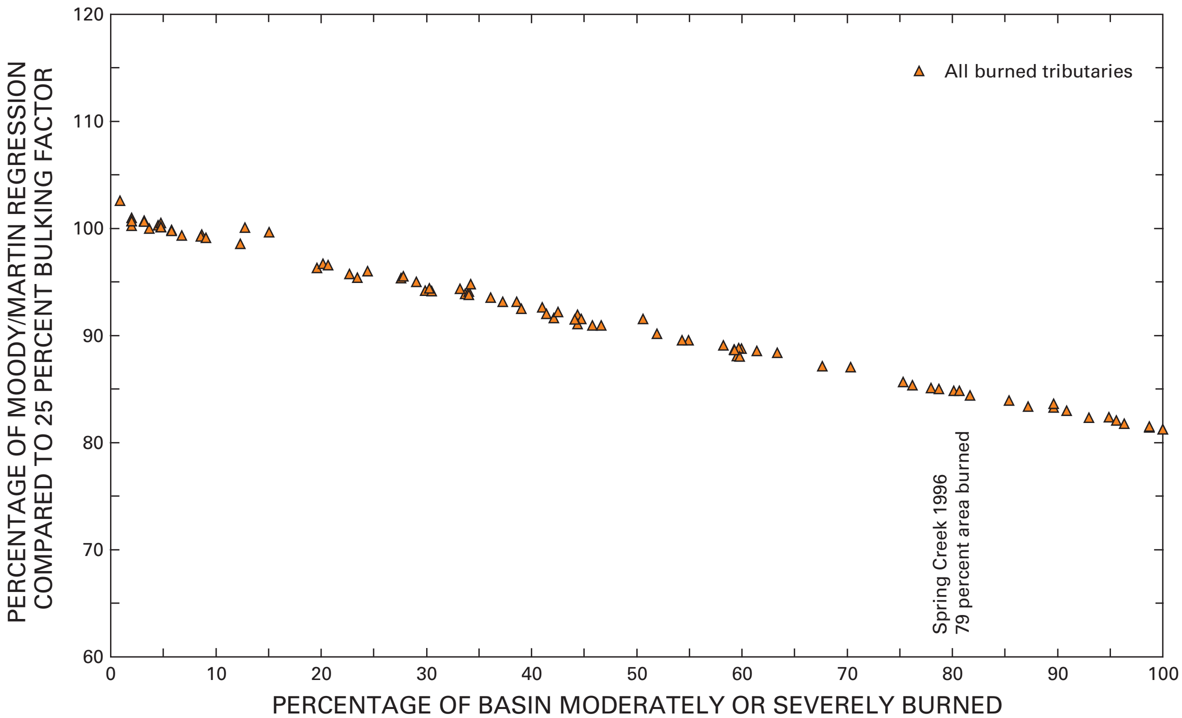

Figure 7. Comparison of post-fire runoff sediment-bulking methods, as a percentage of results from Moody and Martin's (2001a) Spring Creek regression on total drainage-basin area to a 25-percent bulking factor applied to moderately and severely burned areas compared to percentage of drainage basin moderately or severely burned.

wildfire, and hillslope sediment production was declining yearly. Moody and Martin predicted that over time, hillslope sediment yield and fluvial transport of sediment would return to pre-fire rates (Moody and Martin, 2001a).

Yet another explanation could be that the 1.25 BF is insensitive to in-channel storage in valley bottoms and tends to overestimate the efficiency of fluvial transport from some drainage basins. An analysis of in-channel storage in tributary valley bottoms was beyond the scope of this report. The bulked discharges estimated using equation 10 can be considered to be conservative, whereas the discharges estimated using the 1.25 BF can be considered to be maximum values.

Estimated Peak Discharges, South Platte River Tributaries

Post-fire, unbulked tributary peak discharges were increased to reflect the anticipated increased sediment loads by using a 1.25 bulking factor applied to areas of moderate-to-high burn severity. Simulated pre-burn, post-burn, and bulked 100-year discharges for each of the 19 selected subbasins are shown in table 2. Post-burn 100-year peak discharges for the principal subbasins (routed to the point of confluence with the South Platte River) are expected to increase 3 to 90 times over pre-burn peaks. Among all modeled subbasins with substantial (greater than 50 percent) moderate to high burn-severity areas, post-burn bulked peak discharges are expected to be 28 to 91 times greater than pre-burn peaks. For those drainage basins with substantial burned area, average predicted unit-area peak discharges for pre-burn conditions is 12.3 $ft^3/s/mi^2$; average predicted bulked unit-area peak discharge for post-burn conditions is 830 $ft^3/s/mi^2$.

Predicted increases in post-burn peak discharge are in general agreement with the BAER team's hydrologic assessment of the Hayman wildfire (USDA Forest Service, 2002a) and with hydrologic studies of other burned drainage basins (Rowe and others, 1954; Moody and Martin, 2001b; URS Corporation, 2000). The BAER team's assessment included 92 subbasins (all tributary to the 19 selected subbasins modeled in this study) directly affected by the Hayman wildfire. The BAER team analyzed the 25-year, 1-hour storm (1 inch/hour) and found that the average ratio of post- to pre-burn unit-area peak discharge for affected subbasins was about 3; the highest ratios, as much as 7.5, were measured in very small, severely burned subbasins.

Rowe and others (1954) found that the ratio of unit-area peak discharge before and after wildfires in southern California increased as much as 40 times, depending on the recurrence interval of the rainstorm. Ratios tend to be highest in the year following the wildfire, then decrease in subsequent years as vegetation is reestablished and the drainage basin begins to recover (Moody and Martin, 2001a; URS Corporation, 2000).

Moody and Martin (2001b) studied post-fire peak discharges in three burned drainage basins of the Western United States and developed relations for unit-area peak discharge (Q_{bb}/drainage area) as a function of the maximum 30-minute rainfall intensity. Equations developed by Moody and Martin for the Spring Creek drainage basin of Colorado (burned by the Buffalo Creek wildfire of 1996) and the Rendija Canyon drainage basin of New Mexico (burned by the Cerro Grande wildfire of 2000) were used to predict a range of peak discharges that might occur in burned subbasins of the Hayman burned area. The 100-year unit-area peak discharges for the Hayman area simulated using HEC-HMS lie within the range of predicted unit-area peak discharges for the Spring Creek relation (considered to be a lower estimate limit) and the Rendija Canyon relation (considered to be an upper estimate limit). Based on comparison with the results from other burned drainage-basin studies (Moody and Martin, 2001b), the modeling results for the Hayman wildfire are considered reasonable.

Estimated Peak Discharges, Selected Reaches of the South Platte River

Estimated peak discharges on the South Platte River for use in short-term hazard mapping were computed using the manual calibration method as presented to FEMA in 2003 by J.G. Elliott and others (U.S. Geological Survey, written commun.) and described in Appendix 2. Computed peak discharges along the South Platte River, and associated short-term hazard maps, were not revised to reflect model recalibration using the objective calibration method because a comparison showed that model differences (cumulative peak discharges at the outlet of Cheesman Reservoir and at the downstream end of the HEC-HMS model reach) were less than 10 to 17 percent for the two calibration methods. These differences were considered minor with regard to the larger uncertainty associated with modeling post-burn flood peaks, and these differences would not produce substantial differences in mapped areas at the scale of the hazards maps.

Results of the analyses are summarized in a series of hazard maps (fig. 5). Cross sections showing the 100-year floodwater-surface elevation along the South Platte River are shown in figures 8–11, and the extent of the 100-year flood is shown in map view in figures 12–14. The locations of cross sections used in the hazard analysis are presented in Appendix table 4–1.

South Platte River Hydrology and Peak Flow Analysis for Long-Term Recovery—Phase 3

Peak flows were computed to evaluate hydrologic responses at a stage in the post-burn recovery process referred to as the "long-term recovery" period. The long-term recovery period was estimated using methods described in the "Method for Determination of Drainage Basin Recovery—Phase 3" section. In the South Platte River Basin of the Hayman burned area, the long-term recovery period was estimated to be 6 years. Analyses were designed to characterize runoff produced by rainstorms in and near the burned area and to reflect drainage-basin conditions that are expected to exist at a point of recovery approximately 6 years after the wildfire. Values for the HEC-HMS input parameters RCN, initial abstraction, and lag time in individual subbasins were calculated for the long-term recovery by decreasing the RCN in accordance to the long-term recovery decay function and recomputing the initial abstraction and lag time. HEC-HMS was then used to obtain estimates of long-term recovery peak flows. Discharge results from these analyses then were used as input for hydraulic analysis.

Long-term hydrologic analyses were conducted to evaluate the effects of the 10-, 50-, 100-, and 500-year 6-hour rainfall on peak flows in the burned and adjacent delineated unburned South Platte River subbasins after the recovery period. The post-burn 10-, 50-, 100-, and 500-year peak discharges along the main stem of the South Platte River were computed for the Deckers-to-Trumbull detailed study reach. In-stream flow routing, to account for in-channel storage and peak attenuation at successive downstream cross sections, was performed using the routing routines in the HEC-HMS computer model. The Muskingum-Cunge routing routine, which incorporates cross-section and hydraulic properties of the surveyed cross sections, was used to route flows in reaches of the main-stem South Platte River. Routed peaks showed little attenuation. Sensitivity testing indicated that hydrograph attenuation was affected mainly by channel slope; the relatively steep slopes (measured as water-surface slope during the cross-section surveys) through the study reach preclude substantial attenuation. The Modified Puls reservoir routing routine in HEC-HMS was used to route the computed flood hydrograph through Cheesman Reservoir and over the spillway to the downstream reach. Water-surface profile elevations in the detailed study reach were plotted (fig. 16), and floodway computations were made using encroachment routines in the HEC-RAS program for the 100-year profile.

The approach to the long-term detailed hydrologic study included the following steps:

1. Inflow conditions upstream from the burned area were assumed to be the 10-year flood for the South Platte River at the upstream fire perimeter, the 10-year flood for Tarryall Creek at the upstream fire perimeter, and maximum outlet release (1,400 ft^3/s) from Cheesman Reservoir for the South Platte River below Cheesman Dam.

2. Initial pre-flood storage in Cheesman Reservoir was assumed to be 54,039 acre-ft.

3. Drainage-basin parameters for the previously described long-term conditions in the burned subbasins tributary to the South Platte River were used in the HEC-HMS rainfall-runoff model (Appendix table 3–7).

4. Peak flow was simulated for the 10-, 50-, 100-, and 500-year, 6-hour storms by using long-term drainage-basin parameters in burned subbasins tributary to the South Platte River.

5. Rainfall amounts and distributions were determined from the NOAA Atlas 2 guidance (Miller and others, 1973). The 500-year 6-hour storm total was estimated by logarithmic extension of NOAA Atlas 2 data (Appendix table 3–8).

6. Peak flows for post-fire recovery were not bulked due to the probable lack of large sediment loads in the post-fire recovery period.

7. Peak flows for subbasins tributary to the South Platte River were computed (with routing of the runoff hydrograph through the primary subbasins) (Appendix table 3–7).

8. Peak flows for selected reaches of the South Platte River (within and downstream from the burned area) were computed using a hydrograph routing algorithm.

Peak-discharge water-surface elevations from the rainfall-runoff model can be used to create FEMA regulatory maps. However, because a larger flood study is being conducted and a digital flood-insurance rate map (DFIRM) is being created for Douglas County, these results will need to be integrated into the larger scope of the South Platte River. Therefore, no flood-insurance rate map (FIRM) was produced for this report. The flood elevations computed for this study do show overtopping of all three bridges in the detailed reach. The bridge at Trumbull (fig. 16*A*) was overtopped by the 10-yr recurrence floodflow. The next bridge upstream between Deckers and Trumbull (fig. 16*C*) was overtopped by the 50-yr floodflow. The bridge at Deckers (fig. 16*C*) also was overtopped by the 50-yr floodflow. Comparison of the 100-yr flood elevations (Appendix table 3–13) from the 1978 Flood Insurance Study (FIS) (Federal Emergency Management Agency, 1978) to the results in this report for the same cross-section locations indicate that differences ranged from 4 ft higher to 3 ft lower in this study (2004). The median difference was zero.

South Platte River “Detailed” Hydraulic Analysis

Detailed flood hydraulics (known to FEMA as a “Detailed Study”) were computed for the recovered (Phase 3) hydrologic conditions using step-backwater routines in HEC-RAS (U.S. Army Corps of Engineers, 2001a) for a stream reach from a point 5,040 ft upstream from the county road bridge over the South Platte River at Deckers to a point 2,455 ft downstream from the county road bridge over the South Platte River at Trumbull (fig. 15); in this report, this reach is referred to as “the detailed study reach.” Floodway elevations, defined by FEMA as “the channel of a river or other watercourse and the adjacent land areas that must be reserved in order to discharge the base flood without cumulatively increasing the water-surface elevation by more than a designated height” (1 ft in the case of the Deckers-to-Trumbull reach of the South Platte), also were computed for this reach.

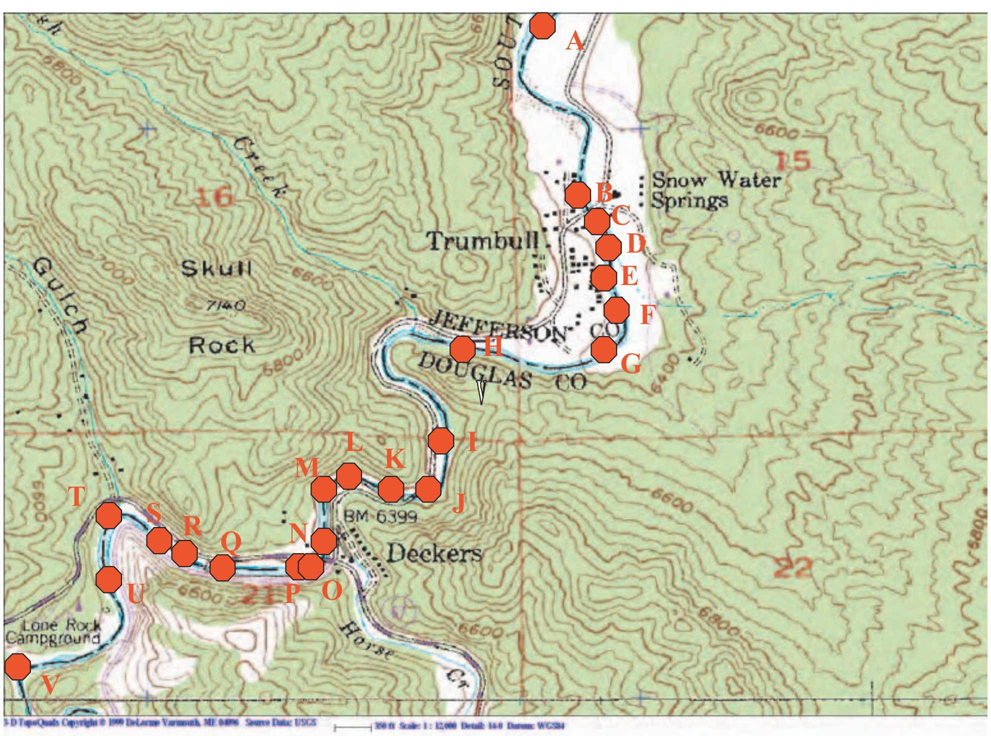

Figure 15. Cross-section location map for South Platte River detailed hydraulic study.

The approach to the hydraulic analyses included the following steps and data:

1. Peak discharges (long-term recovery) based on the 10-, 50-, 100-, and 500-year recurrence intervals (Appendix table 3–9) 6-hour design storm (objective calibration method) for the main-stem South Platte River were used in the detailed study reach.

2. Stream cross sections were delineated using USGS ground surveys and cross-section data from the 1978 detailed flood insurance study (FIS) of Douglas County (Federal Emergency Management Agency, 1978) that overlapped part of this detailed study reach (Appendix table 4–2).

3. Tributary inflows available from HEC-HMS modeling within the detailed study reach were added at the appropriate cross sections in the model to determine the main-stem South Platte peak flows (Appendix table 3–9).

4. Manning's roughness coefficients and distances between cross sections were determined during ground surveys, global positioning system (GPS) surveys, and review of the 1978 FIS data and flood-insurance rate map (FIRM) (Appendix table 3–10).

5. Water-surface elevations and flow characteristics were determined using the HEC-RAS hydraulic model assuming subcritical flow regime (Appendix table 3–11).

6. Water-surface profile elevations in the detailed study reach were plotted at NAVD 88 datum (fig. 16).

7. Floodway computations were made using encroachment routines in the HEC-RAS hydraulic model for the 100-year profile (Appendix table 3–12). For this analysis the flood plain was encroached such that maximum allowable water-surface increase was equal to or less than 1 ft.

Post-Fire Hydrologic Hazards for the Coal Seam Wildfire

The Coal Seam wildfire affected many small subbasins as well as the large subbasin of Mitchell Creek, a perennial tributary of the Colorado River at Glenwood Springs, Colorado (fig. 1). The Coal Seam fire perimeter and Mitchell Creek drainage basin are shown on an oversized map (fig. 17) that accompanies this report. Water flooding and debris flows are potential hazards in the Coal Seam area. Post-fire hydrologic analyses were conducted to evaluate the effects of the 100-year peak flow on the burned and adjacent unburned areas of the Mitchell Creek subbasin. Water-flood and debris-flow analyses also were conducted for subbasins within the Mitchell Creek subbasin. The Mitchell Creek debris-flow analysis is presented in a subsequent section of this report, "Analysis of Debris-Flow-Producing Drainage Basins, Coal Seam Wildfire." For the purpose of flood-hazard mitigation in the present study, the results of a FLO-2D analysis, which includes a combined analysis of water flooding and debris flows in the Mitchell Creek subbasin, have been used to construct the Mitchell Creek hazard map (figs. 18 and 19). The following discussion pertains to water-flood conditions in subbasins and main-stem reaches of Mitchell Creek.

Hydrologic Analysis of Mitchell Creek—Phase 2

Water-flood analyses were designed to characterize increased runoff produced by rainstorms in and near the wildfire area and reflect drainage-basin conditions that are expected to exist during the next several years (before substantial regrowth of vegetation in the burned areas). The results of these analyses were used to delineate a limited-detail hazard-mitigation map for post-fire flooding of Mitchell Creek. The map characterizes short-term (next 1–4 years) runoff conditions and should not be used for regulatory purposes.

Additional hydrologic analyses reflecting more stable drainage-basin conditions (after a recovery period of 5 years) also were performed and are presented in a subsequent section "Mitchell Creek Hydrology and Peak Flow Modeling for Long-Term Recovery—Phase 3." An ongoing study is evaluating the flood hydraulics under long-term recovered conditions of Mitchell Creek in greater detail (known to FEMA as a "Detailed Study"), but findings from the Mitchell Creek long-term study are not included in this report. Results of the "detailed" hydraulic analyses will be used by FEMA to delineate a revised flood-plain map for regulatory purposes. The future map will include analyses of the 10-, 50-, 100-, and 500-year floods.

Assumptions for the short-term, Phase 2 hydrologic hazard-mitigation analysis of Mitchell Creek are as follows:

1. Calibration of a rainfall-runoff model for pre-fire (unburned) conditions in drainage basins tributary to Mitchell Creek. Runoff generated by the 100-year, 1-hour rainstorm (1.64 inches) was calibrated to the existing 100-year discharge for the study area. The existing 100-year discharges are documented in a FEMA Flood Insurance Study (FIS) for Mitchell Creek (Simons, Li & Associates, Inc., 1983).

2. Rainfall runoff was simulated for the 100-year, 1-hour storm for post-fire conditions in burned drainage basins tributary to Mitchell Creek.

3. Peak discharges for selected reaches of Mitchell Creek were computed (with hydrologic routing of the runoff hydrograph).

4. Peak discharges for burned subbasins were increased using a bulking factor to reflect increased sediment loads.

5. Debris-flow hazards were analyzed separately and are covered in the "Analysis of Debris-Flow-Producing Drainage Basins, Coal Seam Wildfire—Phase 2" section of this report.

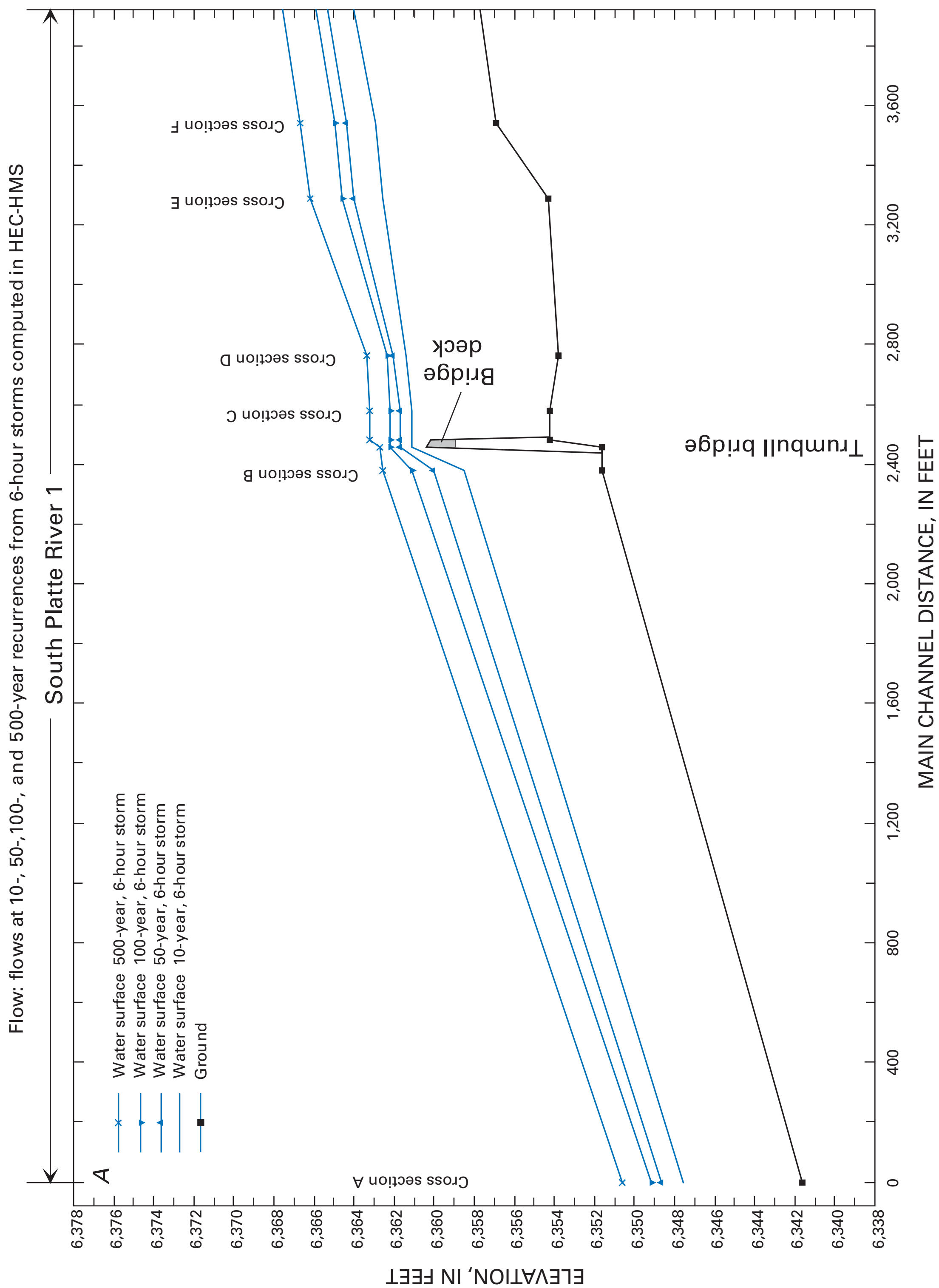

Figure 16. Flood-profile plots of the South Platte River, Colorado, detailed study reach.

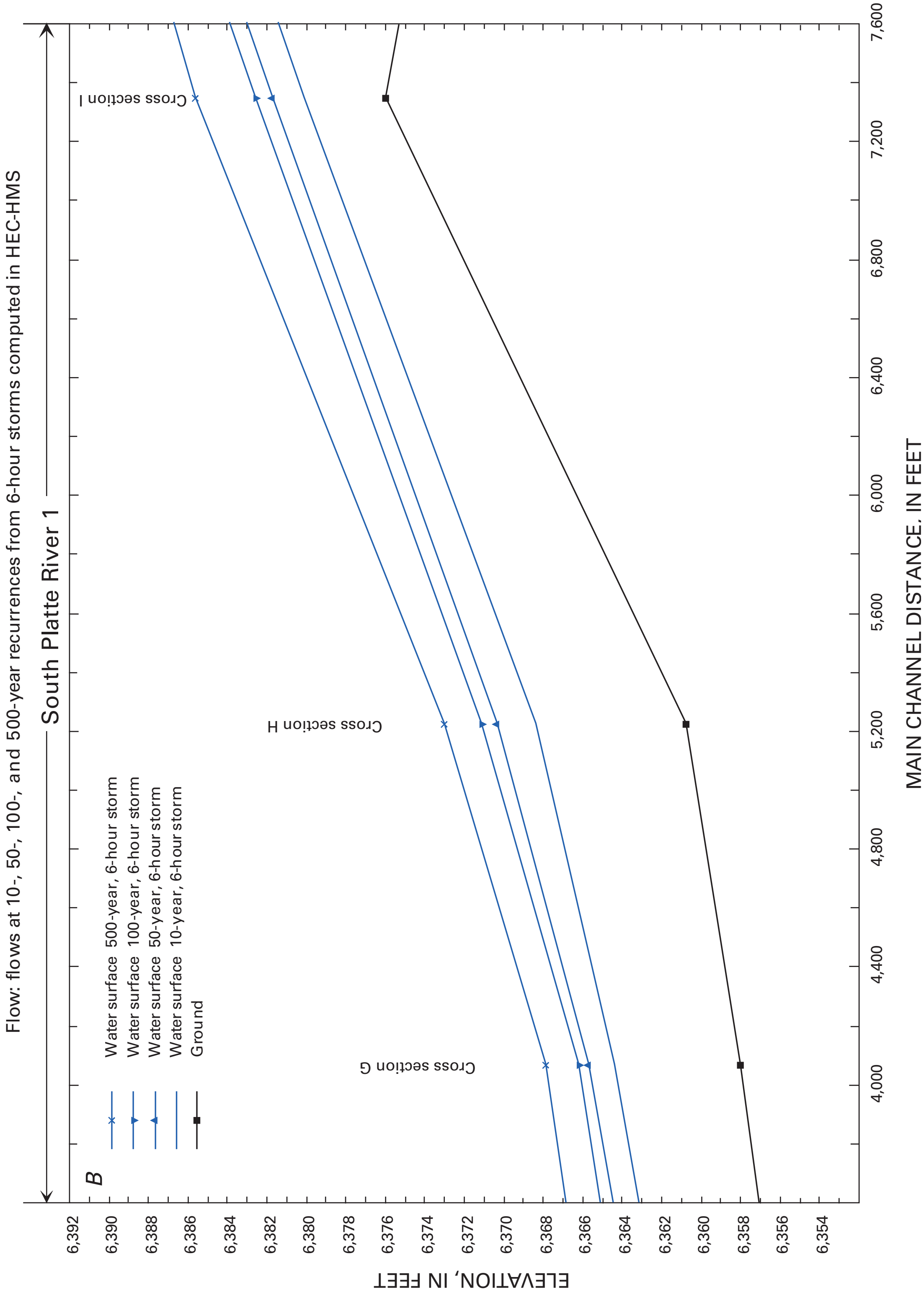

Figure 16. Flood-profile plots of the South Platte River, Colorado, detailed study reach.—Continued

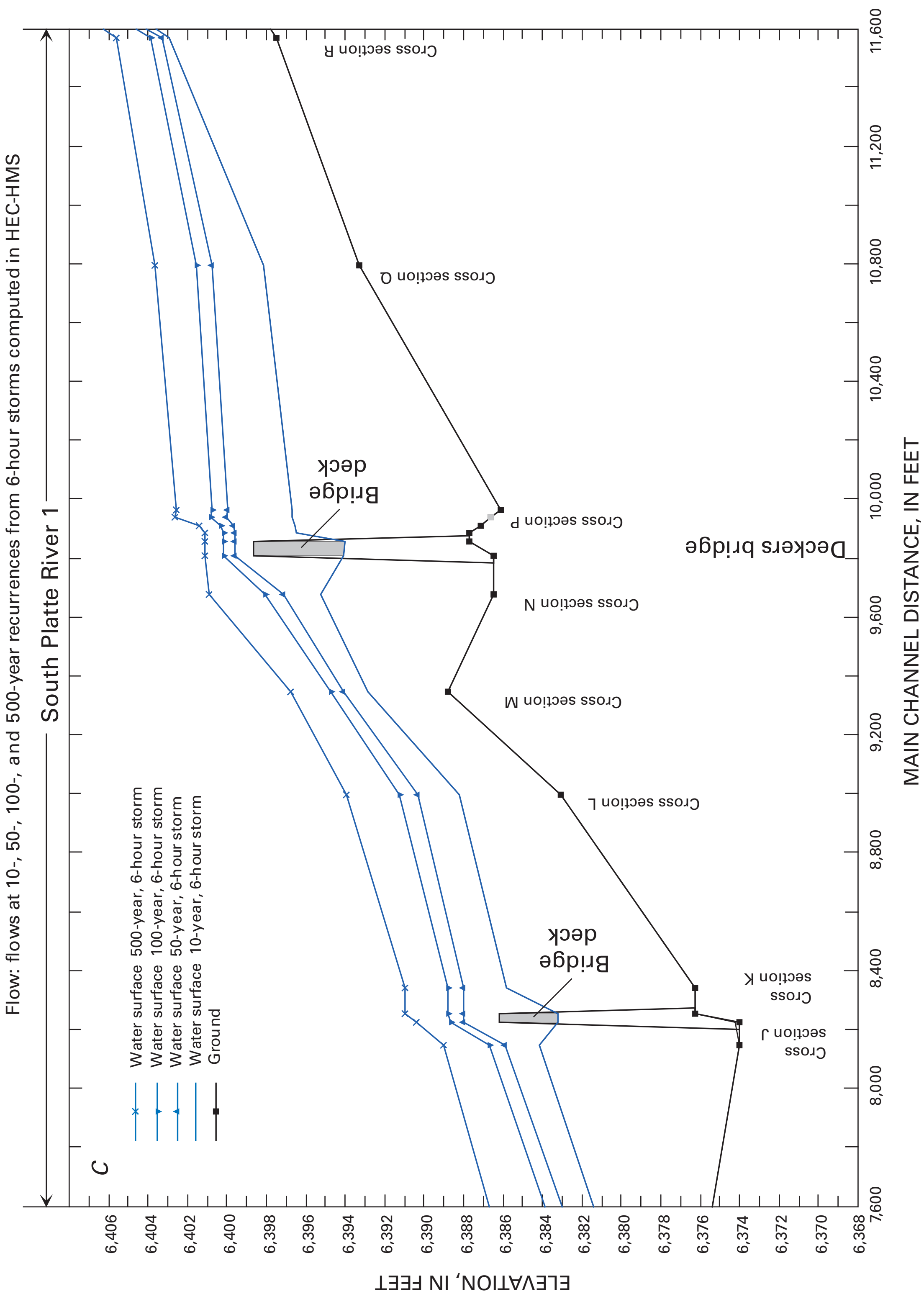

Figure 16. Flood-profile plots of the South Platte River, Colorado, detailed study reach.—Continued

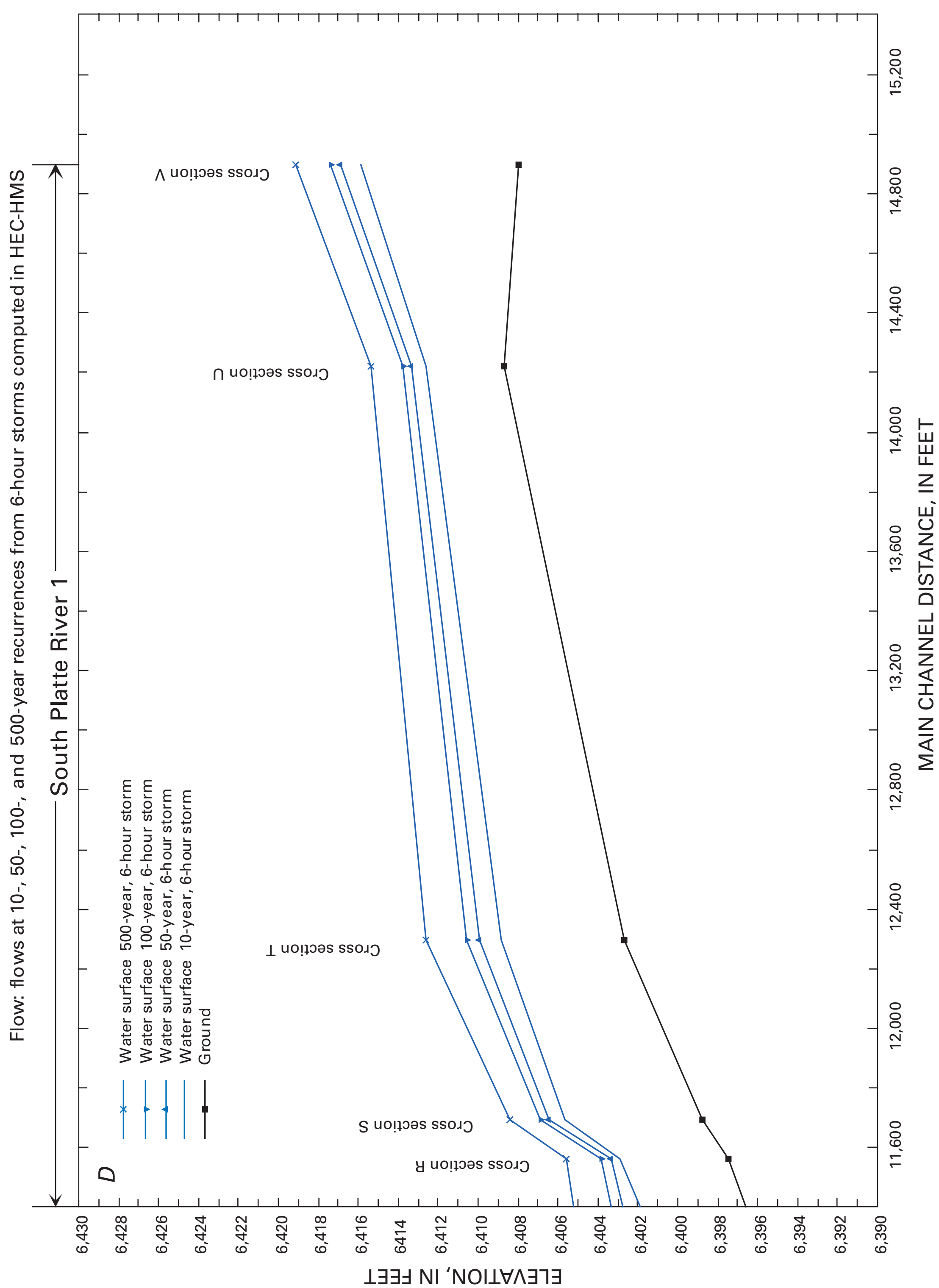

Figure 16. Flood-profile plots of the South Platte River, Colorado, detailed study reach.—Continued

Mitchell Creek has a contributing drainage area of 11.2 mi^2 at Donegan Bridge in Glenwood Springs (fig. 17). A FEMA flood-insurance study (FIS) was completed in 1983 by Simons, Li and Associates, Inc. The accepted 100-year peak discharge for the drainage basin is 360 ft^3/s at a main-stem point upstream from Donegan Bridge (drainage area is 5.9 mi^2). The 1983 hydrologic analysis was based on a detailed regional analysis of streamflow data recorded at nine streamflow-gaging stations. Flood-frequency statistics (log-Pearson III distribution) for Mitchell Creek were based on a regional analysis of Crystal River streamflow-gage data conducted by the U.S. Army Corps of Engineers (1979).

A drainage-area adjustment of this peak discharge was made during the present study to reflect hydrologic conditions in Mitchell Creek at Donegan Bridge. The area-adjusted peak discharge was computed using an equation relating peak discharge for gaged (simulated discharge using HEC-HMS) sites to ungaged sites as a function of relative drainage area (Vaill, 2000). The following equation was used:

$$Q_{100(u)} = Q_{100(g)}\,(A_u/A_g)^X \qquad (11)$$

where

- $Q_{100(u)}$ is the 100-year peak discharge, in cubic feet per second, at the ungaged (nonmodeled) site;
- $Q_{100(g)}$ is the 100-year peak discharge, in cubic feet per second, at the gaged (modeled) site;
- A_u is the drainage area, in square miles, at the ungaged (nonmodeled) site;
- A_g is the drainage area, in square miles, at the gaged (modeled) site;

and

- X is the average exponent for drainage area in the flood region of interest, derived from regression analysis of historical streamflow data.

The computed 100-year peak discharge for Mitchell Creek at Donegan Bridge was 542 ft^3/s.

Mitchell Creek Tributary Rainfall-Runoff Modeling

Rainfall-runoff modeling was used to develop post-fire hydrographs for each of the principal subbasins of Mitchell Creek. Fifteen subbasins (fig. 17, Appendix tables 5–1, 5–2) were delineated using a 10-m DEM. The U.S. Army Corps of Engineers HEC-HMS computer model was used for the analysis (U.S. Army Corps of Engineers, 2001b). The 100-year, 1-hour storm was selected for analysis to reflect flood hazards resulting from spring and summer thunderstorms unique to the study area. Rainfall-runoff modeling was conducted in two steps.

Step 1, Modeling of Unburned Conditions, Mitchell Creek Tributaries

The runoff hydrograph for the 100-year peak discharge was developed for natural, unburned conditions of each subbasin. The accepted 100-year peak discharge of 360 ft^3/s (drainage area of 5.9 mi^2) and the extended 100-year peak discharge of 542 ft^3/s (drainage area of 11.2 mi^2) were used as target discharges for model calibration.

The 100-year, 1-hour storm, as determined from the NOAA Atlas 2 Volume III—Colorado (Miller and others, 1973), is 1.64 inches for most areas of the Mitchell Creek subbasin. The USDA Forest Service BAER team (USDA Forest Service, 2002b) selected a larger rainfall depth (1.85 inches) for analysis in their post-fire study. The larger value reflects rainfall conditions in the most upstream areas of the headwater tributaries and is considered a conservative rainfall depth for the study area.

The U.S. Army Corps of Engineers (1998) used the 1.64-inch rainfall depth for rainfall-runoff modeling in the Glenwood Springs area; a 1-hour storm distribution also was developed from locally measured rainfall data. This temporal distribution was used in the present study because it was derived from local measurements.

The SCS lag-time equation (eq. 2) (Soil Conservation Service, 1985) developed for drainage basins smaller than about 3.25 mi^2 was used to compute the lag time. Drainage-basin areas in the Mitchell Creek subbasin ranged from 0.010 to 4.418 mi^2 (table 3). The SCS method, developed for such small drainage basins, required minimal parameter calibration in simulating the pre-burn, 100-year peak discharges; other methods required additional parameter adjustments for calibration.

The HEC-HMS drainage basin model (U.S. Army Corps of Engineers, 2001b) was used to simulate the pre-burn rainfall-runoff processes in Coal Seam burned area tributaries for (1) unsteady, one- and two-dimensional water flooding in Mitchell Creek and (2) unsteady, two-dimensional debris flows in smaller tributaries affected by the wildfire. An objective calibration method, described in the "Rainfall-Runoff Model Calibration and Simulation" section of this report, was used to calculate optimal pre-burn rainfall-runoff parameters.

Target 100-year peak discharges for each Mitchell Creek subbasin were computed using three published regional equations (Vaill, 2000; Browning, 2001; Kircher and others, 1985). Resulting parameter sets (RCN, initial abstraction, and lag time) then were analyzed using the objective calibration method and HEC-HMS to compute the routed peak discharge at the mouth of Mitchell Creek. Comparison tests showed that the Vaill equation produced target subbasin discharges and resultant RCNs that yielded the best estimate of the accepted 100-year discharge for the main stem of Mitchell Creek. The Vaill equation produced peak discharges that agreed closely with peak discharges from the existing flood insurance study (FIS) (Simons, Li and Associates, Inc., 1983):

- Accepted 100-year peak discharge (5.9 mi^2) = 360 ft^3/s
- Simulated 100-year peak discharge (Vaill, 2000) = 366 ft^3/s (1.67 percent difference)
- Accepted 100-year peak discharge (11.2 mi^2) = 542 ft^3/s
- Simulated 100-year peak discharge (Vaill, 2000) = 587 ft^3/s (8.30 percent difference)

Flow routing within the Mitchell Creek subbasin was performed using the Muskingum method. Values of Muskingum K (defines the time of travel for a flood wave traversing the basin) and X (a weighting factor that describes the backwater storage effects of a channel) were selected within the range of commonly used values for channels in steep, upland drainage basins (McCuen, 1989; John Liou, Federal Emergency Management Agency, oral commun., 2002):

- Muskingum K = 0.6 hour
- Muskingum X = 0.4, to reflect channels in the upper drainage basin with little overbank storage
- Muskingum X = 0.2, to reflect channels in the middle and lower drainage basin with more overbank storage

A summary of pre-burn calibration data (RCN, abstraction, lag-time factors) for all principal and minor subbasins in the Mitchell Creek drainage subbasin is provided in Appendix table 5–1.

Step 2, Modeling of Burned Conditions, Mitchell Creek Tributaries

About 25 percent of the Mitchell Creek drainage basin was burned by the 2002 Coal Seam wildfire. Adjustments to the pre-burn modeling parameters were made to reflect the burned condition within each subbasin. Existing studies documenting the hydrologic response of burned subbasins in other areas were used to guide the calibration for post-burn conditions. The BAER team "Coal Seam Fire Hydrology Report" (USDA Forest Service, 2002b) was used to guide the selection of RCNs for post-burn conditions. Key RCN values used for the present analysis are:

- Unburned drainage basin = 67 to 80
- Low burn severity = 85
- Moderate and high burn severity = 98 (BAER team used RCN = 95)

Where affected drainage basins and subbasins included burned and unburned areas, post-burn RCNs were computed as described in the previous section "Step 2, Modeling of Burned Conditions, South Platte River Tributaries." Post-burn lag times range from 40 to 87 percent of pre-burn lag times, depending on the amount of burned area in the subbasin. A summary of post-burn calibration data (RCNs, abstractions, lag-time factors) for all Mitchell Creek subbasins is

Table 3. Subbasin characteristics, modeling parameters, and computed peak discharge for pre- and post-burn subbasin conditions, Mitchell Creek.

[mi^2, square miles; %, percent; Q_{100}, 100-year discharge; ft^3/s, cubic feet per second]

Subbasin name and number	Drainage area (mi^2)	Area of low burn (%)	Area of moderate-high burn (%)	Runoff-curve number		Q_{100} (ft^3/s)	
				Pre-burn	Post-burn	Pre-burn Q_u	Post-burn Q_b
Storm King 1 (23)	0.201	6.7	74.2	72	95	38.4	415
Storm King 2 (24)	0.055	57.8	35.1	74	91	17.1	107
Mitchell E1 (25)	0.290	42.4	40.7	72	91	48.2	369
Mitchell E2 (26)	0.013	27.7	70.0	79	95	7.84	33.8
Mitchell E3 (27)	0.051	3.0	97.0	80	98	24.7	132
Mitchell E4 (28)	0.045	6.8	89.8	78	97	22.5	130
Mitchell W4–S (29)	0.010	8.6	91.4	79	97	7.80	34.7
Mitchell W3 (30)	0.116	10.5	79.5	74	96	36.8	323
Mitchell W2 (31)	0.133	7.8	76.6	73	95	37.8	353
Mitchell W1 (32)	0.147	24.8	37.5	74	89	40.4	223
Mitchell W4–N (33)	0.031	2.6	89.0	78	97	17.2	95.0
Upper Mitchell West (36)	2.372	11.8	4.1	70	75	175	362
Upper Mitchell East (37)	2.747	11.9	7.7	70	77	192	489
Fish hatchery (38)	0.575	30.3	55.2	67	93	49.2	918
Donegan Bridge (39)	4.418	4.4	5.7	69	74	228	472

in Appendix table 5–2. Table 3 lists the 15 Mitchell Creek subbasins that were modeled and the results of the pre- and post-burn runoff calibrations. A rainfall depth of 1.64 inches (100-year, 1-hour storm) was applied uniformly over each subbasin, with no areal distribution of the storm (Miller and others, 1973).

Sediment Bulking and Peak Flood Discharge for Mitchell Creek

Computed Mitchell Creek peak discharges were increased to account for potential sediment bulking of water floods according to the assumption that sediment concentrations by volume (C_v) could reach the maximum water-flood limit of 20 percent. For the limiting sediment concentration C_v of 20 percent, the corresponding bulking factor is 1.25 (eq. 9). This factor was applied to peak discharges computed for areas of moderate to high burn severity; the bulking factor was weighted according to the relative burned area within each of the modeled subbasins.

Simulated pre-burn, post-burn, and bulked 100-year discharges for each of the 15 Mitchell Creek subbasins are shown in table 4. Post-burn, bulked 100-year peak flows for Mitchell Creek subbasins are expected to increase 2 to 21 times pre-burn peaks (table 4). Post-burn peak discharges for composite subbasins along the main stem of Mitchell Creek (Upstream, Fish Hatchery, and Donegan Bridge) are expected to increase 3 to 4 times pre-burn peaks. Based on comparison with the results of studies of other burned drainage basins (Rowe and others, 1954; Moody and Martin, 2001b; URS Corporation, 2000), the modeling results for post-fire peak flows in Mitchell Creek are considered reasonable.

Combined routing of water-flood (HEC-RAS) and debris-flow (FLO-2D) components in Mitchell Creek are planned as part of a future “detailed” hydraulic study that will delineate the long-term (Phase 3) 10-, 50-, 100-, and 500-year floodplain (and floodway) boundaries for the Mitchell Creek drainage basin. Debris-flow potential in subbasins burned by the Coal Seam wildfire, including tributaries to Mitchell Creek, are evaluated in the subsequent section of this report, “Analysis of Debris-Flow Producing Drainage Basins, Coal Seam Wildfire.”

Table 4. Computed 100-year peak discharges for pre-burn, post-burn, and post-burn (bulked) runoff conditions for modeled subbasins in the Mitchell Creek drainage basin.

[mi^2, square miles; %, percent; Q_{100}, 100-year discharge; ft^3/s, cubic feet per second; Q_u, pre-burn 100-year discharge; Q_b, post-burn 100-year discharge; Q_{bb}, post-burned bulked 100-year discharge; $ft^3/s/mi^2$, cubic feet per second per square mile; N/A, not applicable]

Subbasin name and number	Drainage area (mi^2)	Area of low burn (%)	Area of moderate-high burn (%)	Q_{100} (ft^3/s)				Ratio Q_{bb}/Qu
				Pre-burn (Q_u)	Post-burn (Q_b)	Post-burn bulked (Q_{bb})	Q_{bb} per mi^2 (ft^3/s)	
Storm King 1 (23)	0.201	6.7	74.2	38.4	415	482	2,400	12.6
Storm King 2 (24)	0.055	57.8	35.1	17.1	107	120	2,170	7.0
Mitchell E1 (25)	0.290	42.4	40.7	48.2	369	407	1,400	8.4
Mitchell E2 (26)	0.013	27.7	70.0	7.84	33.8	39.7	3,050	5.1
Mitchell E3 (27)	0.051	3.0	97.0	24.7	132	164	3,200	6.6
Mitchell E4 (28)	0.045	6.8	89.8	22.5	130	159	3,560	7.1
Mitchell W4–S (29)	0.010	8.6	91.4	7.80	34.7	42.6	4,350	5.5
Mitchell W3 (30)	0.116	10.5	79.5	36.8	323	387	3,320	10.5
Mitchell W2 (31)	0.133	7.8	76.6	37.8	353	421	3,160	11.1
Mitchell W1 (32)	0.147	24.8	37.5	40.4	223	244	1,660	6.0
Mitchell W4–N (33)	0.031	2.6	89.0	17.2	95.0	116	3,800	6.8
Upper Mitchell West (36)	2.372	11.8	4.1	175	362	366	154	2.1
Upper Mitchell East (37)	2.747	11.9	7.7	192	489	498	181	2.6
Fish hatchery (38)	0.575	30.3	55.2	49.2	918	1,040	1,810	21.1
Donegan Bridge (39)	4.418	4.4	5.7	22.8	472	479	105	2.1
Composite basin name								
Upstream main stem	5.12	11.8	6.0	216	844	857	167	4.0
Fish hatchery main stem	6.23	13.6	16.1	366	1,070	1,120	180	3.1
Donegan Bridge main stem	11.2	10.8	13.8	587	1,740	1,800	161	3.1

Mitchell Creek Hydrology and Peak Flow Modeling for Long-Term Recovery—Phase 3

Hydrologic responses in Mitchell Creek were computed to evaluate peak flows at a point in the post-burn, long-term recovery period (Phase 3). The long-term recovery was identified using methods described in "Method for Determination of Drainage Basin Recovery—Phase 3" section. In the Mitchell Creek subbasin of the Coal Seam burned area, the long-term recovery was estimated to be 4 years. HEC-HMS input parameters (U.S. Army Corps of Engineers, 2001b) for individual subbasins were calculated for the long-term recovery to facilitate HEC-HMS modeling of peak flows. Discharge results from these analyses can be used as input for hydraulic analysis. Peak-flow hydrographs were developed for 15 tributaries (subbasins) to Mitchell Creek within and downstream from the Coal Seam burned area. These subbasins were delineated using a 30-m DEM. The 1-hour storm duration and distribution used by the USACE for hydrologic analysis in the same area (U.S. Army Corps of Engineers, 1998) was used in this study.

The effects of the 10-, 50-, 100-, and 500-year 1-hour rainfall on peak flows in Mitchell Creek were evaluated. The analysis characterizes increased runoff produced by rainstorms in and near the burned area and reflects drainage-basin conditions that are expected to exist for a 4-year recovery period. The approach to the long-term hydrologic analysis is similar to the approach described previously for pre-burn and post-burn periods and included the following steps and assumptions:

1. Drainage-basin parameters for the previously described long-term conditions in the burned subbasins tributary to Mitchell Creek were used in the HEC-HMS rainfall-runoff model (Appendix table 5–2).

2. Peak flows were simulated in the HEC-HMS rainfall-runoff model for the 10-, 50-, 100-, and 500-year, 1-hour design storms using long-term recovery drainage-basin parameters in burned subbasins tributary to Mitchell Creek (Appendix table 5–3).

3. Rainfall amounts and distributions were determined from the NOAA Atlas 2 guidance. The 500-year 1-hour storm total was estimated by logarithmic extension of NOAA Atlas 2 data (Miller and others, 1973) (Appendix table 5–4).

4. Peak discharges for recovered subbasins were not volumetrically bulked because large sediment loads probably will not be typical in the period following recovery.

5. Peak discharges for subbasins tributary to Mitchell Creek were computed. Runoff hydrographs were routed through the larger subbasins (Appendix table 5–3).

Analysis of Debris-Flow-Producing Drainage Basins, Coal Seam Wildfire—Phase 2

Many of the small subbasins burned by the Coal Seam wildfire have the potential to produce damaging debris flows during the next several years before substantial vegetation regrowth in the burned areas (fig. 17). The Maroon Formation, widely exposed in this area, produced several large debris flows on nearby Storm King Mountain following a wildfire in 1994 (Cannon and others, 1998; Kirkham and others, 2000). The potential for debris flows from larger rainstorms was evaluated in the Coal Seam burned area. Cannon, Michael, and Gartner (2003) and Cannon (Susan H. Cannon, U.S. Geological Survey, oral commun., 2003) assessed approximately 135 tributaries with some potential for flooding and debris flows and estimated the potential peak discharges with Cannon's (2001) regression equation.

Additional debris-flow analysis with FLO-2D was done for 26 of the tributaries Cannon assessed (table 5). These tributaries were identified as having the greatest potential peak debris-flow discharges and for having the potential to damage habitable and commercial structures. Other tributaries also have a potential to produce floods and debris flows but were not included in this analysis. The Mitchell Creek flood potential is covered in the preceding section of this report.

Debris flows from small tributaries (subbasins) to Mitchell Creek were simulated with FLO-2D. A composite model of Mitchell Creek was created in which 10 heavily burned subbasins were modeled as debris-flow-producing tributaries (table 5), and other minimally burned subbasins were modeled as water-flood-producing tributaries. The procedures for simulating Coal Seam burned-area debris flows are presented in the previous section "Methods for Post-Fire Debris-Flow Hazard Analysis."

Drainage areas for the Coal Seam wildfire study subbasins range from 0.01 to 0.75 mi^2. Most of these subbasins are located on Red Mountain south of the Colorado River, in the upland areas north of the golf course in West Glenwood Springs, and are tributaries to Mitchell Creek (fig. 17). All tributaries were modeled using a 10-m grid-element size. Delineation of the potential inundation areas and the maximum depths during the debris flow following a 100-year storm are indicated on maps showing the debris-flow subbasins, existing alluvial fans, and infrastructure visible on the current (2004) USGS topographic maps (figs. 18 and 19).

Debris-flow hydrographs, inundation areas, and maximum flow depths were created in FLO-2D. Subbasins with a relatively large area of moderate and high burn severity were characterized by marked increase in runoff and sediment yield. Estimates of the increase in 100-year discharge resulting from post-fire debris flows, relative to unburned conditions, range from 8 to 14 times in the Red Mountain area, 2 to 9 times in the West Glenwood Springs area, and 8 to 14 times for selected tributaries of Mitchell Creek (table 5). Runoff from tributaries included in the Coal Seam debris-flow analyses

Table 5. Estimated 100-year debris-flow peak discharges for selected Coal Seam burned area tributary subbasins.

[100-year, 1-hour storm total 1.64 inches; sediment concentration, C_v, at water peak = 0.43; USGS, U.S. Geological Survey; USACE, U.S. Army Corps of Engineers; BAER, Burned Area Emergency Rehabilitation team; mi², square miles; ft³/s, cubic feet per second; --, not applicable]

Subbasin number	Tributary subbasin name USGS (fig. 17)	USACE report basin number[1]	BAER report basin number[2]	Tributary to	Drainage area (mi²)	Pre-fire 100-year peak streamflow discharge (ft³/s)	Post-fire 100-year peak streamflow discharge (ft³/s)	Post-fire 100-year peak debris-flow discharge (ft³/s)
1	Red Mtn Basin 1	W–18	14	Wulfsohn Fan	0.07	25	207	363
2	Red Mtn Basin 2	--	15	Wulfsohn Fan/Colo R	0.02	8	61	107
3	Red Mtn Basin 3	W–20	30	Wulfsohn Fan/Colo R	0.06	24	147	258
4	Red Mtn Basin 4	W–21	31	Wulfsohn Fan/Colo R	0.06	25	124	218
5	Red Mtn Basin 5	W–22a	32	Wulfsohn Fan/Colo R	0.06	24	173	304
6	Red Mtn Basin 6	--	33	Wulfsohn Fan/Colo R	0.02	7	47	82
7	Red Mtn Basin 7	W–22b	13	Wulfsohn Fan/Colo R	0.08	28	223	391
8	Red Mtn Basin 9	--	34	Wulfsohn Fan/Colo R	0.04	16	117	205
9	Red Mtn Basin 11	W–24	35	Colorado R	0.55	131	631	1,107
18	"Charo Rd" basin	N–12	22	W Glenwood/Colo R	0.66	148	153	268
19	"Sunny Acres Rd" bsn	N–11		W Glenwood/Colo R	0.11	39	71	125
20	"Cedar Crest Dr" bsn	N–10a	23	W Glenwood/Colo R	0.18	55	270	474
21	"Rock Ledge Dr" bsn	--		W Glenwood/Colo R	0.04	17	69	121
22	"Mel-Ray Rd" basin	N–9	24	W Glenwood/Colo R	0.75	163	757	1,328
23	Storm King 1	--	4	Mitchell Creek	0.20	15	407	714
24	Storm King 2	--	5	Mitchell Creek	0.05	43	110	193
25	Mitchell E1	--		Mitchell Creek	0.29	48	369	647
26	Mitchell E2	--		Mitchell Creek	0.01	8	34	59
27	Mitchell E3	--		Mitchell Creek	0.05	25	132	232
28	Mitchell E4	--		Mitchell Creek	0.04	23	130	228
29	Mitchell W4-S	--		Mitchell Creek	0.01	8	35	61
30	Mitchell W3	--		Mitchell Creek	0.12	37	323	567
31	Mitchell W2	--		Mitchell Creek	0.13	38	353	619
32	Mitchell W1	--		Mitchell Creek	0.15	40	223	391
34	"Ponderosa Dr W"	N–7		W Glenwood/Colo R	0.10	34	130	228
35	"Ponderosa Dr E"	N–8		W Glenwood/Colo R	0.05	19	51	89

[1]Basin number used in U.S. Army Corps of Engineers (1998) report.

[2]Basin number used in Burned Area Emergency Rehabilitation (2002) report.

was not routed within the basin; runoff values used in FLO-2D analyses represent a basin-mouth summary of discharge from the contributing drainage area and are therefore slightly different from the Mitchell Creek water-flood runoff estimates described in the previous Mitchell Creek hydrology section where flow routing was performed (tables 4 and 5).

The debris-flow depths shown in figures 18 and 19 are maximum depths that occurred at some time during the model simulation. In most locations in the depositional zone, depths increased to a maximum as the sediment and water mixture passed and then receded to lesser depths. The time of occurrence of maximum depth varied by location in the depositional zone; therefore these maps do not represent an instant in time of the debris-flow deposit or the final depths at the end of the event. Repetitious, echolike depth patterns on some debris-flow deposits, such as those seen in the West Glenwood Springs area, represent the passage of undulating wave forms during runoff (J.S. O'Brien, FLO Engineering, Inc., oral commun., June 2003).

Some of the simulated 100-year debris-flow depositional areas were extensive. Debris flows from several small subbasins in Red Mountain inundated large areas of the Wulfsohn Fan, and maximum depths of 4 to 6 ft could occur near the west end of the fan (fig. 19). Debris-flow inundation in the West Glenwood Springs area also could be extensive and affect many residences and businesses. Maximum depths in the West Glenwood Springs area could approach 6 to 8 ft with a 100-year storm (fig. 19). If debris flows are generated simultaneously from multiple small tributary subbasins in Mitchell Creek (table 5), the combined maximum debris flows could exceed 10 to 15 feet in the main stem of Mitchell Creek and downstream from the Donegan Bridge (fig. 18).

Post-Fire Hydrologic Hazards for the Missionary Ridge Wildfire

Most of the area affected by the Missionary Ridge wildfire is underlain by sedimentary rocks including the Cutler, Hermosa, and Morrison Formations, known sources of debris-flow sediments (Cannon and others, 2003). Numerous steep drainage basins in the burned area have the potential to produce debris flows that threaten homes, businesses, several major roads, bridges, and the dams at Lemon and Vallecito Reservoirs during the next several years before substantial vegetation regrowth in the burned areas.

Analysis of Debris-Flow-Producing Drainage Basins, Missionary Ridge Wildfire—Phase 2

The potential for debris flows from larger rainstorms was evaluated in the Missionary Ridge burned area. The Missionary Ridge wildfire area is shown in figure 20. Cannon and others (2003) and Cannon (Susan H. Cannon, U.S. Geological Survey, oral commun., 2003) assessed approximately 121 tributaries with some potential for flooding and debris flows and estimated the potential peak discharges with Cannon's (2001) regression equation.

Twenty-five of the tributaries Cannon assessed were selected for additional debris-flow analysis with FLO-2D (table 6). These tributaries were identified as having the greatest potential peak debris-flow discharges and for having the potential to damage habitable and commercial structures. The procedures for simulating Missionary Ridge burned-area debris flows are presented in the section "Methods for Post-Fire Debris-Flow Hazard Analysis." Other tributaries also have a potential to produce floods and debris flows but were not included in this analysis.

Subbasins of the Missionary Ridge burned area differ greatly in size; drainage areas range from 0.07 to 9.78 mi^2. These subbasins are tributaries to the Animas, Florida, and Los Pinos Rivers. A delineation of the potential inundation areas and the maximum depths during a debris flow following a 100-year, 1-hour storm (1.77 inches) are indicated in figures 21 and 22 showing the debris-flow subbasins, existing alluvial fans, and infrastructure visible on the current (2004) USGS topographic maps.

Debris-flow hydrographs, inundation areas, and maximum flow depths were created in FLO-2D. All tributaries initially were modeled using a 10-m grid-element size. Five large subbasins producing large peak discharges that inundated extensive areas were modeled with 30-m grid elements. These larger subbasins were Stevens Creek, a tributary of the Animas River; True, Shearer, and Red Creeks, tributaries of the Florida River; and Red Creek, a tributary of the Los Pinos River (figs. 21 and 22). The FLO-2D models for these five subbasins approached the grid-element number maximum when 10-m elements were used. Consequently, the outflow graphics from these five subbasins do not have the high resolution of the other subbasins in this study, but the extensive hazard area is adequately shown.

The debris-flow depths shown in figures 21 and 22 are maximum depths that occurred at some time during the model simulation. In most locations in the depositional zone, depths increased to a maximum as the sediment and water mixture passed and then receded to lesser depths. The time of occurrence of maximum depth varied by location in the depositional zone; therefore, these maps do not represent an instant in time of the debris-flow deposit or the final depths at the end of the debris flow.

The largest increase from estimated pre-burn discharge to post-burn debris flow 100-year discharge is expected to occur in the Coon Creek subbasin (fig. 21) where peak discharges could increase by a factor of greater than 240 (table 6). Approximately 96 percent of the 7.99-mi^2 Coon Creek subbasin was burned by the Missionary Ridge wildfire, and 78 percent of the subbasin was moderately to severely burned (USDA Forest Service, 2002c). Maximum debris-flow depths downstream from the Coon Creek canyon mouth could be in the range of 8 to 10 ft with isolated depths in excess of 15 ft. Estimates of the increase in 100-year discharge resulting from post-fire debris flows, relative to unburned conditions in most of the Missionary Ridge area, are not as great as those in Coon Creek. In the Animas River area, the increases range from 9 to 38 times; in the Florida River area, from 22 to 31 times; and in the Vallecito Reservoir and Los Pinos River area, from 9 to 30 times (figs. 21 and 22).

The large contributing drainage areas and large 100-year debris-flow peak discharges from some Missionary Ridge burned-area tributaries (subbasins) result in extensive inundation areas (figs. 21 and 22). Existing topography in these areas includes older alluvial and debris fans, terraces, hillslopes, valley-floors, and flood plains. Isolated areas of deeper flow on the debris fan, such as those downstream from Freed Canyon, Haflin Canyon, Woodard Canyon, and Kroeger Canyon, are most likely the result of sediment and water accumulations in topographic low spots, such as at a terrace margin or in abandoned and active stream channels.

Repetitious, echolike depth patterns on some debris-flow deposits, such as for Coon Creek and Lost Creek, represent the passage of undulating wave forms during runoff (J.S. O'Brien, FLO Engineering, Inc., oral commun., June 2003). The repetitious fan-shaped inundation patterns, such as those downstream from Elkhorn Canyon, Stevens Creek, and Freed Canyon, may be the result of a prolonged debris-flow event advancing over a series of topographic irregularities, or

Table 6. Estimated 100-year debris-flow peak discharges for selected Missionary Ridge burned area tributary subbasins.

[100-year, 1-hour storm total 1.77 inches; sediment concentration, C_v, at water peak = 0.43; USGS, U.S. Geological Survey; BAER, Burned Area Emergency Rehabilitation team; mi², square miles; ft³/s, cubic feet per second; --, not applicable]

Subbasin number	Tributary subbasin name USGS (figs. 20–22)	BAER report basin number or name[1]	Tributary to	Drainage area (mi²)	Pre-fire 100-year peak streamflow discharge (ft³/s)	Post-fire 100-year peak streamflow discharge (ft³/s)	Post-fire 100-year peak debris-flow discharge (ft³/s)
18	Coon Creek	N Fk, M Fk, S Fk	Animas River Valley	7.99	149	20,653	36,234
21	Unnamed 1st order	--	Animas River Valley	2.16	182	3,946	6,923
30	Elkhorn Canyon	--	Animas River Valley	0.46	79	1,075	1,886
35	Stevens Creek	N10	Animas River Valley	6.02	414	2,186	3,835
50	Freed Canyon	Freed Canyon	Animas River Valley	2.16	216	4,094	7,183
66	Unnamed 1st order	--	Animas River Valley	0.18	43	449	788
69	Unnamed 1st order	--	Animas River Valley	0.07	26	156	274
71	Haflin Canyon	X-Sec near N19	Animas River Valley	1.61	179	3,050	5,351
92	Woodard Canyon	V21	Animas River Valley	0.91	124	1,817	3,188
106	Kroeger Canyon	Kroeger Cr 2	Animas River Valley	1.22	150	2,555	4,482
61	Unnamed 2nd order	E26	Lemon Reservoir and dam	0.57	90	1,276	2,239
83	True Creek	--	Florida River	2.56	238	2,977	5,223
96	Shearer Creek	--	Florida River	7.07	455	7,847	13,767
119	Red Creek	E34 Red Creek	Florida River	7.75	471	8,231	14,440
16	Lost Creek	--	Grimes/Vallecito Creeks	2.30	225	1,157	2,030
23	Unnamed 2nd order	--	Vallecito Reservoir	0.35	67	910	1,597
24	Unnamed 0 order	--	Vallecito Reservoir	0.54	87	799	1,402
29	Freeman Creek	E4-12	Vallecito Reservoir	2.32	226	2,965	5,202
53	Unnamed 1st order	--	Vallecito Reservoir	0.24	53	607	1,065
55	Root Creek	--	Vallecito Reservoir	0.72	105	1,590	2,789
63	Jack Creek	E1 Jack Cr/E1A	Vallecito Reservoir and dam	1.99	198	3,366	5,905
65	Wilson Creek	Wilson Cr E23-25	Vallecito Reservoir	1.58	175	2,590	4,544
68	Gut Canyon	--	Vallecito Reservoir	0.38	69	839	1,472
73	Red Creek	--	Los Pinos River	9.78	560	9,459	16,595
111	Patton Canyon	--	Vallecito Reservoir and dam	0.70	102	1,516	2,660

[1]Basin number used in USDA Forest Service (2002c) report.

they could be computational relicts related to the model limit of eight possible directions for the mixture to flow from one square grid element into an adjacent grid element.

Debris-flow deposition into water bodies, such as Lemon and Vallecito Reservoirs, was not accurately simulated by FLO-2D because no bathymetric data were available. Consequently, the reservoir water surface was treated in the model as a solid, planar feature. Debris-flow depths beyond the water's edge are overstated by an undetermined amount; however, flow depths at the tributary mouth are within the tolerance of the model, and flow depths on the existing land surface are reasonably accurate where not affected by backwater effects from the artificial reservoir surface.

Summary

Drought conditions in Colorado made the 2002 wildfire season unusually active. Several wildfires substantially changed the hydrologic, hydraulic, and geomorphologic characteristics of the affected drainage basins. In cooperation with the Federal Emergency Management Agency (FEMA), a team from the U.S. Geological Survey (USGS) and the Bureau of Reclamation (BOR) assessed and ranked the 2002 Colorado wildfires (as of July 2, 2002) in terms of relative hazard to population centers and infrastructure. The team also conducted detailed assessments of the hydrologic, hydraulic,

and geomorphologic effects of selected, high-priority wildfires on burned and adjacent unburned parts of the drainage basins, providing information for use by water managers about the effects of wildfire on runoff and sediment from burned drainage basins. The technical assessment focused on population centers and infrastructure affected by the wildfires. Existing National Flood Insurance Program (NFIP) maps (where available) needed to be revised to reflect post-fire drainage-basin conditions. The technical response team, consisting of experts in hydrology, hydraulics, sediment transport, geomorphology, and GIS mapping, used NFIP study data to evaluate post-fire changes to flood-inundation maps where these data existed.

The objective of this study was to conduct three phases of hydrologic activities in response to the Colorado wildfires in 2002:

Phase 1.—Post-wildfire reconnaissance-hazard maps were created for 16 Colorado wildfires identified as of July 2, 2002. These maps were used to rank the relative priority of each of the wildfires in terms of anticipated hydrologic hazard. These maps were developed for reconnaissance purposes only and are not included in this report. Three highest priority wildfires were selected for more detailed hydrologic analysis under Phase 2 of the study.

Phase 2.—More detailed hydrologic studies were conducted for those wildfires having the highest priority defined in Phase 1, leading to the production of revised flood- or debris-flow hazard maps for areas with existing NFIP maps and for other flood-prone areas where post-fire flooding could threaten downstream population centers or infrastructure.

Phase 3.—Long-term runoff characteristics that reflect post-fire drainage-basin recovery and stabilizing hydrologic conditions expected to develop over a period of several years after the wildfire also were analyzed for two channel reaches: the South Platte River between Deckers and Trumbull, Colo., and Mitchell Creek in Glenwood Springs, Colo.

An additional study task included a detailed hydraulic analysis of the South Platte River between Deckers and Trumbull. Detailed 10-, 50-, 100-, and 500-year flood-plain elevations were developed for the Deckers-to-Trumbull reach. Floodway elevations also were computed for this reach.

The 16 wildfires that had burned or were burning as of July 2, 2002, ranged from the Trinidad Complex wildfire in south-central Colorado to the Pinyon Ridge wildfire near Meeker in northwestern Colorado, to the Missionary Ridge wildfire near Durango, in southwestern Colorado. Three wildfires were determined to have a high priority in terms of anticipated hazard and potential threat to infrastructure and life and were selected for additional, more detailed hydrologic assessments. These were the Hayman wildfire in the Colorado Front Range Mountains southwest of Denver, the Coal Seam wildfire at the southern edge of the Flat Tops region and along the Colorado River near Glenwood Springs, and the Missionary Ridge wildfire in the southern San Juan Mountains near Durango.

The Hayman wildfire started in June 2002 near Lake George in the South Platte River Basin and burned approximately 138,000 acres (216 mi^2). Elevations in the burned area ranged from 6,289 to over 11,000 ft. The drainage area of the South Platte River at South Platte, Colo., is 2,580 mi^2. The South Platte River flows from southwest to the northeast through the interior of the burned area. Most of the burned area is composed of shallow, easily eroded, weathered soils from the Pikes Peak batholith. The landscape is highly dissected in the upland forested part of the burned area. Annual precipitation is composed of snowfall during the winter and high-intensity rainstorms during the summer.

The Coal Seam wildfire started on June 8, 2002, near Glenwood Springs and burned approximately 12,200 acres (19.1 mi^2). Elevations in the burned area ranged from 5,800 to 10,500 ft. In the Coal Seam area, abundant, fine-grained sediment is available for debris-flow entrainment originating from tributaries underlain by weathered sedimentary rocks of the Maroon and other formations. Flooding in Mitchell Creek, a major tributary entering the Glenwood Springs area from the north, is another potential hazard in the Coal Seam burned area. Approximately 25 percent of Mitchell Creek's 11.9-mi^2 drainage area was burned by the Coal Seam wildfire.

The Missionary Ridge wildfire burned from June 9 to July 14, 2002, and affected approximately 70,500 acres (110 mi^2) in La Plata County, Colorado. Elevations in the burned area ranged from approximately 6,500 to 11,400 ft. The wildfire affected tributaries of three major drainage basins near Durango: the Animas, Florida, and Los Pinos River drainage basins. Approximately 61 percent of the area was burned with a moderate or high severity. Most of the area affected by the wildfire is underlain by sedimentary rocks including the Cutler, Hermosa, and Morrison Formations, which are known sources of debris-flow sediments.

The predominant potential hazard process in the Hayman wildfire area is flooding by sediment-laden water along the large tributaries to, and the main stem of, the South Platte River. Although much sediment is available for erosion and transport by storm runoff in the Hayman area, there is little potential for debris-flow activity because the amount of silt- and clay-size material derived from the weathered parent rock is relatively small. The other two high-priority burned areas had a substantial potential for debris-flow activity that could adversely affect life and infrastructure. Debris flows pose a hazard distinct from other sediment-laden flows because of their unique destructive power; debris flows can occur with little warning and can exert great impulsive loads on objects in their paths. Even small debris flows can strip vegetation, block drainageways, damage structures, and endanger human life. The marine shales exposed in formations within the Coal Seam and Missionary Ridge burned areas weather into fine-grained sediments including clays that are essential to the mobility and transport competence of debris flows.

Many of the rainfall-runoff model parameters used in this study were extracted from the topography captured in digital elevation models (DEMs). Ten-meter digital elevation model

(10-m DEM) data and Intermap IFSAR 2.5-m data were prepared for this study with the LT4X program using elevation contour lines (hypsography) from standard USGS 1:24,000-scale topographic maps. The accuracy of an elevation value in the 10-m DEM is ±20 ft in mountainous areas and ±10 ft in flatter areas. The ground condition represented in the elevation data is that of the original orthophotography used to produce each 1:24,000 quadrangle map; in general, for the study area, this orthophotography was flown between 1950 and 1980. Interferometric Synthetic Aperture Radar (IFSAR) data from Intermap Technologies was used over the Hayman burned area to provide a more accurate DEM.

Streamflow-gage data for most tributary drainage basins of the Hayman, Coal Seam, and Missionary Ridge drainage basins were not available; therefore, hydrographs and peak discharge values for pre-burn, post-burn short-term, and post-burn long-term scenarios were simulated for each subbasin by using a rainfall-runoff model. Most model parameters are abstract conceptual representations of non-measurable characteristics that must be estimated through a calibration process.

Two calibration approaches were used to estimate the pre-burn parameter values in this study: the manual calibration method and the objective calibration method. The manual calibration method initially was used for the Hayman rainfall-runoff model and involved a trial-and-error estimation of parameter values for all subbasins. Because there was no way to ensure the optimal estimation of parameter values or to quantify the degree of uniqueness and(or) uncertainty associated with the estimated parameter values, a second approach, the objective calibration method based on nonlinear regression, was used to recalibrate the Hayman rainfall-runoff model. The objective calibration method was used to calibrate the Coal Seam and Missionary Ridge rainfall-runoff models.

Simulated peak discharge values were computed using the HEC–1 rainfall-runoff model. Subbasin characteristics were derived using a geographical information system and included area, length, and slope. The rainfall-runoff model parameters RCN, initial abstraction, and lag time were defined by the SCS curve number method. Where affected drainage basins and subbasins included both burned and unburned areas, post-burn RCNs were computed by weighting the respective drainage-basin conditions according to the equations of the SCS curve number method. After the model calibration process was complete, the post-burn parameter values and associated GIS information were used as input to the HEC-HMS rainfall-runoff model for drainage-basin hydrograph generation.

Computed water-peak discharges from the HEC-HMS modeling were "bulked," or increased volumetrically, to account for increased sediment concentrations that are expected to occur as a result of accelerated erosion after burning. Bulking analyses and computations were based on previous studies of post-fire runoff in other areas of the Western United States and on published research documenting the physical behavior of combined water and sediment flows. The amount of sediment bulking varied in the study depending on whether predominantly water floods or debris flows were anticipated in response to the 100-year storm. Peak-discharge estimates for the predominant water floods anticipated in the South Platte River Basin were bulked by a factor that assumed a volumetric sediment concentration (C_v) of 20 percent. Flood hydrographs were routed down main-stem channels by using routing routines included in the HEC-HMS rainfall-runoff model, and post-fire flood elevations were computed for bulked peak discharges at selected cross-section locations in the South Platte River and Mitchell Creek.

Debris-flow behavior is dependent on the concentration and particle-size range of the entrained sediment and on the relative proportion of inertial and viscous forces. A relatively high proportion of clay-size particles (diameter less than 0.004 mm, or 0.0002 inch) in the transported sediment increases debris-flow matrix strength and helps maintain the high pore pressure necessary to support larger particles in the flow. Sediment concentrations used in simulations at Coal Seam and Missionary Ridge are based on results from previous studies. The assumed volumetric concentrations for the input debris-flow hydrograph were varied through the event and for this study were initial C_v 20 percent, mean C_v approximately 31 percent, maximum C_v 48 percent (preceding the input water hydrograph peak), C_v at the time of the input water hydrograph peak 43 percent, and C_v for the duration of the event 20 percent.

A two-dimensional flood-routing model, FLO-2D, was used to delineate the area of unconfined debris-flow inundation on selected alluvial fan and valley floor areas in the Coal Seam and Missionary Ridge burned areas. The model uses a specified input hydrograph, volumetric sediment concentration, and existing topography to route a debris flow from the originating tributary to the depositional zone. Debris-flow discharges presented in this study were generated by 100-year rainfall events, and the inflow hydrographs at the alluvial fan heads or tributary mouths were generated with the objective calibration method used in the South Platte River analysis. The 100-year, 1-hour rainfall was 1.64 inches for the Coal Seam area and 1.77 inches for the Missionary Ridge area.

Interpretation of FLO-2D model output is limited by several factors. FLO-2D treats debris-flow composition as a temporally and spatially unvarying mixture; coarse material does not settle out during the simulation as it does in actual mud and debris flows. When the input sediment concentrations are decreased in FLO-2D, the debris-flow mixture travels a farther distance down a fan or valley; when concentrations are increased, the debris flow travels a shorter distance before stopping. The FLO-2D model is a quasi-two-dimensional model and, although often used in unconfined flow situations, it only routes flow in a downslope direction toward the nearest neighbor grid cell rather than in a truly lateral or transverse direction. Outflow from one square grid element into an adjacent square grid element is limited to eight possible directions (N, NE, E, SE, S, SW, W, NW). Model output is limited by the resolution of the topographic data supplied; in this study, 10-meter digital elevation data. Most roughness elements less than 10 m in size are not accounted for. Also, the original topography remains static during a model run and is insensitive to large-scale channel scour or aggradation. Small-scale differences in grid-cell elevation values influence the direction of cell-to-cell flow propagation. Errors in the input elevation values or changes in elevation over time, such as from land use or subsequent debris-flow deposition, could render the existing model output inaccurate.

Inundation areas and depositional depths generated in the FLO-2D simulations reflect the median of predicted values. Minimum and maximum likelihood areas and depths are not presented in the model output, and there is large, unquantified variability in the expected outcome of the 100-year storm. Another limitation of the analyses is that estimated inundation areas and depths from the model output are not verifiable without onsite observations of actual debris flows and the rainfall amounts that generated them.

Runoff characteristics that reflect post-fire drainage-basin recovery and stabilizing hydrologic conditions are expected to develop over a period of several years after the wildfire. A method was developed to objectively determine the number of years over which this recovery could occur. Assumptions for this method are that (1) a wildfire will raise the RCN in a burned drainage basin from a pre-fire RCN to a post-burn RCN as a function of burned area and severity; (2) during the recovery period, the post-burn RCN will "decay" back to some function of the pre-fire curve number; (3) although it is recognized as a simplification, recovery will be some function of time; and (4) initial decay will be the most rapid and will take place as a function of the magnitude of the pre-fire RCN and the difference between pre- and post-fire RCNs.

Estimates for both pre- and post-fire RCNs are available for all subbasins in the Hayman and Coal Seam burned areas on the basis of HEC-HMS modeling. Although there are very few field data that describe post-burn recovery, a study in the Frijoles Canyon at Bandolier National Monument in New Mexico provides a nearly complete description of post-fire recovery based streamflow records collected in a burned area. The study describes post-fire recovery in terms of the magnitude and frequency of flood peaks; the description was used in Hayman and Coal Seam wildfire recovery characterizations developed here, as a basis for a post-fire recovery equation that is a function of initial RCN, change in RCN due to wildfire, and time. The equation has the form of an exponential decay equation and can be used to estimate an RCN at any point in the recovery process.

A family of curves was generated with this post-fire recovery equation. These curves indicate estimates for RCN for a recovery period beginning with post-fire conditions and continuing for 50 years in a hypothetical drainage basin with an assumed pre-burn RCN of 50, raised to post-burn RCNs of 55 to 100 in increments of 5. In order to obtain an estimate of overall recovery in each wildfire area, the equation was used to determine values for RCN for all drainage basins for a period beginning with post-fire conditions and continuing through 50 years. The resultant time-series values were evaluated to identify a time in the recovery process when the change in estimated 100-year flood peak became less than 5 percent per year. The recovery times were rounded to the nearest whole year and used as the basis to prepare input for HEC-HMS to obtain estimates of the 100-year flood peak at the recovery time. The recovery-time estimates are: 6 years upstream from Cheesman Reservoir; 6 years downstream from Cheesman Reservoir; and 4 years for Mitchell Creek. Times in this range are consistent with BAER-team estimates of about 5 years due to vegetation regrowth, and with field observations from the USGS National Research Program of about 6 to 7 years in the Buffalo Creek burned area.

Hayman Wildfire

The South Platte River within and downstream from the Hayman wildfire is regulated by a series of reservoirs. In order to assess the effects of the 100-yr storm and subsequent flooding on burned and adjacent unburned areas of the South Platte River drainage basin, boundary flow conditions were established at the upstream edge of the fire perimeter and at the outflow from Cheesman Dam.

Because of the large contributing drainage area of the South Platte River Basin upstream from the fire perimeter and the substantial regulation/storage capacity of upstream reservoirs, it is extremely unlikely that a 100-year flood would occur throughout the entire basin during a single runoff event; consequently, the 10-year peak discharge at streamflow-gaging station 06696000 South Platte River near Lake George was selected as the boundary inflow condition. The 10-year peak discharge was computed for the period of record since completion of Elevenmile Canyon Reservoir (1933–98). The 10-year peak discharge was adjusted to account for the contributing drainage area between the streamflow-gaging station and the upstream edge of the Hayman fire perimeter, using a regional regression equation developed by the USGS for mountain regions of Colorado. The adjusted 10-year peak discharge, 940 ft^3/s, was used as the inflow peak for the South Platte River at the upstream limit of the burned area.

Cheesman Reservoir is operated as a water-supply reservoir; therefore, the boundary condition at the outflow at Cheesman Dam was determined to be a full reservoir, with uncontrolled flow over the spillway in response to upstream runoff. The reservoir is assumed to pass the entire flood volume but none of the sediment entrained from upstream.

Rainfall-runoff modeling was used to develop post-fire hydrographs for 19 selected subbasins tributary to the South Platte River within and downstream from the Hayman burned area. The U.S. Army Corps of Engineers HEC-HMS computer model was used for the analysis with the 100-year, 6-hour storm (2.4 inches).

A comparison of measured 100-year peak flows at five stream gages on tributaries near Cheesman Reservoir with the results of the regional regression equations developed for mountain areas of Colorado showed that the regional equations substantially overestimated the observed 100-year peaks by a factor of 2 or more. As an alternative, the five streamflow gages in the Goose Creek and Tarryall Creek drainages were used to develop a local regional equation for the study area. An ordinary-least-squares regression model to predict 100-year peak discharge (Q_{100}) as a function of drainage area (A) was developed using the stream-gage data. The regression model was used as the basis for calibration of the pre-burn, 100-year peak discharge of drainage basins modeled using HEC-HMS. Calibration of parameters in HEC-HMS was performed, to the extent possible, in the general range of drainage areas defined by the five streamflow gages used in the regression analysis.

The objective calibration method was used to estimate drainage-basin losses in all of the South Platte River tributaries (subbasins) affected by the Hayman wildfire. Larger drainage basins (Turkey Creek, Goose Creek, Wigwam Creek, and Horse Creek) were divided into smaller subbasins, and the subbasin hydrographs were routed to the basin mouth. Pre-burn runoff curve numbers (RCN) between 55 and 67 were selected for each subbasin. The pre-burn abstraction values were selected using default model computations based on pre-burn subbasin characteristics and are reflective of the weathered rock soils that dominate the area.

The SCS dimensionless unit hydrograph method was used to compute the resultant hydrograph. After examination of several lag-time equations, the SCS lag-time equation was selected for use in modeling. In the SCS equation, lag time is calculated directly from the RCN.

Simulated peak discharge for pre-burn conditions was calibrated to the 100-year peak discharge computed using the locally derived regional equation. Parameter estimation for each subbasin was done using the objective calibration method. Flow routing within the five larger subbasins was performed using the Muskingum method. Because observed hydrograph or field data were not available for calibration of the routing parameters, values of Muskingum K and X were selected within the range of commonly used values for channels in steep, upland subbasins.

Existing studies documenting the hydrologic response of burned drainage basins in other areas were used to guide the calibration for post-burn conditions. The post-burn RCNs selected by the BAER team were adopted for post-burn-discharge estimates in South Platte River tributaries (subbasins). Where affected drainage basins and subbasins included burned and unburned areas, post-burn RCNs were computed by weighting the respective drainage-basin conditions according to the governing equations of the SCS curve number method. Post-burn lag times were adjusted according to the SCS lag-time equation, which is a function of the post-burn RCN. Post-burn lag times were estimated using the SCS equation and ranged from 24 to 93 percent of pre-burn lag times in South Platte River subbasins.

To account for the potential sediment bulking of flood-flows in burned drainage basins, computed peak discharges were increased according to the assumption that sediment concentrations by volume (C_v) could reach the maximum water-flood limit of 20 percent. For a C_v of 20 percent, the corresponding bulking factor (BF) is 1.25. This factor was applied to peak water discharges computed by the HEC-HMS model for areas of moderate to high burn severity; the bulking factor was weighted according to relative burned area within each of the modeled drainage basins.

Post-burn 100-year peak discharges for the 19 selected subbasins, routed to the point of confluence with the South Platte River, are expected to increase 3 to 90 times pre-burn peaks. Among all modeled drainage basins, including subbasins of the larger tributaries, with substantial (greater than 50 percent) moderate to severe burned areas, post-burn bulked peak discharges are expected to be 28 to 91 times greater than pre-burn peaks. For those drainage basins with substantial burned area, average predicted unit-area peak discharge for pre-burn conditions is 12.3 $ft^3/s/mi^2$; average predicted bulked unit-area peak discharge for post-burn conditions is 830 $ft^3/s/mi^2$. Predicted increases in post-burn peak discharge are in general agreement with the BAER team's hydrologic assessment of the Hayman wildfire and with hydrologic studies of other burned drainage basins. Results of the analyses are summarized in a series of hazard maps showing the extent of the 100-year flood, and cross sections showing the 100-year flood water-surface elevation along the South Platte River.

The post-burn 10-, 50-, 100-, and 500-year peak discharges along the main stem of the South Platte River were computed for the Deckers-to-Trumbull detailed study reach. In-stream flow routing, to account for in-channel storage and peak attenuation at successive downstream cross sections, was performed using the routing routines in the HEC-HMS computer model. The Muskingum-Cunge routing routine, which incorporates cross-section and hydraulic properties of the surveyed cross sections, was used to route flows in reaches of the main-stem South Platte River. Routed peaks showed little attenuation. Sensitivity testing indicated that hydrograph attenuation was affected mainly by channel slope; the relatively steep slopes (measured as water-surface slope during the cross-section surveys) through the study reach preclude substantial attenuation. The Modified Puls reservoir routing routine in HEC-HMS was used to route the computed flood hydrograph through Cheesman Reservoir and over the spillway to the downstream reach.

Post-fire recovery-time estimates are 6 years for drainage basins upstream from Cheesman Reservoir, and 6 years for drainage basins downstream from Cheesman Reservoir. Detailed flood hydraulics were computed using step-backwater routines in HEC-RAS for a stream reach from a point 5,040 ft upstream from the county road bridge over the South Platte River at Deckers to a point 2,455 ft downstream from the county road bridge over the South Platte River at Trumbull. Peak flows from the 10-, 50-, 100-, and

500-year recurrence intervals 6-hour design storm for the main-stem South Platte River were used in the detailed reach. Water-surface profile elevations in the detailed study reach were plotted, and floodway computations were made using encroachment routines in the HEC-RAS program for the 100-year profile.

Coal Seam Wildfire

The Coal Seam wildfire affected many small subbasins as well as the large subbasin of Mitchell Creek, a perennial tributary of the Colorado River at Glenwood Springs, Colo. Water flooding in Mitchell Creek and debris flows from smaller tributaries are potential hazards in the Coal Seam area. Post-fire hydrologic analyses were conducted to evaluate the effects of the 100-year, 1-hour storm (1.64 inch) on the burned and adjacent unburned areas of the Mitchell Creek subbasin and other subbasins.

Mitchell Creek has a contributing drainage area of 11.2 mi^2 at Donegan Bridge in Glenwood Springs. Earlier studies determined the 100-year peak discharge is 360 ft^3/s at a main-stem point upstream from Donegan Bridge (drainage area is 5.9 mi^2). A drainage-area adjustment of this peak discharge was made to reflect hydrologic conditions at Donegan Bridge. The area-adjusted peak discharge was computed using an equation relating peak discharge for gaged sites to ungaged sites as a function of relative drainage area. The computed, 100-year peak discharge for Mitchell Creek at Donegan Bridge was 542 ft^3/s. Rainfall-runoff modeling was used to develop post-fire hydrographs for 15 principal subbasin drainage basins of Mitchell Creek. Subbasin areas in the Mitchell Creek drainage ranged from 0.010 to 4.42 mi^2.

Unburned conditions first were modeled using the 100-year peak discharges of 360 ft^3/s at the point upstream from the Donegan Bridge and 542 ft^3/s at the Donegan Bridge as target discharges for model calibration. The SCS lag-time equation developed for drainage basins smaller than about 3.25 mi^2 was used to compute the lag time. The objective calibration method was used to estimate optimal pre-burn rainfall-runoff parameters for use in simulating the effects of wildfires on (1) unsteady, one- and two-dimensional water flooding and (2) unsteady, two-dimensional, debris flows. The HEC-HMS model was used to simulate the pre-burn rainfall-runoff processes. Model calibration was achieved by applying a nonlinear-parameter estimation algorithm to the HEC-HMS model.

Target 100-year peak discharges for each unburned Mitchell Creek subbasin were computed using three published regional equations. Resulting parameter sets (RCN, initial abstraction, and lag time) then were analyzed using the PEST algorithm and HEC-HMS to compute the routed peak discharge at the mouth of Mitchell Creek. Comparison tests showed that of the three regional equations evaluated, the Vaill equation produced target subbasin discharges and resultant RCNs that yielded the best estimate of the accepted 100-year discharge for the main stem of Mitchell Creek. The Vaill equation produced peak discharges that agreed closely with peak discharges from the existing flood-insurance study. Flow routing within the Mitchell Creek subbasin was performed using the Muskingum method.

About 25 percent of the Mitchell Creek drainage basin was burned by the Coal Seam wildfire in 2002. Adjustments to the pre-burn modeling parameters were made to reflect the burned condition within each subbasin as was done for tributaries to the South Platte River. The BAER team “Coal Seam Fire Hydrology Report” was used to guide the selection of RCNs for post-burn conditions in the Mitchell Creek subbasin. Post-burn lag times range from 40 to 87 percent of pre-burn lag times, depending on the amount of burned area in the subbasin.

Computed Mitchell Creek peak discharges were increased to account for potential sediment bulking of water floods according to the assumption that sediment concentrations by volume (C_v) could reach the maximum water-flood limit of 20 percent. This factor was applied to peak discharges computed for areas of moderate to high burn severity; the bulking factor was weighted according to relative burned area within each of the modeled subbasins. Post-burn, bulked 100-year peak flows for Mitchell Creek subbasins are expected to increase 2 to 21 times pre-burn peaks. Post-burn peak discharges for points along the main stem of Mitchell Creek are expected to increase 3 to 4 times pre-burn peaks.

Many of the small subbasins burned by the Coal Seam wildfire have the potential to produce damaging debris flows. Debris-flow analysis with FLO-2D was done for 26 tributaries (subbasins) identified as having the greatest potential peak debris-flow discharges and for having the potential to damage to habitable and commercial structures. Debris flows from 10 small tributaries to Mitchell Creek also were simulated with FLO-2D. Drainage areas for the Coal Seam burned-area subbasins range from 0.01 to 0.75 mi^2.

Subbasins with a relatively large area of moderate and high burn severity were characterized by marked increase in runoff and sediment yield. Estimates of the increase in 100-year discharge resulting from post-fire debris flows, relative to unburned conditions, range from 8 to 14 times in the Red Mountain area, 2 to 9 times in the West Glenwood Springs area, and 8 to 14 times for selected tributaries of Mitchell Creek. Runoff from tributaries included in the Coal Seam debris-flow analyses was not routed within the Mitchell Creek drainage basin; runoff values used in FLO-2D analyses represent a basin-mouth summary of discharge from the contributing drainage area and are therefore slightly different from the Mitchell Creek water-flood runoff estimates where flow routing was performed. Post-fire recovery-time estimates were not made for the smaller subbasins burned by the Coal Seam wildfire; however, the estimated recovery time for Mitchell Creek is 4 years.

The debris-flow depths in this report are maximum depths that occurred at some time during the model simulation. In most locations in the depositional zone, depths increased to a maximum as the sediment and water mixture passed and then receded to lesser depths. The time of occurrence of maximum depth varied by location in the depositional zone. Some debris-flow depositional areas were extensive. Debris flows from several small subbasins in Red Mountain inundated large areas of the Wulfsohn Fan, and maximum depths of 4 to 6 ft could occur near the west end of the fan. Maximum depths in the West Glenwood Springs area could approach 6 to 8 ft with a 100-year storm, and if debris flows are generated simultaneously from multiple small tributary drainage basins in Mitchell Creek, the combined maximum debris flows could exceed 10 to 15 ft in the main stem of Mitchell Creek and downstream from the Donegan Bridge.

Missionary Ridge Wildfire

Numerous steep drainage basins in the Missionary Ridge burned area have the potential to produce debris flows. Post-fire hydrologic analyses were conducted to evaluate the effects of the 100-year, 1-hour storm (1.77 inch) in 25 burned tributaries. Subbasins of the Missionary Ridge burned area differ greatly in size; drainage areas range from 0.07 to 9.78 mi^2. These subbasins are tributaries to the Animas, Florida, and Los Pinos Rivers.

Debris-flow hydrographs, inundation areas, and maximum flow depths were created in FLO-2D. All tributaries initially were modeled with FLO-2D using a 10-m grid-element size. Five subbasins with relatively large drainage areas producing large peak discharges that inundated extensive areas were modeled using 30-m grid elements. These drainage basins were Stevens Creek, a tributary of the Animas River; True, Shearer, and Red Creeks, tributaries of the Florida River; and Red Creek, a tributary of the Los Pinos River.

The debris-flow depositional depths in most locations increased to a maximum as the sediment and water mixture passed and then receded to lesser depths. The time of occurrence of maximum depth varied by location in the depositional zone. The largest increase from estimated pre-burn discharge to post-burn debris flow 100-year discharge is expected to occur in the Coon Creek subbasin where peak discharges could increase by a factor greater than 240. Approximately 96 percent of the 7.99-mi^2 Coon Creek subbasin was burned by the Missionary Ridge wildfire, and 78 percent of the subbasin was moderately to severely burned. Maximum debris-flow depths downstream of the Coon Creek canyon mouth could be in the range of 8 to 10 ft with isolated depths in excess of 15 ft. Estimates of the increase in 100-year discharge resulting from post-fire debris flows, relative to unburned conditions in most of the Missionary Ridge area, are not as great as those in Coon Creek. In the Animas River area, the increases range from 9 to 38 times; in the Florida River area, from 22 to 31 times; and in the Vallecito Reservoir and Los Pinos River area, from 9 to 30 times.

References Cited

Browning, T.W., 2001, Guidelines for determining 100-year flood flows for approximate floodplains in Colorado, version 5.0 (draft): Denver, Colorado Water Conservation Board, 37 p.

Cannon, S.H., 2001, Debris-flow generation from recently burned drainage basins: Environmental and Engineering Geoscience, v. 7, no. 4, p. 321–341.

Cannon, S.H., Kirkham, R.M., and Parise, Mario, 2001, Wildfire-related debris-flow initiation processes, Storm King Mountain, Colorado: Geomorphology, v. 39, p. 171–188.

Cannon, S.H., Michael, J.A., and Gartner, J.E., 2003, Assessment of potential debris flow peak discharges from basins burned by the 2002 Coal Seam Fire, Colorado: U.S. Geological Survey Open-File Report 03–333.

Cannon, S.H., Michael, J.A., Gartner, J.E., and Gleason, J.A., 2003, Assessment of potential debris flow peak discharges from basins burned by the 2002 Missionary Ridge Fire, Colorado: U.S. Geological Survey Open-File Report 03–332.

Cannon, S.H., Powers, P.S., and Savage, W.Z., 1998, Fire-related hyperconcentrated and debris flows on Storm King Mountain, Glenwood Springs, Colorado, USA: Environmental Geology, v. 34, no. 2–3, p. 210–218.

Costa, J.E., 1988, Rheologic, geomorphic, and sedimentologic differentiation of water floods, hyperconcentrated flows, and debris flows, *in* Flood geomorphology: New York, John Wiley and Sons, p. 113–122.

Costa, J.E., and Jarrett, R.D., 1981, Debris flows in small mountain stream channels of Colorado and their hydrologic impacts: Bulletin of the Association of Engineering Geologists, v. XVIII, no. 3, p. 309–322.

Cubworth, A.G., Jr., 1989, Flood hydrology manual—A water resources technical publication: Bureau of Reclamation, Denver, 243 p.

Doherty, John, 1998, PEST—Model-independent parameter estimation: Bethesda, Md., Watermark Numerical Computing, S.S. Papadopuoulous Associates, 200 p.

Doherty, John, 2001, PEST-ASP upgrade notes: Brisbane, Watermark Numerical Computing, 21 p.

Duan, Nathan, 1983, Smearing estimate—A nonparametric retransformation method: Journal of the American Statistical Association, v. 78, no. 383, p. 605–610.

Elliott, J.G., and Parker, R.S., 2001, Developing a post-fire flood chronology and recurrence probability from alluvial stratigraphy in the Buffalo Creek drainage basin, Colorado, USA, , *in* Hydrologic processes, v. 15: John Wiley and Sons, Ltd., p. 3039–3051.

Environmental Systems Research Institute, 2002, Getting started with ArcGIS: Environmental Systems Research Institute user's manual, 253 p.

Environmental Systems Research Institute, 2004, Using ArcGIS Spatial Analyst, 232 p.

Federal Emergency Management Agency, 1978, WSP2 computer model runs in Douglas County FIS study by Howard, Needles, Tammen, and Bergendoff, under contract no. H–4016.

Foster Wheeler Environmental Corporation, 1999, Landscape assessment, Upper South Platte Watershed: USDA Forest Service, South Platte Ranger District, Morrison, Colo., *http://www.fs.fed.us/r2/psicc/spl/south_platte_web/volume_1_contents.htm* (accessed November 25, 2002), variously paginated.

Griffiths, P.G., Webb, R.H., and Melis, T.S., 1996, Initiation and frequency of debris flows in Grand Canyon, Arizona: U.S. Geological Survey Open-File Report 96–491, 35 p.

Guy, H.P., 1970, Fluvial sediment concepts: Techniques of Water-Resources Investigations of the U.S. Geological Survey, book 3, chap. C1, 55 p.

Hansen, W.R., Chronic, J., and Matelock, J., 1978, Climatography of the Front Range urban corridor and vicinity, Colorado: U.S. Geological Survey Professional Paper 1019, Washington, D.C., 59 p.

Hungr, O., Morgan, G.C., and Kellerhals, R., 1984, Quantitative analysis of debris-torrent hazards for design of remedial measures: Canadian Geotechnical Journal, v. 21, p. 663–677.

Infotek Development, Inc., 1993, LT4X Data conversion software reference manual, v. II.

Interagency Advisory Committee on Water Data, 1982, Guidelines for determining flood flow frequency, Bulletin 17B: U.S. Department of the Interior, U.S. Geological Survey, Office of Water Data Coordination, Reston, Va.

Jarrett, R.D., and Costa, J.E., 1988, Evaluation of the flood hydrology in the Colorado Front Range using precipitation, streamflow, and paleoflood data for the Big Thompson River basin: U.S. Geological Survey Water-Resources Investigations Report 87–4117, 37 p.

Key, C.H., and Benson, N.C., 2002, Measuring and remote sensing of burn severity, *in* Coffelt, J.L. and Livingston, R.K., U.S. Geological Survey Wildland Fire Workshop, Los Alamos, N. Mex., October 31–November 3, 2000: U.S. Geological Survey Open-File Report 02–11, p. 55.

Kircher, J.E., Choquette, A.F., and Richter, B.D., 1985, Estimation of natural streamflow characteristics in western Colorado: U.S. Geological Survey Water-Resources Investigations Report 85–4068, 28 p.

Kirkham, R.M., Parise, Mario, and Cannon, S.H., 2000, Geology of the 1994 South Canyon wildfire area, and a geomorphic analysis of the September 1, 1994, debris flows, south flank of Storm King Mountain, Glenwood Springs, Colorado: Colorado Geological Survey Special Publication 46, 39 p.

Major, J.J., 1993, Rheometry of natural sediment slurries: Proceedings of the 1993 Conference, Hydraulics Division, American Society of Civil Engineers, San Francisco, California, p. 1415–1421.

McCuen, R.H., 1989, Hydrologic analysis and design: Englewood Cliffs, N. J., Prentice-Hall, 867 p.

Miller, J.F., Frederick, R.H., and Tracey, R.J., 1973, NOAA Atlas 2, Precipitation-frequency atlas of the western United States, v. 3—Colorado: U.S. Department of Commerce, National Oceanic and Atmospheric Administration, National Weather Service, Silver Spring, Md., 67 p.

Moody, J.A., and Martin, D.A., 2001a, Hydrologic and sedimentologic response of two burned drainage basins in Colorado: U.S. Geological Survey Water-Resources Investigations Report 01–4122, variously paginated.

Moody, J.A., and Martin, D.A., 2001b, Post-fire, rainfall-intensity-peak discharge relations for three mountainous drainage basins in the western USA, *in* Hydrologic Processes, v. 15: John Wiley and Sons, Ltd., p. 2981–2993.

O'Brien, J.S., 1993, FLO-2D two-dimensional flood routing system, version 2001.06: FLO-2D Software, Inc., Nutrioso, Ariz., CD-ROM.

O'Brien, J.S., 2001, FLO-2D user's manual, version 2001.06: FLO-2D Software, Inc., Nutrioso, Ariz., variously paginated.

O'Brien, J.S., and Fullerton, W.T, 1989, Hydraulic and sediment transport study of Crown Pointe flood wall: Breckenridge, Colo., Lenzotti and Fullerton Consulting Engineers, Inc., 34 p.

Pierson, T.C., and Costa, J.E., 1987, A rheologic classification of subaerial sediment-water flows: Geological Society of America, Reviews in Engineering Geology, v. VII, 12 p.

Pierson, T.C., and Scott, K.M., 1985, Downstream dilution of a lahar—Transition from debris flow to hyperconcentrated streamflow: Water Resources Research, v. 21, p. 1511–1524.

Rowe, P.B., Countryman, C.M., and Story, H.C., 1954, Hydrologic analysis used to determine effects of fire on peak discharge and erosion rates in southern California drainage basins: U.S. Department of Agriculture, Water Resources Center Archives, University of California, Berkeley, 48 p.

Simons, Li & Associates, Inc., 1983, Hydrology report for Town of Rangely, City of Rifle and Garfield County flood insurance studies: FEMA Contract No. EMW–C–0942, Denver, Colorado, variously paginated.

Soil Conservation Service, 1985, National engineering handbook, sec. 4: U.S. Department of Agriculture, Washington, D.C.

Taylor, A.B., and Schwarz, H.E., 1952, Unit hydrograph lag and peak flow related to basin characteristics: Transactions of the American Geophysical Union, v. 33, p. 235–246.

URS Corporation, 2000, The Cerro Grande post-fire hydrologic analysis: Denver, Colo., URS Corporation, variously paginated.

U.S. Army Corps of Engineers, 1957, Flood prediction techniques: U.S. Department of the Army, TB 5–550–3, Washington D.C.

U.S. Army Corps of Engineers, 1979, Hydrology, Crystal River, Colorado: U.S. Department of the Army, Sacramento District, Internal Office Report, Sacramento, Calif.

U.S. Army Corps of Engineers, 1998, Technical data notebook, Flood Insurance Study, April 1998, Glenwood Springs and Garfield County, Colorado: U.S. Army Corps of Engineers, Sacramento, Calif., variously paginated.

U.S. Army Corps of Engineers, 2000, Post Cerro Grande fire hydrology to support project formulation for grade control structure design, Guaje Arroyo near Los Alamos, NM: Internal Office Report, U.S. Department of the Army Albuquerque District, Albuquerque, New Mexico, variously paginated.

U.S. Army Corps of Engineers, 2001a, HEC-RAS River Analysis System version 3.0: U.S. Army Corps of Engineers Hydrologic Engineering Center, Davis, Calif., variously paginated.

U.S. Army Corps of Engineers, 2001b, Hydrologic modeling system HEC-HMS: U.S. Army Corps of Engineers Hydrologic Engineering Center, Davis, Calif., 188 p.

U.S. Army Corps of Engineers, 1998, HEC–1 flood hydrograph package user's manual: U.S. Army Corps of Engineers Hydrologic Engineering Center, Davis, Calif., version 4.1, 434 p.

USDA Forest Service, 2002a, Burned area emergency stabilization and rehabilitation plan, Hayman fire: U.S. Department of Agriculture, PSICC, June 2002 Hydrology Report, unpublished report.

USDA Forest Service, 2002b, Burned area emergency stabilization and rehabilitation plan, Coal Seam Fire: U.S. Department of Agriculture, PSICC, June 2002 Hydrology Report, unpublished report.

USDA Forest Service, 2002c, Burned area emergency stabilization and rehabilitation plan, Missionary Ridge and Valley fires: U.S. Department of Agriculture, July 2002 Hydrology Report, *http://www.fs.fed.us/r2/sanjuan/bulletin_board/baerreport.htm* (accessed August 9, 2002), variously paginated.

Vaill, J.E., 2000, Analysis of the magnitude and frequency of floods in Colorado: U.S. Geological Survey Water-Resources Investigations Report 99–4190, 35 p.

Varnes, D.J., 1978, Slope movement types and processes, *in* Schuster, R.L., and Krizek, R.J., eds., Landslides analysis and control: Washington, D.C., National Academy of Sciences, Transportation Research Board Special Report 176, p. 11–33.

Veenhuis, J.E., 2002, Effects of wildfire on the hydrology of Capulin and Rito de los Frijoles canyons, Bandolier National Monument, New Mexico: U.S. Geological Survey Water-Resources Investigations Report 02–4152, 39 p.

Wright-McLaughlin Engineers, 1975, Urban storm drainage criteria manual: Denver Regional Council of Governments, volumes I and II.

Appendixes

Appendix 1. Summary of Methods for Post-Fire Flood and Debris-Flow Hazard Analyses

[Methods are described in greater detail in the previous sections of this report]

Procedures for All Hydrologic Hazards: Sediment-Laden Water Floods and Debris Flows

Short-Term Hazards

1. Determine the dominant hydrologic processes likely to create hazards in the short term (perhaps 3–6 years) before substantial drainage basin recovery from the effects of fire.

2. Acquire or construct digital elevation model (DEM) data for the burned drainage basins and downstream areas with potential for flood or debris-flow inundation. Identify the appropriate resolution of DEM data based on data availability, modeling requirements, and project cost. Compute drainage-basin area, length, and slope using a geographical information system (GIS).

3. Acquire or survey detailed channel cross sections along main stem of channels, if flood-plain mapping will be done.

4. Compile historical peak-discharge data from streamflow-gaging stations located within or near the burned area (if available), or from drainage basins with similar climate and geography to those of the affected area. If recorded streamflow data are not available for the affected area, regional regression equations derived from gage data collected in hydrologically similar regions may be appropriate.

5. Acquire precipitation data from nearby weather stations or from the NOAA precipitation-frequency atlas (Miller and others, 1973). An observed or design hyetograph representative of the study area is needed for rainfall-runoff modeling.

6. Select an appropriate computer program to be used for rainfall-runoff modeling. In this study, the U.S. Army Corps of Engineers' Hydrologic Modeling System (HEC-HMS) was selected (U.S. Army Corps of Engineers, 2000).

7. Select an appropriate mathematical model to estimate the precipitation-runoff and routing process. In this study, the SCS Curve Number Loss Model (Soil Conservation Service, 1985) was selected to estimate runoff volume as a function of the precipitation hyetograph and drainage-basin characteristics. The SCS Curve Number Loss Model includes a transformation to convert runoff volume to a streamflow hydrograph, and hydrologic routing to "account for storage and energy flux as water moves through stream channels" (U.S. Army Corps of Engineers, 2000).

8. Estimate pre-burn rainfall-runoff model parameters for all drainage basins in the burned area in terms of the loss/transform model to be used. Parameters required for the SCS Curve Number Model are the runoff curve number, initial abstraction, and basin lag time. Calibration of pre-burn rainfall-runoff model parameters may be done manually (trial-and-error), or by using an objective method based on nonlinear regression. In this study, the objective calibration method was used to incrementally adjust the parameter values until the modeled peak discharge at the basin outlet matched the "t-year" peak discharge (where the "t-year" value characterizes the recurrence interval of interest). In the objective calibration method, an appropriate precipitation hyetograph, of specific depth-duration-frequency (such as the 6-hour, 100-year storm), is used in conjunction with a rainfall-runoff model and an optimization algorithm to estimate the optimal set of drainage-basin parameters.

9. Once the pre-burn rainfall-runoff model has been calibrated to local or regional hydrologic conditions, the pre-burn drainage-basin parameters are adjusted to reflect post-burn conditions. Post-burn runoff curve numbers for various burn severities, documented by the USDA Forest Service BAER Teams, were used in this study (see for example, USDA Forest Service, 2002c). Photogrammetric methods, which can provide a measure of the burn intensity, also may be used.

10. Where affected drainage basins and subbasins include burned and unburned areas, composite post-burn runoff curve numbers are derived using a weighting procedure based on the governing relation between runoff and precipitation excess. In this study, the weighting procedure was defined in terms of precipitation excess according to the governing equations of the SCS runoff curve number method (Soil Conservation Service, 1985).

11. Estimate post-burn peak discharges (t-year recurrence interval) and post-burn runoff hydrographs for the burned drainage basins, using the rainfall-runoff model (for example, HEC-HMS), the computed post-burn rainfall-runoff model parameters, and the t-year rainfall distribution defined by amount, duration, and cumulative density function (as previously selected).

12. Route the main-stem peak discharge for post-burn conditions using a hydraulic model such as HEC-RAS (U.S. Army Corps of Engineers, 2001a), and complete the flood-hazard map according to conventional procedures.

Long-Term Hazards

1. Evaluate the post-fire recovery period and estimate hydrologic conditions for the drainage basin over a longer period of time. The long-term recovery period reflects the time in years for the drainage basin to reach a generally stable condition, not the time required for the drainage basin to return to pre-burn conditions.

2. In this study an exponential decay equation, developed on the basis of assumptions and a limited amount of measured data, was used to estimate input drainage-basin parameters for a time-series of 50 years, beginning with post-fire conditions. The rainfall-runoff model was then used to obtain a series of estimated peaks for t-year design storm at the downstream end of the modeled area.

3. The resultant series of estimated peaks was evaluated to identify the period of time (in years) in the recovery process for which the annual reduction in the estimated peak discharge becomes relatively stable (less than 5 percent per year). This period of time is called "long-term recovery."

4. Estimate peak discharges and runoff hydrographs for long-term recovery (t-year recurrence interval), using the rainfall-runoff model (for example, HEC-HMS).

5. Route the main-stem peak discharge for long-term recovery using a hydraulic model such as HEC-RAS (U.S. Army Corps of Engineers, 2001a), and complete the flood-hazard map according to conventional procedures.

Additional Procedures for Sediment-Laden Water Floods

1. Bulk or increase the discharge hydrograph volumetrically, to account for the addition of entrained sediment (the result will be increased water discharge as surrogate for sediment load). In this study, a bulking factor was applied to basin areas determined to have moderate to high burn severity. Application of a bulking factor is an interpretive decision that will be based on the drainage-basin characteristics of a given study area. For water flooding, the theoretical upper limit of sediment concentration by volume is 20 percent. This may be considered the upper limit of adjustment of the hydrograph for sediment-laden water floods. A sediment concentration of 20 percent by volume translates to a bulking factor of 1.25, which was used in this study (O'Brien and Fullerton, 1989).

2. Route the sediment-adjusted flood hydrographs through the drainage basin by using hydrologic routing routines included in the rainfall-runoff model. In this study, Muskingum and Muskingum-Cunge routing methods were applied in HEC-HMS.

3. Compute post-fire flood elevations for post-burn peak discharges at selected cross-section locations along the study reach using an appropriate hydraulic model (for example, HEC-RAS), and delineate the resulting flood-plain boundaries on a topographic map using DEM (or photogrammetric) data. This constitutes the short-term "Hazards Map."

Additional Procedures for Debris Flows

1. Debris flows are modeled using an appropriate flood and debris-flow routing model. In this study, the FLO-2D two-dimensional debris-flow-routing model was used (O'Brien, 1993, 2001).

2. Convert DEM maps into an ArcGIS (Environmental Systems Research Institute, 2002) GRID format. Divide the grid data sets into subsets covering the channel and depositional areas to be modeled. Import the grid data into FLO-2D (or other appropriate debris-flow routing model).

3. Import the post-burn inflow hydrograph (generated using HEC-HMS) into FLO-2D. In this study, hydrographs corresponding to the 100-year post-burn peak discharges were used. Note: Procedures to compute the post-burn inflow hydrograph (water only, no sediment bulking) were described in the previous section ("Additional Procedures for Sediment-Laden Water Floods").

4. Apply variable volumetric sediment concentrations (C_v) to the input hydrograph. In this study, the following concentrations were applied to each inflow hydrograph: initial C_v 20 percent, mean C_v approximately 31 percent, maximum C_v 48 percent (preceding the input water hydrograph peak), C_v 43 percent at the time of the input water hydrograph peak, and C_v 20 percent for the duration of the event.

5. Generate FLO-2D model output files, including maximum velocity and inundation depth files. In this study, maximum debris-flow depths in each grid element were overlaid on a topographic map.

6. Delineate debris-flow inundation maps using FLO-2D output files, DEM data, and an appropriate GIS.

Appendix 2. The Manual Calibration Method for the Hayman Burned Area

This Appendix presents the results obtained with the manual calibration method. The manual calibration method involved incremental adjustment of runoff curve numbers (RCN) to obtain discharges at the mouth of each drainage basin tributary to the South Platte River to match results from the regional 100-year peak-flow equations. Results from the manual calibration method were the basis for the flood hazard maps presented in this report (figs. 8 through 14) and in a previously composed USGS Administrative Report presented to FEMA in July 2003 (J.G. Elliott and others, written commun.).

The material in this Appendix, including figures and tables, is the same as that presented in the USGS 2003 Administrative Report to FEMA and are the final products for the short-term (approximately 1 to 5 years) hazard assessment of the Hayman burn area. The material in this Appendix is included for comparison to results from the objective rainfall-runoff model calibration method.

South Platte River "Limited-Detail" Hydrologic Analysis

Post-fire hydrologic analyses were conducted to evaluate the effects of the 100-year peak flow on the burned and adjacent unburned areas of the South Platte River drainage basin and reflect drainage-basin conditions that are expected to exist during the next several years (in the short-term, prior to substantial regrowth of vegetation in the burned areas). The results of these analyses (known to FEMA as a "Limited Detail Analysis") were used to delineate a hazard-mitigation map for post-fire, 100-year flooding of the South Platte River and will not be used for regulatory purposes (John Liou, Federal Emergency Management Agency, oral commun., 2003).

The approach to the post-fire "limited-detail" hydrologic analyses included the following steps:

1. Inflow conditions were established for the South Platte River at the upstream boundary of the burned area and for the South Platte River downstream from Cheesman Dam.

2. A rainfall-runoff model was calibrated for pre-fire (unburned) conditions in the affected drainage basins tributary to the South Platte River. Runoff generated by the 100-year, 6-hour rainstorm (2.4 inches) was calibrated to computed 100-year peak discharge (flood-frequency analysis) at selected stream-gage sites in the study area.

3. Rainfall-runoff of the 100-year, 6-hour storm for post-fire conditions in burned drainage basins tributary to the South Platte River was modeled.

4. Peak discharges for drainage basins tributary to the South Platte River were computed (with routing of the runoff hydrograph through the larger drainage basins).

5. Peak discharges for burned drainage basins were increased using a bulking factor to reflect the increased runoff volume due to large sediment loads.

6. Peak discharges (bulked flow) for selected reaches of the South Platte River (within and downstream from the burned area) were computed using a hydrograph routing algorithm.

South Platte River Inflow Conditions

Boundary flow conditions at the upstream edge of the fire perimeter and at the outflow from Cheesman Dam were established as follows.

Upstream Edge of Burn Perimeter

Discharge records for streamflow-gaging station 06696000 (South Platte River near Lake George, drainage area 963 mi^2) are available for the period 1930–98; the gage was located downstream from the outlet of Elevenmile Canyon Reservoir (owned and operated by the Denver Water Board). Because of the large contributing drainage area of the South Platte River basin upstream from the wildfire area and the substantial regulation/storage capacity of upstream reservoirs, it is extremely unlikely that a 100-year flood would occur throughout the entire basin during a single runoff event. To account for potential antecedent runoff and reservoir releases into the burned area, a 10-year peak discharge was selected as the boundary inflow condition. The 10-year peak discharge for streamflow-gaging station 06696000 was computed for the period of record since completion of Elevenmile Canyon Reservoir (1933–98). The resulting discharge is 840 ft^3/s.

The 10-year peak discharge was adjusted to account for contributing drainage area between streamflow-gaging station 06696000 and the upstream edge of the Hayman fire perimeter (drainage area 1,133 mi^2), using a regional regression equation for ungaged sites near gaging stations developed by the USGS for mountain regions of Colorado (Vaill, 2000). The adjusted 10-year peak discharge is 940 ft^3/s, which was used as the inflow peak for the South Platte River at the upstream edge of the fire perimeter. A similar analysis was used to compute the pre-burn discharge for Tarryall Creek, which also is regulated. The computed 10-year peak discharge was 715 ft^3/s (Tarryall Creek near Lake George). Tarryall Creek flows into the burned area of the Hayman fire and was treated as a boundary inflow point.

Outflow from Cheesman Dam

Cheesman Reservoir is owned and operated by the Denver Water Board as a water-supply reservoir for the City of Denver. It is not designated for flood control, so hydrologic analysis of the 100-year flood assumes fill-and-spill operation of the dam. That is, the reservoir is allowed to fill to capacity then freely spill excess over the spillway. Based on discussions with staff of the Denver Water Board (Robert Steger, Denver Water Board, oral commun., 2003), the boundary condition at Cheesman Dam was determined to be a full reservoir, with uncontrolled flow over the spillway in response to upstream runoff. The outlet works (release capacity 1,400 ft^3/s) were assumed to be closed; the spillway (release capacity 22,370 ft^3/s) would pass the entire flood (subject to peak attenuation by the reservoir) and produce the base flow to be used for modeling of the South Platte River downstream from the dam. Outflow from Cheesman Dam was assumed to contain no sediment.

Cheesman Reservoir could be filled with water at any time within 1 to 4 years after the fire, or more, in response to either operational considerations (Cheesman evaporation rates are smaller than upstream reservoirs on the South Platte River system) or natural runoff. As a result, both short-term (hazard-mitigation) and long-term modeling scenarios reflect a full-reservoir condition.

South Platte River Tributary Rainfall-Runoff Modeling—Manual Calibration Method

Rainfall-runoff modeling was used to develop post-fire hydrographs for 19 principal drainage basins tributary to the South Platte River within and downstream from the Hayman burn area. These principal drainage basins and an additional 22 minor contributing drainages were analyzed with the U.S. Army Corps of Engineers HEC-HMS computer model (U.S. Army Corps of Engineers, 2001b) and by using the 100-year, 6-hour storm (2.4 inches).

Rainfall-Runoff Model Methodology for the Hayman Fire

Rainfall-runoff modeling was conducted in two steps to simulate (1) preburned or unburned conditions, and (2) burned conditions.

Step 1, Modeling of Unburned Conditions

The runoff hydrograph for the 100-year peak discharge was developed for natural, unburned conditions of each drainage basin. Because streamflow data for most tributary drainage basins were not available, a hydrograph and peak discharge for each drainage basin were computed using the rainfall-runoff model; basin hydrographs were generated in the model using the Soil Conservation Service (SCS) Curve Number Loss model (Soil Conservation Service, 1985) as described previously in the "Rainfall-Runoff Model Calibration and Simulation" section of the report.

A comparison of measured 100-year peak flows (Interagency Advisory Committee on Water Data, 1982) at five streamflow gaging stations in the Goose and Tarryall Creek drainages with the results of regional regression equations developed for mountain areas of Colorado (Vaill, 2000; Browning, 2001; Kircher and others, 1985) showed that the regional equations substantially overestimated the observed 100-year peaks (by a factor of 2 or more). As an alternative, the five streamflow gaging stations in the Goose and Tarryall Creek drainages were used to develop a local regional equation for the study area. Table 2–1 shows a summary of the drainage basin characteristics and the computed 100-year peak discharges used to develop the relation (Interagency Advisory Committee on Water Data, 1982). The resulting peak discharges computed using the local regression model, along with those predicted by the Vaill regional equation (2000), are shown in table 2–1 for comparison. The sites generally are unaffected by regulation and are considered to reflect meteorological and hydrological characteristics representative of the burned and adjacent unburned drainage basins affected by the fire. Because of the short period of historical record for each gage, no mixed-population analyses (snowmelt and rainfall peaks) were performed.

Table 2–1. Characteristics of streamflow-gaging stations used for calibration of 100-year peak discharge for pre-burn conditions, South Platte drainage basin.

[mi^2, square miles; ft, feet; ft/ft, feet per feet; ft^3/s, cubic feet per second; Q_{100}, 100-year peak discharge]

Streamflow-gaging station	Period of record	Drainage area (mi^2)	Gage elevation (ft)	Basin slope (ft/ft)	Q_{100} at gage (ft^3/s)	Predicted Q^{100}, equation A–1 (ft^3/s)	Predicted Q_{100}, Vaill[1] (ft^3/s)
Tarryall Creek at Upper Station near Como (06696980)	1978–86	23.7	9,935	0.316	236	192	569
Michigan Creek above Jefferson (06697450)	1978–86	23.1	9,503	0.246	196	188	513
Jefferson Creek near Jefferson (06698000)	1978–86	11.8	9,600	0.333	81	108	355
Tarryall Creek below Rock Creek, near Jefferson (06699005)	1983–97	236	9,020	0.182	1,050	1,270	2,390
Goose Creek above Cheesman Lake (06700500)	1924–82	86.6	6,910	0.317	646	559	1,410

[1]Vaill, 2000.

An ordinary-least-squares regression model to predict 100-year peak discharge, Q_{100}, as a function of drainage area, A, was developed using the gage data shown in table 2–1. The resulting equation and regression statistics were:

	R squared	Standard error of estimate	(2–1)
$Q_{100} = 14.21\ A^{0.823}$	0.995	28 percent	

The regression coefficient (14.21) in the equation includes a bias correction factor to correct for bias introduced in the process of converting the results of log-space regression analysis back to rectangular coordinates (Duan, 1983).

Similar one-parameter models for Q_{100} have been developed by Browning (2001) and by Jarrett and Costa (1988). A plot of the new regression analysis showing the best-fit line defined by the equation is shown in figure 2–1; all five data points lie within the computed 95-percent confidence intervals (not shown) for the regression. The regression line generally plots lower and parallel to the equation defined by Jarrett and Costa (not shown) for a larger dataset (basins below 8,000 ft elevation) developed for the South Platte River Basin.

The regression model was used as the basis for calibration of the pre-burn, 100-year peak discharge of drainage basins modeled using HEC-HMS. The regression model is limited by the small number of streamflow gages available for analysis within the study area and by the relatively short period of record at each gage (which reduces the reliability of the peak-flow statistics).

The Soil Conservation Service (SCS) curve number method was used to estimate rainfall-runoff losses in individual, smaller tributaries. The objective calibration method, described in the “Rainfall-Runoff Model Calibration and Simulation” section of the report, was used to estimate rainfall-runoff losses in the larger tributary drainage basins that were a composite of several smaller drainage basins (Turkey Creek, Goose Creek, Wigwam Creek, and Horse Creek) (fig. 4 of the main body of the report). These larger composite drainage basins were divided into smaller subbasins that generally correspond to basin delineations defined by the BAER Team (USDA Forest Service, 2002a) in their post-fire analysis of the Hayman area; routing of subbasin hydrographs to the basin mouth was conducted for these large basins.
On the basis of existing reports that describe pre-fire drainage basin conditions within the study area (Foster Wheeler Environmental Corporation, 1999; USDA Forest Service, 2002a) and assessment of aerial photography, pre-burn runoff curve numbers (RCN) between 55 and 67 were selected for each drainage basin (pre-burn RCNs used in this study are somewhat lower than those selected by the BAER Team). In addition to drainage basin RCN values, the initial abstraction (infiltration) and the percentage of impervious area were entered into the model. The pre-burn abstraction values were selected using default model computations based on pre-burn drainage basin characteristics and are reflective of the weathered rock soils that dominate the area. Impervious areas (rock outcrops, roads, and so forth) were mapped by the BAER Team and were accounted for in the model by adjusting RCNs for those areas.

The SCS dimensionless unit hydrograph method was used to compute the resultant hydrograph. The Taylor-Schwarz (1952) lag-time equation was selected for use in modeling after testing with several lag-time computation methods; other methods considered include the SCS lag-time equation (Soil Conservation Service, 1985) and the Denver lag-time equation (Wright-McLaughlin Engineers, 1975). The Taylor-Schwarz method required minimal parameter calibration in modeling

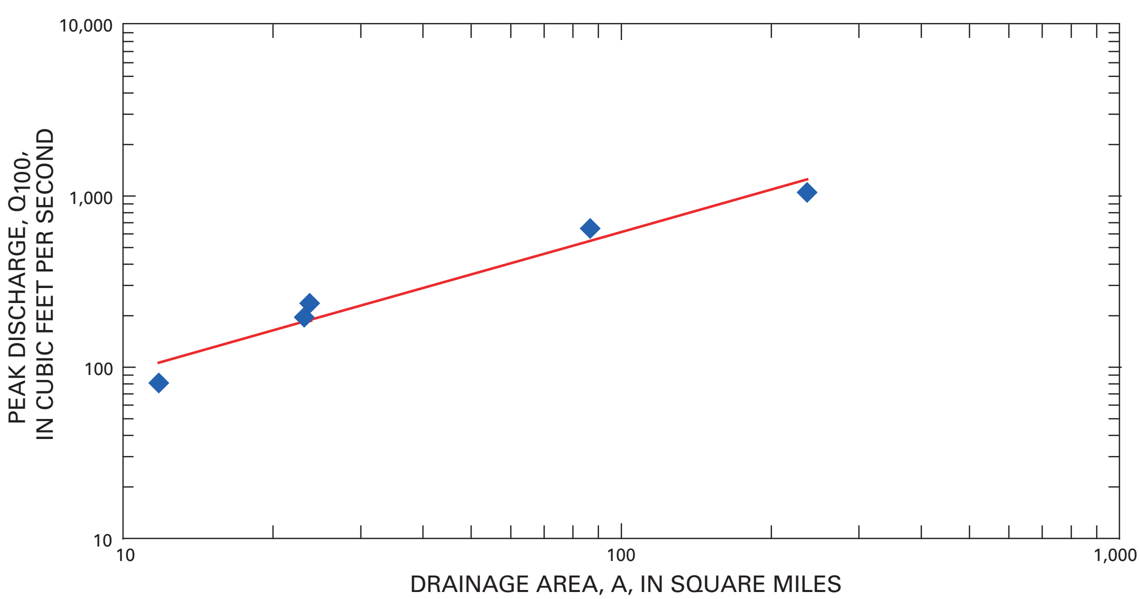

Figure 2–1. Relation of 100-year flood peaks and drainage area showing the best-fit regression line using an ordinary-least-squares regression model.

pre-burn, 100-year peak discharges for the study area. Other methods resulted in parameter values outside of the range of values that would be expected for the study area. The Taylor-Schwarz equation has the following form:

$$L_t = C_t\,(LL_{ca})^{0.3} \quad (2–2)$$

$$Ct = 0.6/S^{0.5} \quad (2–3)$$

where

- L_t is the Taylor-Schwarz lag time, in hours;
- C_t is a coefficient of basin topography based on basin slope;
- L is the basin length, measured along the main channel to the furthest point on the basin perimeter, in miles;
- L_{ca} is the length from the basin mouth to the basin centroid, measured along the main channel from its origin (as determined from the base map) to a point opposite the centroid, in miles;

and

- S is the average basin slope.

Simulated 100-year peak discharge for pre-burn conditions was calibrated to the 100-year peak discharge computed with equation 2-1. Calibration generally was conducted within the range of drainage area represented by the regression analysis. Calibration of the four larger basins (Turkey Creek, Goose Creek, Wigwam Creek, and Horse Creek) was designed to produce peak discharges that correspond to values predicted by equation 2–1 for the basin mouth (confluence with the South Platte River). Calibration of each drainage basin was done manually, by adjusting RCN values (and associated initial abstractions) incrementally until the simulated peak discharge at the drainage basin outlet was equal to the peak discharge predicted by equation 2–1.

Flow routing within the larger basins was performed using the Muskingum method (McCuen, 1989). Because observed hydrograph or field data were not available for calibration of the routing parameters, values of Muskingum K (defines the time of travel for a flood wave traversing the basin) and X (a weighting factor that describes the backwater storage effects of a channel) were selected within the range of commonly used values for channels in steep, upland drainage basins (McCuen, 1989; John Liou, FEMA, oral commun., 2003):

- Muskingum K = 0.6 hour;
- Muskingum X = 0.4, to reflect channels with little over-bank storage.

A summary of pre-burn calibration data (RCN, abstraction, lag-time factors) for all principal and minor drainage basins is provided in Appendix table 3–3.

Step 2, Modeling of Burned Conditions

Adjustments of the pre-burn peak discharge were made to reflect the burned conditions within each drainage basin. Existing studies documenting the hydrologic response of burned drainage basins in other areas were used to guide the calibration for post-burn conditions. The "Hayman Fire Hydrology Report" (USDA Forest Service, 2002a) was used to guide the selection of RCNs for post-burn conditions. The BAER Team study reports that marked increases in runoff occur in areas of moderate-to-high burn severity; low burn severity also contributes to increased runoff. Because of the detailed mapping of the post-burn drainage basins (including burn severity, rock outcrops, unburned area, and water courses) conducted by the BAER Team, and because of extensive USDA Forest Service experience with post-fire hydrology, the post-burn runoff curve numbers selected by the BAER Team generally were adopted for this study. Exceptions were the use of lowered RCNs for some unburned areas (as noted previously), and a slightly higher RCN for areas of moderate to high severity burn (explained herein). RCNs used for the modeling described in this report are:

- Rocky areas = 90
- Unburned forest = 55–60
- Low burn severity = 85
- Moderate and high burn severity = 98 (BAER Team used 95)

Where affected drainage basins and subbasins included burned and unburned areas, post-burn RCNs were computed by weighting the respective drainage basin conditions according to the governing equations of the SCS curve number method. The relation between RCN and drainage-basin runoff is nonlinear, such that small burned areas can be expected to cause substantial increases in runoff. Initial abstraction values generally decrease as a result of moderate to severe burned conditions (URS Corporation, 2000). In the SCS method, initial abstraction is a function of RCN. An RCN value of 95 produces an initial abstraction of 0.11 inch; an RCN value of 98 produces an initial abstraction of 0.04 inch. Runoff data and field observations made by the USGS (Robert Jarrett, oral commun., 2002) suggest that runoff in burned areas of the Buffalo Creek fire and Hayman fire (as well as other fires in the Western United States) can occur with as little as 0.1 inch of rainfall, indicating that initial abstractions (especially where burned soils may be hydrophobic) may be less than 0.1 inch. In view of these observations, a lower limit (conservative) abstraction value of 0.04 inch was used for areas of moderate-high burn severity (RCN = 98). This modification of RCN for moderate-high burn severity (from 95 to 98) resulted in an increase in computed peak discharges in the South Platte River of as much as 20 percent.

Removal of surface vegetation by wildfire can be expected to decrease the runoff lag time in an affected drainage basin (URS Corporation, 2000; U.S. Army Corps of Engineers, 2000). Because site-specific data are not available to calibrate this response, post-burn lag times were reduced as a function of the percentage of moderate-to-high burned area in each drainage basin. Adjustment of post-burn lag times was made using a lag-time equation developed by the BOR for the Rocky Mountain region (Cubworth, 1989, p. 74). The BOR equation has the same basic form as the Taylor-Schwarz equation, with the inclusion of a basin-slope parameter (U.S. Army Corps of Engineers, 1957). The BOR found that the Taylor-Schwarz coefficient C_t was related to the average Manning's n value representing the hydraulic characteristics of a drainage basin's drainage network. The following equation was used to compute lag time, L_g (in hours):

$$L_g = 26K_n\,[(LL_{ca})/S^{0.5}]^{0.33} \qquad (2\text{–}4)$$

where

- K_n is the average Manning's n value for the drainage basin;
- L is the basin length, measured along the main channel from its origin (as determined from the base map) to the furthest point on the basin perimeter, in miles;
- L_{ca} is the length to the basin centroid, measured along the main channel to a point opposite the centroid, in miles;

and

- S is the average basin slope.

Note that the term 26 K_n is a basin coefficient similar to the coefficient C_t in the Taylor-Schwarz equation. In order to better characterize the post-burn lag-time conditions, the following procedure was used:

1. Pre-burn lag times, calibrated using the Taylor-Schwarz equation and the regression equation for peak discharge data, were used to derive the corresponding value for K_n in equation 2-4; this essentially was a calibration process. The approach appears to fit well with the observed BOR data for the Rocky Mountains. Their relation predicts Manning's n to be in the range of 0.050 to 0.073 for thunderstorm lag times in the Rocky Mountains. Most of the Hayman pre-burn lag times lie within this range.

2. Post-burn lag-time conditions were adjusted using n = 0.030 for moderate-high burn areas and n = 0.040 for low-burn areas. A composite, weighted n value for each basin (based on percentage of unburned, low burn, and moderate-high burn areas) was used in the BOR lag-time equation. Manning's n values for post-burn conditions were selected on the basis of professional judgment and are considered to be the lower bound for post-burn drainage basin roughness.

Weighted, post-burn lag times can be as low as 39 percent of pre-burn lag times, depending on the area of drainage basin burned. A summary of post-burn calibration data (RCNs, abstractions, lag-time factors) for all principal and minor drainage basins is in Appendix table 3–4.

Table 2–2 shows the 19 principal drainage basins for which modeling was conducted and the results of the pre- and post-burn runoff calibrations. A rainfall depth of 2.4 inches (100-year, 6-hour storm) was applied uniformly over each basin, with no aerial distribution of the storm (Miller and others, 1973).

Runoff curve numbers for larger drainage basins are shown as a range of values determined for the subbasins within each drainage basin. Model data for all primary drainage basins, contributing subbasins, and minor drainages in the Hayman burn area are in Appendix tables 3–1, 3–2, 3–3, and 3–4.

Estimated Peak Discharges, South Platte River Tributaries

To account for the potential sediment bulking of floodflows in burned drainage basins, computed peak discharges were increased according to the assumption that sediment concentrations by volume (C_v) could reach the maximum water-flood limit of 20 percent (Costa, 1988). The equation of O'Brien and Fullerton (1989) was used to compute the bulking factor (BF):

$$BF = 1/(1 - C_v) \qquad (2\text{–}5)$$

For a C_v of 20 percent, the corresponding BF is 1.25. This factor was applied to peak water discharges computed by the HEC-HMS model for areas of moderate to high burn severity. The bulking factor was weighted according to relative burned area within each of the modeled drainage basins.

Simulated pre-burn, post-burn, and bulked 100-year discharges for each of the principal drainage basins are shown in table 2–2. Post-burn 100-year peak discharges for the 19 principal drainage basins (routed to the point of confluence with the South Platte River) are expected to increase 2 to 34 times pre-burn peaks. Among all modeled drainage basins (including subbasins) with substantial (>50 percent) moderate to severe burned areas, post-burn peak discharges are expected to be 8 to 44 times greater than pre-burn peaks. For those drainage basins with substantial burned area, average predicted peak discharges per square mile for pre-burn conditions is 15.8 $ft^3/s/mi^2$; average predicted peak discharges per square mile for post-burn conditions is 425 $ft^3/s/mi^2$. Predicted increases in post-burn peak discharge are in general agreement with the BAER Team's hydrologic assessment of the Hayman fire (USDA Forest Service, 2002a) and with hydrologic studies of other burned drainage basins (Rowe and others, 1954; Martin and Moody, 2001b; URS Corporation, 2000).

Estimated Peak Discharges, Selected Reaches of the South Platte River

As part of the hydrologic assessment of the Hayman fire on affected reaches of the South Platte River, the 100-year peak discharge for selected points along the river were computed on the basis of tributary inflow from drainage basins within and adjacent to the burned area. Cumulative peak discharge in the main-stem South Platte River was computed as the sum of the main-stem flow and tributary peak discharges (table 2–2) at the point of interest. In-stream flow routing, to account for in-channel storage and peak attenuation at successive downstream sections, was performed using the routing routines in the HEC-HMS computer model.

Table 2–2. Drainage-basin characteristics, modeling parameters, and computed peak discharges for pre-burn, post-burn, and post-burn (bulked) conditions in the 19 principal drainage basins affected by the Hayman fire.

[mi^2, square miles; %, percent; Q_{100}, 100-year discharge; in, inches; ft^3/s, cubic feet per second; Q_u, pre-burn 100-year discharge; Q_b, post-burn 100-year discharge; Q_{bb}, post-burned bulked 100-year discharge; $ft^3/s/mi^2$, cubic feet per second per square mile; N/A, not applicable]

Basin name and number (downstream order)	Drainage area (mi^2)	Area of low burn (%)	Area of moderate to high burn (%)	Rainfall depth[1] (in)	Curve number*		Q_{100} (ft^3/s)				Ratio Q_{bb}/Q_u
					Pre-burn	Post-burn (weighted)	Pre-burn, Q_u	Post-burn, Q_b	Post-burn (bulked), Q_{bb}	Qbb ($ft^3/s/mi^2$)	
Vermillion Creek (1)	4.93	50.0	27.6	2.4	58	86	52.6	665	711	144	13.5
Crystal Creek (2)	5.27	46.4	29.0	2.4	59	86	55.5	663	711	135	12.8
Beaver Creek (3)	3.54	51.5	33.7	2.4	59	88	40.3	531	576	163	14.3
Hackett Gulch (4)	6.56	37.2	33.2	2.4	56	86	66.4	954	1,030	157	15.5
Tarryall Creek (5)	443	0.96	0.89	2.4	N/A	86	715	2,160	2,160	N/A	N/A
Longwater Gulch (6)	2.34	29.3	67.6	2.4	57	94	28.8	641	749	320	26.0
Corral Creek (7)	4.38	15.7	70.3	2.4	55	93	47.6	1,150	1,350	308	28.4
Northrup Gulch (8)	3.84	37.2	58.2	2.4	58	93	43.5	844	967	252	22.2
Turkey Creek (9)	28.2	32.4	50.6	2.4	57–61	77–98	222	3.390	3,820	135	17.2
Goose Creek (10)	95.2	5.29	15.1	2.4	57–58	58–98	607	4,120	4,280	45.0	7.1
Cheesman Reservoir											
Schoonover Gulch (11)	1.71	11.7	85.4	2.4	57	96	22.0	607	737	431	33.5
Sixmile/Wigwam Creek (12)	36.7	13.7	34.2	2.4	58–60	78–96	274	2,510	2,720	74.1	9.9
Fourmile Creek (13)	8.22	11.7	59.7	2.4	61	90	80.8	958	1,100	134	13.6
Horse Creek (14)	212	9.06	12.8	2.4	58–66	58–98	1,150	4,010	4,140	19.5	3.6
Lazy Gulch (15)	1.23	54.2	39.0	2.4	56	90	17.0	309	339	276	19.9
Brush Creek (16)	2.33	29.2	59.3	2.4	58	92	28.7	507	582	250	20.3
Unnamed drainage (17)	1.16	0.00	0.00	2.4	57	57	15.8	15.8	15.8	N/A	N/A
Saloon Gulch (18)	1.26	39.7	46.6	2.4	58	90	17.2	290	324	257	18.8
Gunbarrel/Kelsey Creek (19)	10.2	8.00	2.00	2.4	57	63	96.8	220	221	21.7	2.3

[1]NOAA Atlas 2 Volume III—Colorado (Miller and others, 1973).

Twenty river cross sections were surveyed through the study reach upstream and downstream from Cheesman Reservoir. These cross sections were located to improve the flood-plain delineation of the existing FEMA regulatory maps (designated by FEMA as an Approximate Study area) and to establish discrete flood elevations for the post-fire, 100-year flood through the affected reach. Each cross section was surveyed to the North American Vertical Datum of 1988 (NAVD88, vertical control) and to the North American Datum of 1983 (NAD83, horizontal control) by Global Positioning System (GPS) surveys. Left and right ends of each cross section were monumented (rebar rods with stamped, aluminum caps) to facilitate resurveys. Control coordinates (Universal Transverse Mercator) and elevations (NAVD88) for all cross sections are shown in Appendix 4; cross-section data (x-y coordinate pairs) are available from the U.S. Geological Survey, Colorado District, Denver, Colo.

Because of the distance between surveyed cross sections (generally 1 to 2 miles), water-surface elevations for computed peak discharges were determined using a normal-depth calculation (steady, uniform flow); step-backwater flow routing was not performed.

Main-Stem Peak Discharge Within the HEC-HMS Model Area

Cumulative drainage areas for each cross section were computed from GIS data. The 100-year peak discharge at each South Platte cross section within the HEC-HMS model area was determined from the routing computations. The Muskingum-Cunge routing routine, which incorporates cross-section and hydraulic properties of the surveyed cross sections, was used to route flows in reaches of the main-stem South Platte River. Routed peaks showed little attenuation. Sensitivity testing indicated that hydrograph attenuation was affected mainly by channel slope; the relatively steep slopes (measured as water-surface slope during the cross-section surveys) through the study reach preclude substantial attenuation.

The Modified Puls reservoir routing routine in HEC-HMS was used to route the computed flood hydrograph through Cheesman Reservoir and over the spillway to the downstream reach. As noted previously, the study assumes that Cheesman Reservoir is full, so that an inflow hydrograph would pass through the reservoir and over the spillway, into the downstream reach. The computed inflow hydrograph to Cheesman Reservoir consists of two components:

- Routed water-flood hydrograph, consisting of inflows from burned and unburned drainage basins.

- Computed sediment hydrograph to account for sediment bulking of South Platte River flows. The sediment hydrograph was computed by applying the bulking factor (eq. 2–5) to the portion of main-stem water discharge attributed to areas of moderate to high severity burn; the resulting peak was 1,750 ft^3/s.

These two components were combined to form the bulked inflow hydrograph. Because most sediment is assumed deposited in Cheesman Reservoir, a clear water (equivalent to the water-flood hydrograph plus the water discharge resulting from the displaced volume of inflowing sediment) was routed through the reservoir and over the spillway. On the basis of the conditions described herein, the computed peak discharge for the combined inflow hydrograph to Cheesman Reservoir was 19,000 ft^3/s; the computed total inflow volume was 19,800 acre-feet.

The routed outflow peak discharge (clear water) from Cheesman Reservoir was 11,900 ft^3/s. Peak discharges (with sediment bulking) computed for cross sections surveyed along the South Platte River downstream from Cheesman Reservoir range from 12,900 ft^3/s (at cross section DXS1) to 18,900 ft^3/s (at cross section DXS7).

Main-Stem Peak Discharge Downstream from the HEC-HMS Model Area

For South Platte reaches downstream from the area modeled using HEC-HMS (and downstream from the burn perimeter), peak discharge was adjusted for contributing drainage area using an equation relating peak discharge for "gaged" (simulated discharge using HEC-HMS) sites to ungaged sites as a function of relative drainage area (Vaill, 2000). The following equation was used:

$$Q_{100(u)} = Q_{100(g)}\,(A_u/A_g)^x \qquad (2–7)$$

where

$Q_{100(u)}$ is the 100-year peak discharge, in cubic feet per second, at the ungaged (unmodeled) site;

$Q_{100(g}$ is the 100-year peak discharge, in cubic feet per second, at the gaged (modeled) site;

A_u is the drainage area, in square miles, at the ungaged (unmodeled) site;

A_g is the drainage area, in square miles, at the gaged (modeled) site;

and

X is the average exponent for drainage area in the flood region of interest, derived from regression analysis of historical streamflow data.

Peak discharges computed for channel cross sections surveyed along the South Platte River downstream from the burned area range from 18,900 ft^3/s (at cross section DXS8), to 22,200 ft^3/s (at cross section DXS13 downstream from the confluence with the North Fork South Platte River), and 22,400 ft^3/s (at cross section WXS3 in Waterton Canyon). A summary of peak discharge and computed water-surface elevations for all South Platte channel cross sections is shown in table 2–3. Hazard-mitigation maps were constructed from the computed water-surface elevations to assist State and local emergency-response officials in planning for possible post-fire flooding. These oversized maps, including cross sections, are presented in figures 8 through 14 and accompany this report.

Table 2–3. Channel cross-section properties (normal-depth computation) for South Platte River reaches upstream and downstream from Cheesman Reservoir.

[ft^3/s, cubic feet per second; ft, feet; ft/ft, feet per feet; ft/s, feet per second; NAVD 88, North American Vertical Datum of 1988]

Name of cross section	Peak discharge (ft^3/s)	Water-surface elevation (ft) (NAVD88)	Channel slope (ft/ft)	Top width (ft)	Mean depth (ft)	Mean velocity (ft/s)	Froude number	Note
Reach upstream from Cheesman Reservoir								
Cross section UXS1	9,670	7,116.29	0.0047	314	4.10	7.51	0.70	Used average cross-section properties for entire reach
Cross section UXS2	10,400	6,950.71	0.0095	130	7.83	10.2	0.64	
Cross section UXS3	10,400	6,855.61	0.0038	125	7.37	11.3	0.73	
Reach downstream from Cheesman Reservoir								Routed peak outflow over spillway = 11,400 ft^3/s
Cross section DXS1	12,900	6,490.90	0.0018	223	8.77	6.60	0.39	Above Wigwam Creek confluence
Cross section DXS2	14,700	6,461.44	0.0027	203	8.97	8.07	0.48	Below Wigwam Creek confluence
Cross section DXS3	15,800	6,425.48	0.0031	195	8.62	9.40	0.59	Below Fourmile Creek confluence
Cross section DXS4	16,000	6,414.76	0.0067	145	9.54	11.6	0.66	Above Deckers and Horse Creek confluence
Cross section DXS4.5	18,600	6,380.28	0.0025	140	11.7	11.4	0.61	Trumbull stream gage
Cross section DXS5	18,700	6,359.44	0.0027	601	5.40	5.75	0.59	
Cross section DXS6	18,900	6,342.79	0.0039	334	6.77	8.36	0.67	Wide, flat flood plain through this reach
Cross section DXS7	18,900	6,298.31	0.0018	353	9.27	5.77	0.38	
Cross section DXS8	18,900	6,285.51	0.0027	612	6.74	4.58	0.44	End Hayman burn perimeter
Cross section DXS8.5	18,900	6,269.91	0.0016	241	10.9	7.22	0.40	
Cross section DXS9	18,900	6,226.30	0.0013	253	10.5	7.14	0.42	
Cross section DXS10	19,000	6,194.24	0.0039	249	8.39	9.09	0.58	
Cross section DXS11	19,200	6,163.26	0.0010	202	13.1	7.23	0.35	
Cross section DXS12	19,200	6,117.41	0.0024	164	11.1	10.58	0.60	
Cross section DXS13	22,200	6,100.36	0.0031	186	12.8	9.33	0.47	Below confluence of N.F. South Platte
Reach downstream from Strontia Springs Reservoir (Waterton Canyon)								
Cross section WXS2	22,300	5,725.81	0.0092	135	12.4	13.35	0.70	Waterton Canyon
Cross section WXS3	22,400	5,690.71	0.0038	204	11.0	9.96	0.54	Waterton Canyon

Appendix 3. Appendix Tables 3–1—3–14

Table 3–1. South Platte River basins and subbasins used in the HEC-HMS model upstream and downstream from Cheesman Reservoir.

[mi^2, square miles; BAER, Burned Area Emergency Rehabilitation; n/a, not applicable]

Model basin ID	Corresponding BAER basin(s)	Name of basin or drainage	Basin area (mi^2)
South Platte River basins and subbasins upstream from Cheesman Dam			
0.1	84	Unnamed	0.60
PA	80, 77, 75	South Platte Reach A	3.87
UBB1	-	Unburned basin 1ac	n/a
UBB2	-	Unburned basin 2ac	n/a
1	78	Vermillion Creek	4.93
UBB3	-	Unburned basin 3ac	n/a
2	76	Crystal Creek	5.27
UBB4	-	Unburned basin 4ac	0.32
PB	891	South Platte Reach B	11.3
3	74	Beaver Creek	3.54
4	65	Hackett Gulch	6.56
5A	58	Tarryall Creek	8.42
5B	58, 72	Tarryall Creek	3.11
5C	-	Tarryall Creek (upstream)	431
6	63	Longwater Gulch	2.34
7	53	Corral Creek	4.38
7.1	57	Motberry Gulch	1.60
7.2	47	Wildcat Creek	1.98
8	51	Northrup Gulch	3.84
8.1	44	Unnamed drainage A	1.03
8.2	45	Unnamed drainage B	0.72
PC	892	South Platte Reach C	6.49
9A	37	Turkey Creek	0.61
9B	92	Turkey Creek	1.99
9C	46	Turkey Creek	8.09
9D	37	Turkey Creek	0.99
9E	40	Turkey Creek	0.97
9F	43	Turkey Creek	1.57
9G	91	Turkey Creek	6.44
9H	90	Turkey Creek	2.16
9I	54	Turkey Creek	0.27
9J	59	Turkey Creek	0.40
9K	62	Turkey Creek	0.48
9L	67	Turkey Creek	0.88
9M	73	Turkey Creek	2.97
9N	46 (partial)	Turkey Creek	0.37
9.1	33	Unnamed drainage C	0.87
9.2	34	Sand Draw	0.67
9.3	31	Unnamed drainage D	0.75
10A	26	Goose Creek	2.13
10B	26	Goose Creek	4.67

Table 3–1. South Platte River basins and subbasins used in the HEC-HMS model upstream and downstream from Cheesman Reservoir.—Continued

[mi², square miles; BAER, Burned Area Emergency Rehabilitation; n/a, not applicable]

Model basin ID	Corresponding BAER basin(s)	Name of basin or drainage	Basin area (mi²)
South Platte River basins and subbasins upstream from Cheesman Dam—Continued			
10C	25	Goose Creek	2.82
10D	87	Goose Creek	7.38
10E	30	Goose Creek	1.88
10F	39	Goose Creek	6.27
10G	32	Goose Creek	3.55
10H	-	Goose Creek	7.64
10I	-	Goose Creek	4.69
10J	-	Goose Creek	5.48
10K	-	Goose Creek	10.9
10L	-	Goose Creek	12.2
10M	-	Goose Creek	13.9
10N	-	Goose Creek	11.7
Basins downstream from Cheesman Dam			
11	28	Schoonover	1.71
12A	3	Sixmile and Wigwam	18.2
12B	2	Sixmile and Wigwam	5.22
12C	6	Sixmile and Wigwam	3.43
12D	5	Sixmile and Wigwam	7.78
12E	19	Sixmile and Wigwam	0.88
12F	22	Sixmile and Wigwam	1.19
13	21	Fourmile Creek	8.22
14A	11	Horse Creek	3.58
14B	23	Horse Creek	1.36
14C	24	Horse Creek	0.64
14D	20	Horse Creek	0.63
14E	11, 50, 52, 55, 61, 68, 70	Horse Creek	18.8
14F	27	Horse Creek	2.05
14G	29	Horse Creek	0.55
14H	36	Horse Creek	0.76
14I	38	Horse Creek	1.16
14J	42	Horse Creek	1.89
14K	49	Horse Creek	15.5
14L	56	Horse Creek	1.19
14M	60	Horse Creek	0.40
14N	64	Horse Creek	0.65
14O	66	Horse Creek	0.49
14P	71	Horse Creek	0.58
14Q	None	Horse Creek	12.3
14R	None	Horse Creek	12.8
14S	85	Horse Creek	17.4
14T	85	Horse Creek	8.85
14U	85	Horse Creek	7.39
14V	35	Horse Creek	2.71

Table 3–1. South Platte River basins and subbasins used in the HEC-HMS model upstream and downstream from Cheesman Reservoir.—Continued

[mi^2, square miles; BAER, Burned Area Emergency Rehabilitation; n/a, not applicable]

Model basin ID	Corresponding BAER basin(s)	Name of basin or drainage	Basin area (mi^2)
Basins downstream from Cheesman Dam—Continued			
14W	85	Horse Creek	7.20
14X	88	Horse Creek	16.0
14Y	88	Horse Creek	12.8
14Z	88	Horse Creek	15.5
14AA	None	Horse Creek	1.83
14BB	None	Horse Creek	9.45
14CC	None	Horse Creek	6.43
14DD	None	Horse Creek	9.00
14EE	None	Horse Creek	13.3
14FF	None	Horse Creek	8.88
15	8	Lazy Gulch	1.23
16	7	Brush Creek	2.33
17	9	Unnamed drainage	1.16
UB1	None	Unburned drainage 1bc	1.75
18	4	Saloon Gulch	1.26
UB2	None	Unburned drainage 2bc	1.07
19A	1	Gunbarrel and Kelsey	0.69
19B	1	Gunbarrel and Kelsey	4.72
19C	1	Gunbarrel and Kelsey	4.79
UB3	None	Unburned drainage 3bc	13.1
M1	893	South Platte Reach 1	3.26
M2	893	South Platte Reach 2	2.57
M3	93, 893	South Platte Reach 3	2.98
M4	93	South Platte Reach 4	4.19

Table 3–2. Burn data for South Platte River basins and subbasins upstream and downstream from Cheesman Reservoir.

[ID, identification number; mi^2, square miles; %, percent; BAER, Burned Area Emergency Rehabilitation]

Single basins (yellow) | Composite basins (pink) | Subbasins of composite basins (blue)

Model basin ID	Name of basin or drainage	Total basin area (mi^2)	Percentage of low burned area	Low burned area (mi^2)	Percentage of medium-high burned area	Medium-high burned area (mi^2)	Total burned area (%)	Total burned area (mi^2)
South Platte River basins and subbasins upstream from Cheesman Dam								
0.1	Unnamed	0.60	44.00	0.27	19.62	0.119	63.62	0.384
PA	South Platte Reach A	3.87	82.00	3.17	4.50	0.174	86.50	3.35
UBB1	Unburned basin 1ac	19.8	0.00	0.00	0.00	0.000	0.00	0.000
UBB2	Unburned basin 2ac	8.70	0.00	0.00	0.00	0.000	0.00	0.000
1	Vermillion Creek	4.93	50.00	2.47	27.58	1.360	77.58	3.82
UBB3	Unburned basin 3ac	1.20	0.00	0.00	0.00	0.000	0.00	0.000
2	Crystal Creek	5.27	46.40	2.45	29.05	1.531	75.45	3.98
UBB4	Unburned basin 4ac	0.32	0.00	0.00	0.00	0.000	0.00	0.000
PB	South Platte Reach B	11.3	46.00	5.20	38.59	4.364	84.59	9.57
3	Beaver Creek	3.54	51.50	1.82	33.70	1.194	85.20	3.02
4	Hackett Gulch	6.56	37.20	2.44	33.19	2.177	70.39	4.62
5	Mouth of Tarryall Creek	443	0.96	4.27	0.89	3.922	1.85	8.19
5A	Tarryall Creek	8.42	37.00	3.12	34.02	2.865	71.02	5.98
5B	Tarryall Creek	3.11	37.00	1.15	34.02	1.057	71.02	2.21
5C	Tarryall upstream (regulated in and above 5C)	431	0.00	0.00	0.00	0.000	0.00	0.000
6	Longwater Gulch	2.34	29.00	0.68	67.64	1.583	96.64	2.26
7	Corral Creek	4.38	16.00	0.70	70.32	3.080	86.32	3.78
7.1	Motberry Gulch	1.60	20.00	0.32	80.12	1.282	100.12	1.60
7.2	Wildcat Creek	1.98	19.00	0.38	80.65	1.593	99.65	1.97
8	Northrup Gulch	3.84	37.00	1.42	58.22	2.234	95.22	3.65
8.1	Unnamed drainage A	1.03	22.00	0.23	77.95	0.803	99.95	1.03
8.2	Unnamed drainage B	0.72	18.00	0.13	81.67	0.591	99.67	0.722
PC	South Platte Reach C	6.49	21.00	1.36	61.42	3.987	82.42	5.35
9	Mouth of Turkey Creek	28.2	32.41	9.13	50.60	14.253	83.01	23.4

Table 3–2. Burn data for South Platte River basins and subbasins upstream and downstream from Cheesman Reservoir.—Continued

[ID, identification number; mi², square miles; %, percent; BAER, Burned Area Emergency Rehabilitation]

Single basins (yellow) | Composite basins (pink) | Subbasins of composite basins (blue)

Model basin ID	Name of basin or drainage	Total basin area (mi²)	Percentage of low burned area	Low burned area (mi²)	Percentage of medium-high burned area	Medium-high burned area (mi²)	Total burned area (%)	Total burned area (mi²)
South Platte River basins and subbasins upstream from Cheesman Dam—Continued								
9A	Turkey Creek	0.61	1.00	0.01	98.72	0.599	99.72	0.605
9B	Turkey Creek	1.99	5.00	0.10	94.90	1.889	99.90	1.99
9C	Turkey Creek	8.09	34.00	2.75	44.37	3.588	78.37	6.34
9D	Turkey Creek	0.99	1.00	0.01	98.72	0.980	99.72	0.990
9E	Turkey Creek	0.97	0.00	0.00	100.00	0.968	100.00	0.968
9F	Turkey Creek	1.57	9.00	0.14	90.85	1.425	99.85	1.57
9G	Turkey Creek	6.44	42.00	2.70	37.26	2.400	79.26	5.10
9H	Turkey Creek	2.16	62.00	1.34	20.17	0.435	82.17	1.77
9I	Turkey Creek	0.27	65.00	0.17	23.46	0.063	88.46	0.236
9J	Turkey Creek	0.40	50.00	0.20	3.67	0.015	53.67	0.216
9K	Turkey Creek	0.48	66.00	0.31	6.75	0.032	72.75	0.347
9L	Turkey Creek	0.88	43.00	0.38	42.11	0.369	85.11	0.746
9M	Turkey Creek	2.97	30.00	0.89	44.71	1.327	74.71	2.22
9N	Turkey Creek	0.37	34.00	0.13	44.37	0.164	78.37	0.290
9.1	Unnamed drainage C	0.87	4.00	0.03	95.57	0.831	99.57	0.866
9.2	Sand Draw	0.67	4.00	0.03	96.33	0.641	100.33	0.667
9.3	Unnamed drainage D	0.75	7.00	0.05	93.00	0.698	100.00	0.750
10	Mouth of Goose Creek	95.2	5.29	5.04	15.06	14.335	20.35	19.4
10A	Goose Creek	2.13	10.00	0.21	89.61	1.909	99.61	2.12
10B	Goose Creek	4.67	10.00	0.47	89.61	4.181	99.61	4.65
10C	Goose Creek	2.82	32.00	0.90	59.96	1.690	91.96	2.59
10D	Goose Creek	7.38	26.00	1.92	63.36	4.677	89.36	6.60
10E	Goose Creek	1.88	31.00	0.58	54.94	1.030	85.94	1.61
10F	Goose Creek	6.27	9.00	0.56	8.67	0.544	17.67	1.11
10G	Goose Creek	3.55	11.00	0.39	8.57	0.304	19.57	0.695
10H	Goose Creek	7.64	0.00	0.00	0.00	0.000	0.00	0.000

Table 3–2. Burn data for South Platte River basins and subbasins upstream and downstream from Cheesman Reservoir.—Continued

[ID, identification number; mi², square miles; %, percent; BAER, Burned Area Emergency Rehabilitation]

Single basins (yellow) | Composite basins (pink) | Subbasins of composite basins (blue)

Model basin ID	Name of basin or drainage	Total basin area (mi^2)	Percentage of low burned area	Low burned area (mi^2)	Percentage of medium-high burned area	Medium-high burned area (mi^2)	Total burned area (%)	Total burned area (mi^2)
South Platte River basins and subbasins upstream from Cheesman Dam—Continued								
10I	Goose Creek	4.69	0.00	0.00	0.00	0.000	0.00	0.000
10J	Goose Creek	5.48	0.00	0.00	0.00	0.000	0.00	0.000
10K	Goose Creek	10.9	0.00	0.00	0.00	0.000	0.00	0.000
10L	Goose Creek	12.2	0.00	0.00	0.00	0.000	0.00	0.000
10M	Goose Creek	13.9	0.00	0.00	0.00	0.000	0.00	0.000
10N	Goose Creek	11.7	0.00	0.00	0.00	0.000	0.00	0.000
South Platte River basins and subbasins downstream from Cheesman Dam								
11	Schoonover	1.71	11.70	0.20	85.37	1.461	97.07	1.66
12	Mouth of Sixmile and Wigwam	36.7	13.68	5.02	34.24	12.555	47.91	17.6
12A	Sixmile and Wigwam	18.2	15.00	2.73	27.80	5.053	42.80	7.78
12B	Sixmile and Wigwam	5.22	13.00	0.68	42.50	2.219	55.50	2.90
12C	Sixmile and Wigwam	3.43	11.00	0.38	51.90	1.778	62.90	2.15
12D	Sixmile and Wigwam	7.78	11.00	0.86	24.40	1.897	35.40	2.75
12E	Sixmile and Wigwam	0.879	24.00	0.21	76.20	0.670	100.20	0.881
12F	Sixmile and Wigwam	1.19	14.00	0.17	78.70	0.938	92.70	1.11
13	Fourmile Creek	8.22	11.70	0.96	59.71	4.906	71.41	5.87
14	Mouth of Horse Creek	212	9.06	19.22	12.75	27.048	21.82	46.3
14A	Horse Creek	3.58	33.00	1.18	20.65	0.738	53.65	1.92
14B	Horse Creek	1.36	18.00	0.24	75.30	1.021	93.30	1.27
14C	Horse Creek	0.641	0.00	0.00	100.00	0.641	100.00	0.641
14D	Horse Creek	0.633	48.00	0.30	45.80	0.290	93.80	0.594
14E	Horse Creek	18.8	27.00	5.08	36.10	6.788	63.10	11.9
14F	Horse Creek	2.05	11.00	0.23	54.30	1.110	65.30	1.34
14G	Horse Creek	0.547	45.00	0.25	29.90	0.164	74.90	0.410
14H	Horse Creek	0.764	33.00	0.25	30.50	0.233	63.50	0.485

Table 3–2. Burn data for South Platte River basins and subbasins upstream and downstream from Cheesman Reservoir.—Continued

[ID, identification number; mi², square miles; %, percent; BAER, Burned Area Emergency Rehabilitation]

Single basins (yellow) | Composite basins (pink) | Subbasins of composite basins (blue)

Model basin ID	Name of basin or drainage	Total basin area (mi²)	Percentage of low burned area	Low burned area (mi²)	Percentage of medium-high burned area	Medium-high burned area (mi²)	Total burned area (%)	Total burned area (mi²)
South Platte River basins and subbasins downstream from Cheesman Dam—Continued								
14I	Horse Creek	1.16	46.00	0.53	44.10	0.509	90.10	1.04
14J	Horse Creek	1.89	50.00	0.94	30.30	0.572	80.30	1.52
14K	Horse Creek	15.5	33.00	5.13	41.00	6.370	74.00	11.5
14L	Horse Creek	1.19	52.00	0.62	41.40	0.494	93.40	1.11
14M	Horse Creek	0.399	30.00	0.12	59.50	0.237	89.50	0.357
14N	Horse Creek	0.653	13.00	0.08	87.20	0.569	100.20	0.654
14O	Horse Creek	0.492	6.00	0.03	59.80	0.294	65.80	0.324
14P	Horse Creek	0.582	48.00	0.28	22.70	0.132	70.70	0.411
14Q	Horse Creek	12.3	0.00	0.00	3.00	0.369	3.00	0.369
14R	Horse Creek	12.8	0.00	0.00	0.00	0.000	0.00	0.000
14S	Horse Creek	17.4	5.00	0.87	4.77	0.831	9.77	1.70
14T	Horse Creek	8.85	5.00	0.44	4.77	0.422	9.77	0.865
14U	Horse Creek	7.39	5.00	0.37	4.77	0.353	9.77	0.722
14V	Horse Creek	2.71	38.00	1.03	59.24	1.603	97.24	2.63
14W	Horse Creek	7.20	5.00	0.36	4.77	0.343	9.77	0.703
14X	Horse Creek	16.0	2.00	0.32	3.18	0.509	5.18	0.828
14Y	Horse Creek	12.8	2.00	0.26	3.18	0.406	5.18	0.662
14Z	Horse Creek	15.5	2.00	0.31	3.18	0.494	5.18	0.805
14AA	Horse Creek	1.83	0.00	0.00	3.18	0.058	3.18	0.058
14BB	Horse Creek	9.45	0.00	0.00	3.18	0.300	3.18	0.300
14CC	Horse Creek	6.43	0.00	0.00	3.18	0.204	3.18	0.204
14DD	Horse Creek	9.00	0.00	0.00	3.18	0.286	3.18	0.286
14EE	Horse Creek	13.3	0.00	0.00	3.18	0.423	3.18	0.423
14FF	Horse Creek	8.88	0.00	0.00	3.18	0.282	3.18	0.282

Table 3–2. Burn data for South Platte River basins and subbasins upstream and downstream from Cheesman Reservoir.—Continued

[ID, identification number; mi^2, square miles; %, percent; BAER, Burned Area Emergency Rehabilitation]

Single basins (yellow) | Composite basins (pink) | Subbasins of composite basins (blue)

Model basin ID	Name of basin or drainage	Total basin area (mi^2)	Percentage of low burned area	Low burned area (mi^2)	Percentage of medium-high burned area	Medium-high burned area (mi^2)	Total burned area (%)	Total burned area (mi^2)
South Platte River basins and subbasins downstream from Cheesman Dam—Continued								
15	Lazy Gulch	1.23	54.20	0.67	39.05	0.480	93.25	1.15
16	Brush Creek	2.33	29.20	0.68	59.31	1.380	88.51	2.06
17	Unnamed drainage	1.16	0.00	0.00	0.00	0.000	0.00	0.000
UB1	Unburned drainage 1bc	1.75	0.00	0.00	0.00	0.000	0.00	0.000
18	Saloon Gulch	1.26	39.70	0.50	46.63	0.588	86.33	1.088
UB2	Unburned drainage 2bc	1.07	0.00	0.00	0.00	0.000	0.00	0.000
19	Mouth of Gunbarrel and Kelsey	10.2	8.00	0.82	2.00	0.204	10.00	1.02
19A	Gunbarrel and Kelsey	0.686	8.00	0.05	2.00	0.014	10.00	0.069
19B	Gunbarrel and Kelsey	4.72	8.00	0.38	2.00	0.094	10.00	0.472
19C	Gunbarrel and Kelsey	4.79	8.00	0.38	2.00	0.096	10.00	0.479
UB3	Unburned drainage 3bc	13.1	0.00		0.00	0.000	0.00	0.000
M1	South Platte Reach 1	3.26	21.00	0.68	5.77	0.188	26.77	0.872
M2	South Platte Reach 2	2.57	21.00	0.54	5.77	0.148	26.77	0.687
M3	South Platte Reach 3	2.98	31.00	0.92	9.05	0.269	40.05	1.19
M4	South Platte Reach 4	4.19	40.00	1.67	12.33	0.516	52.33	2.19

Table 3–3. Pre- and post-burn model parameters for South Platte River basins and subbasins upstream and downstream from Cheesman Reservoir used in the manual calibration method.

[ID, identification number; BAER, Burned Area Emergency Rehabilitation; mi², square miles; RCN, runoff curve number; IA, initial abstraction; na, not applicable]

Model basin ID	Corresponding BAER basin(s)	Name of basin or drainage	Drainage area (mi²)	Pre-burned RCN	Default IA	Taylor lag time	Remarks
South Platte River basins and subbasins upstream from Cheesman Dam							
0.1	84	Unnamed	0.60	59	1.40	3.23	
PA	80, 77, 75	South Platte Reach A	3.87	65	1.07	10.72	
UBB1	-	Unburned basin 1ac	19.82	62	1.25	9.86	
UBB2	-	Unburned basin 2ac	8.70	61	1.26	8.70	
1	78	Vermillion Creek	4.93	58	1.42	4.76	
UBB3	-	Unburned basin 3ac	1.20	67	0.97	1.20	
2	76	Crystal Creek	5.27	59	1.40	5.13	
UBB4	-	Unburned basin 4ac	0.32	56	1.57	1.05	
PB	891	South Platte Reach B	11.31	63	1.17	10.56	
3	74	Beaver Creek	3.54	59	1.39	4.84	
4	65	Hackett Gulch	6.56	57	1.53	3.62	
5A	58	Tarryall Creek	8.42	59	1.37	6.15	
5B	58, 72	Tarryall Creek	3.11	57	1.50	3.38	
5C	-	Tarryall upstream	431.05	na	na	na	Tarryall is regulated in this area
6	63	Longwater Gulch	2.34	57	1.49	3.20	
7	53	Corral Creek	4.38	56	1.60	2.53	
7.1	57	Motberry Gulch	1.60	56	1.55	2.43	
7.2	47	Wildcat Creek	1.98	56	1.55	2.54	
8	51	Northrup Gulch	3.84	58	1.45	4.15	
8.1	44	Unnamed drainage A	1.03	56	1.57	1.82	
8.2	45	Unnamed drainage B	0.72	56	1.60	1.35	
PC	892	South Platte Reach C	6.49	60	1.35	6.02	
9A	37	Turkey Creek	0.61	57	1.50	1.84	
9B	92	Turkey Creek	1.99	57	1.50	3.07	
9C	46	Turkey Creek	8.09	59	1.39	6.99	
9D	37	Turkey Creek	0.99	57	1.50	2.60	
9E	40	Turkey Creek	0.97	58	1.46	2.95	
9F	43	Turkey Creek	1.57	57	1.50	2.69	
9G	91	Turkey Creek	6.44	61	1.26	9.13	
9H	90	Turkey Creek	2.16	58	1.47	3.38	
9I	54	Turkey Creek	0.27	57	1.50	1.73	
9J	59	Turkey Creek	0.40	57	1.50	2.01	
9K	62	Turkey Creek	0.48	57	1.50	2.05	
9L	67	Turkey Creek	0.88	58	1.45	3.43	
9M	73	Turkey Creek	2.97	58	1.45	3.84	
9N	46 (partial)	Turkey Creek	0.37	58	1.45	1.25	
9.1	33	Unnamed drainage C	0.87	56	1.57	1.75	
9.2	34	Sand Draw	0.67	57	1.50	2.17	
9.3	31	Unnamed drainage D	0.75	58	1.47	2.59	
10A	26	Goose Creek	2.13	58	1.46	2.96	
10B	26	Goose Creek	4.67	58	1.46	3.63	
10C	25	Goose Creek	2.82	58	1.46	2.29	
10D	87	Goose Creek	7.38	59	1.42	4.88	

Table 3–3. Pre- and post-burn model parameters for South Platte River basins and subbasins upstream and downstream from Cheesman Reservoir used in the manual calibration method.—Continued

[ID, identification number; BAER, Burned Area Emergency Rehabilitation; mi², square miles; RCN, runoff curve number; IA, initial abstraction; na, not applicable]

Model basin ID	Corresponding BAER basin(s)	Name of basin or drainage	Drainage area (mi²)	Pre-burned RCN	Default IA	Taylor lag time	Remarks
South Platte River basins and subbasins upstream from Cheesman Dam—Continued							
10E	30	Goose Creek	1.88	58	1.45	1.83	
10F	39	Goose Creek	6.27	58	1.45	3.45	
10G	32	Goose Creek	3.55	58	1.46	2.90	
10H	-	Goose Creek	7.64	58	1.43	4.68	
10I	-	Goose Creek	4.69	58	1.45	3.26	
10J	-	Goose Creek	5.48	58	1.46	3.19	
10K	-	Goose Creek	10.95	58	1.45	3.84	
10L	-	Goose Creek	12.16	58	1.44	5.98	
10M	-	Goose Creek	13.86	58	1.46	6.73	
10N	-	Goose Creek	11.70	59	1.41	8.04	
South Platte River basins and subbasins downstream from Cheesman Dam							
11	28	Schoonover	1.71	57	1.52	2.70	
12A	3	Sixmile and Wigwam	18.18	60	1.33	8.80	
12B	2	Sixmile and Wigwam	5.22	62	1.23	3.96	
12C	6	Sixmile and Wigwam	3.43	61	1.28	3.74	
12D	5	Sixmile and Wigwam	7.78	60	1.33	4.77	
12E	19	Sixmile and Wigwam	0.88	60	1.33	1.81	
12F	22	Sixmile and Wigwam	1.19	61	1.28	1.67	
13	21	Fourmile Creek	8.22	62	1.25	8.22	
14A	11	Horse Creek	3.58	59	1.37	5.26	
14B	23	Horse Creek	1.36	61	1.26	1.99	
14C	24	Horse Creek	0.64	58	1.42	1.67	
14D	20	Horse Creek	0.63	62	1.21	1.56	
14E	11, 50, 52, 55, 61, 68, 70	Horse Creek	18.80	61	1.26	16.20	
14F	27	Horse Creek	2.05	63	1.15	2.52	
14G	29	Horse Creek	0.55	64	1.11	1.53	
14H	36	Horse Creek	0.76	66	1.01	1.46	
14I	38	Horse Creek	1.16	62	1.21	1.65	
14J	42	Horse Creek	1.89	59	1.37	3.28	
14K	49	Horse Creek	15.54	58	1.42	12.78	
14L	56	Horse Creek	1.19	61	1.26	2.36	
14M	60	Horse Creek	0.40	58	1.42	1.67	
14N	64	Horse Creek	0.65	59	1.37	1.60	
14O	66	Horse Creek	0.49	59	1.37	1.89	
14P	71	Horse Creek	0.58	63	1.15	1.70	
14Q	None	Horse Creek	12.29	59	1.37	10.35	
14R	None	Horse Creek	12.75	58	1.42	9.84	
14S	85	Horse Creek	17.42	60	1.31	6.62	
14T	85	Horse Creek	8.85	60	1.31	7.82	
14U	85	Horse Creek	7.39	60	1.31	5.84	
14V	35	Horse Creek	2.71	59	1.37	3.77	
14W	85	Horse Creek	7.20	60	1.31	6.09	

Table 3–3. Pre- and post-burn model parameters for South Platte River basins and subbasins upstream and downstream from Cheesman Reservoir used in the manual calibration method.—Continued

[ID, identification number; BAER, Burned Area Emergency Rehabilitation; mi², square miles; RCN, runoff curve number; IA, initial abstraction; na, not applicable]

Model basin ID	Corresponding BAER basin(s)	Name of basin or drainage	Drainage area (mi²)	Pre-burned RCN	Default IA	Taylor lag time	Remarks
South Platte River basins and subbasins downstream from Cheesman Dam—Continued							
14X	88	Horse Creek	15.99	59	1.37	6.24	
14Y	88	Horse Creek	12.78	59	1.37	5.64	
14Z	88	Horse Creek	15.54	59	1.37	7.48	
14AA	None	Horse Creek	1.83	58	1.42	2.90	
14BB	None	Horse Creek	9.45	58	1.42	12.14	
14CC	None	Horse Creek	6.43	58	1.42	6.47	
14DD	None	Horse Creek	9.00	58	1.42	5.58	
14EE	None	Horse Creek	13.32	58	1.42	7.61	
14FF	None	Horse Creek	8.88	58	1.42	8.43	
15	8	Lazy Gulch	1.23	57	1.54	2.21	
16	7	Brush Creek	2.33	58	1.45	3.66	
17	9	Unnamed drainage	1.16	57	1.50	2.67	
UB1	None	Unburned drainage 1bc	1.75	58	1.48	3.24	
18	4	Saloon Gulch	1.26	57	1.51	2.57	
UB2	None	Unburned drainage 2bc	1.07	57	1.53	2.36	
19A	1	Gunbarrel and Kelsey	0.69	57	1.50	2.33	
19B	1	Gunbarrel and Kelsey	4.72	57	1.50	4.23	
19C	1	Gunbarrel and Kelsey	4.79	57	1.50	4.07	
UB3	None	Unburned drainage 3bc	13.12	58	1.44	5.50	
M1	893	South Platte Reach 1	3.26	58	1.44	4.16	
M2	893	South Platte Reach 2	2.57	58	1.45	3.77	
M3	93, 893	South Platte Reach 3	2.98	58	1.42	4.19	
M4	93	South Platte Reach 4	4.19	58	1.42	4.60	

Explanation of Parameters

Regr. Q = Local peak discharge regression equation, determined by Q = 14.21 × A0.823

Unburn RCN = RCN determined from composite and individual BAER team basins (base RCN for natural forest min. 55)

Default IA = Initial Abstraction value determined by SCS method, IA = 0.2 × [(1,000/RCN) – 10]

Taylor lag time = Lag time determined by Taylor-Schwartz method

Table 3–4. Post-burn model parameters for South Platte River basins upstream and downstream from Cheesman Reservoir used in the manual calibration method.

[ID, identification number; BAER, Burned Area Emergency Rehabilitation; mi², square miles; %, percent; RCN, runoff curve number; IA, initial abstraction; LT, lag time; BOR, Bureau of Reclamation source; na, not applicable]

Model basin ID	Corresponding BAER basin(s)	Name of basin or drainage	Area (mi²)	Unburned RCN	Medium and high burn %	Burned RCN	Change in RCN	Burned default IA	Unburned Taylor LT	Burned LT BOR	Percentage of unburned LT	Note
South Platte River basins and subbasins upstream from Cheesman Dam												
0.1	84	Unnamed	0.60	59	19.6	82.5	24	0.42	3.23	2.55	78.9	
PA	80, 77, 75	South Platte Reach A	3.87	65	4.5	84.1	19	0.38	10.72	4.11	38.4	
UBB1	-	Unburned basin 1ac	19.82	62	0.0	Unburned		Unburned	9.86	9.86	100.0	
UBB2	-	Unburned basin 2ac	8.70	61	0.0	Unburned		Unburned	8.70	8.70	100.1	
1	78	Vermillion Creek	4.93	58	27.6	86.2	28	0.32	4.76	3.31	69.6	
UBB3	-	Unburned basin 3ac	1.20	67	0.0	Unburned		Unburned	1.20	1.20	99.6	
2	76	Crystal Creek	5.27	59	29.1	86.2	27	0.32	5.13	3.68	71.8	
UBB4	-	Unburned basin 4ac	0.32	56	0.0	Unburned		Unburned	1.05	1.05	100.1	
PB	891	South Platte Reach B	11.31	63	38.6	89.1	26	0.24	10.56	5.52	52.3	
3	74	Beaver Creek	3.54	59	33.7	88.3	29	0.27	4.84	3.35	69.2	
4	65	Hackett Gulch	6.56	57	33.2	85.9	29	0.33	3.62	2.83	78.1	
5A	58	Tarryall Creek	8.42	59	34.0	86.3	27	0.32	6.15	4.17	67.8	
5B	58, 72	Tarryall upstream	3.11	57	34.0	86.4	29	0.31	3.38	2.74	81.2	
5C	-	Rest of Tarryall	431.05	na	0.0	Unburned		Unburned	na	na	na	Tarryall regulated in this area
6	63	Longwater Gulch	2.34	57	67.6	94.2	37	0.12	3.20	2.17	67.7	
7	53	Corral Creek	4.38	56	70.3	93.3	38	0.14	2.53	2.15	84.9	
7.1	57	Motberry Gulch	1.60	56	80.1	95.9	40	0.09	2.43	1.67	68.6	
7.2	47	Wildcat Creek	1.98	56	80.7	96.0	40	0.08	2.54	1.71	67.4	
8	51	Northrup Gulch	3.84	58	58.2	92.9	35	0.15	4.15	2.73	65.7	
8.1	44	Unnamed drainage A	1.03	56	78.0	95.7	40	0.09	1.82	1.10	60.6	
8.2	45	Unnamed drainage B	0.72	56	81.7	96.1	40	0.08	1.35	0.87	64.5	
PC	892	South Platte Reach C	6.49	60	61.4	91.9	32	0.18	6.02	3.15	52.4	
9A	37	Turkey Creek	0.61	57	98.7	97.9	41	0.04	1.84	1.00	54.2	
9B	92	Turkey Creek	1.99	57	94.9	97.5	40	0.05	3.07	1.69	55.0	
9C	46	Turkey Creek	8.09	59	44.4	89.0	30	0.25	6.99	4.80	68.7	
9D	37	Turkey Creek	0.99	57	98.7	97.9	41	0.04	2.60	1.58	60.6	
9E	40	Turkey Creek	0.97	58	100.0	98.0	40	0.04	2.95	1.77	60.1	
9F	43	Turkey Creek	1.57	57	90.9	97.1	40	0.06	2.69	1.71	63.7	
9G	91	Turkey Creek	6.44	61	37.3	88.1	27	0.27	9.13	5.85	64.0	
9H	90	Turkey Creek	2.16	58	20.2	85.7	28	0.33	3.38	2.52	74.6	
9I	54	Turkey Creek	0.27	57	23.5	87.2	30	0.29	1.73	1.24	71.8	
9J	59	Turkey Creek	0.40	57	3.7	76.9	20	0.60	2.01	1.71	85.1	

Table 3–4. Post-burn model parameters for South Platte River basins upstream and downstream from Cheesman Reservoir used in the manual calibration method. —Continued

[ID, identification number; BAER, Burned Area Emergency Rehabilitation; mi², square miles; %, percent; RCN, runoff curve number; IA, initial abstraction; LT, lag time; BOR, Bureau of Reclamation source; na, not applicable]

Model basin ID	Corresponding BAER basin(s)	Name of basin or drainage	Area (mi²)	Un-burned RCN	Medium and high burn %	Burned RCN	Change in RCN	Burned default IA	Unburned Taylor LT	Burned LT BOR	Percentage of unburned LT	Note
South Platte River basins and subbasins upstream from Cheesman Dam—Continued												
9K	62	Turkey Creek	0.48	57	6.8	81.5	24	0.45	2.05	1.53	74.7	
9L	67	Turkey Creek	0.88	58	42.1	89.6	32	0.23	3.43	2.18	63.5	
9M	73	Turkey Creek	2.97	58	44.7	88.4	31	0.26	3.84	2.45	63.7	
9N	46 (partial)	Turkey Creek	0.37	58	44.4	89.0	31	0.25	1.25	0.89	70.8	
9.1	33	Unnamed drainage C	0.87	56	95.6	97.6	41	0.05	1.75	1.11	63.3	
9.2	34	Sand Draw	0.67	57	96.3	97.6	40	0.05	2.17	1.37	63.0	
9.3	31	Unnamed drainage D	0.75	58	93.0	97.3	40	0.06	2.59	1.56	60.4	
10A	26	Goose Creek	2.13	58	89.6	97.0	39	0.06	2.96	1.15	38.9	
10B	26	Goose Creek	4.67	58	89.6	97.0	39	0.06	3.63	1.54	42.5	
10C	25	Goose Creek	2.82	58	60.0	92.7	35	0.16	2.29	1.54	67.1	
10D	87	Goose Creek	7.38	59	63.4	92.9	34	0.15	4.88	3.20	65.5	
10E	30	Goose Creek	1.88	58	54.9	91.4	33	0.19	1.83	1.26	68.9	
10F	39	Goose Creek	6.27	58	8.7	69.2	11	0.89	3.45	3.28	95.1	
10G	32	Goose Creek	3.55	58	8.6	69.5	12	0.88	2.90	2.83	97.6	
10H	-	Goose Creek	7.64	58	0.0	Unburned		Unburned	4.68	4.68	100.0	
10I	-	Goose Creek	4.69	58	0.0	Unburned		Unburned	3.26	3.26	100.0	
10J	-	Goose Creek	5.48	58	0.0	Unburned		Unburned	3.19	3.19	100.1	
10K	-	Goose Creek	10.95	58	0.0	Unburned		Unburned	3.84	3.84	99.9	
10L	-	Goose Creek	12.16	58	0.0	Unburned		Unburned	5.98	5.98	100.1	
10M	-	Goose Creek	13.86	58	0.0	Unburned		Unburned	6.73	6.73	100.0	
10N	-	Goose Creek	11.70	59	0.0	Unburned		Unburned	8.04	8.04	100.0	
South Platte River basins and subbasins downstream from Cheesman Dam												
11	28	Schoonover	1.71	57	85.4	96.2	39	0.08	2.70	1.71	63.6	
12A	3	Sixmile and Wigwam	18.18	60	27.8	80.6	21	0.48	8.80	7.45	84.8	
12B	2	Sixmile and Wigwam	5.22	62	42.5	85.8	24	0.33	3.96	3.16	79.7	
12C	6	Sixmile and Wigwam	3.43	61	51.9	88.2	27	0.27	3.74	2.96	79.1	
12D	5	Sixmile and Wigwam	7.78	60	24.4	78.5	19	0.55	4.77	4.20	88.0	
12E	19	Sixmile and Wigwam	0.88	60	76.2	95.5	36	0.09	1.81	1.15	63.5	
12F	22	Sixmile and Wigwam	1.19	61	78.7	95.1	34	0.10	1.67	1.33	79.6	
13	21	Fourmile Creek	8.22	62	59.7	90.4	29	0.21	8.22	5.51	67.1	

Table 3–4. Post-burn model parameters for South Platte River basins upstream and downstream from Cheesman Reservoir used in the manual calibration method.—Continued

[ID, identification number; BAER, Burned Area Emergency Rehabilitation; mi^2, square miles; %, percent; RCN, runoff curve number; IA, initial abstraction; LT, lag time; BOR, Bureau of Reclamation source; na, not applicable]

Model basin ID	Corresponding BAER basin(s)	Name of basin or drainage	Area (mi^2)	Un-burned RCN	Medium and high burn %	Burned RCN	Change in RCN	Burned default IA	Unburned Taylor LT	Burned LT BOR	Percentage of unburned LT	Note
South Platte River basins and subbasins downstream from Cheesman Dam—Continued												
14A	11	Horse Creek	3.58	59	20.7	81.2	22	0.46	5.26	3.37	64.1	
14B	23	Horse Creek	1.36	61	75.3	94.8	33	0.11	1.99	1.40	70.4	
14C	24	Horse Creek	0.64	58	100.0	98.0	40	0.04	1.67	0.99	59.3	
14D	20	Horse Creek	0.63	62	45.8	91.2	29	0.19	1.56	1.21	77.8	
14E	11, 50, 52, 55, 61, 68, 70	Horse Creek	18.80	61	36.1	83.0	22	0.41	16.20	11.16	68.9	
14F	27	Horse Creek	2.05	63	54.3	89.1	26	0.24	2.52	2.04	81.0	
14G	29	Horse Creek	0.55	64	29.9	86.7	22	0.31	1.53	1.33	87.3	
14H	36	Horse Creek	0.76	66	30.5	85.6	19	0.34	1.46	1.23	84.0	
14I	38	Horse Creek	1.16	62	44.1	90.5	28	0.21	1.65	1.29	78.4	
14J	42	Horse Creek	1.89	59	30.3	87.2	28	0.29	3.28	2.35	71.5	
14K	49	Horse Creek	15.54	58	41.0	87.8	29	0.28	12.78	8.10	63.4	
14L	56	Horse Creek	1.19	61	41.4	90.5	29	0.21	2.36	1.56	66.2	
14M	60	Horse Creek	0.40	58	59.5	92.4	34	0.16	1.67	1.16	69.5	
14N	64	Horse Creek	0.65	59	87.2	96.7	37	0.07	1.60	0.99	62.0	
14O	66	Horse Creek	0.49	59	59.8	89.6	30	0.23	1.89	1.43	75.5	
14P	71	Horse Creek	0.58	63	22.7	84.8	21	0.36	1.70	0.91	53.5	
14Q	None	Horse Creek	12.29	59	3.0	Unburned		Unburned	10.17	10.17	100.0	
14R	None	Horse Creek	12.75	58	0.0	Unburned		Unburned	9.84	9.84	100.1	
14S	85	Horse Creek	17.42	60	4.8	66.4	6	1.01	6.62	6.36	96.1	
14T	85	Horse Creek	8.85	60	4.8	66.4	6	1.01	7.82	7.50	95.9	
14U	85	Horse Creek	7.39	60	4.8	66.4	6	1.01	5.84	5.63	96.4	
14V	35	Horse Creek	2.71	59	59.2	93.3	34	0.14	3.77	2.19	58.2	
14W	85	Horse Creek	7.20	60	4.8	66.4	6	1.01	6.09	5.85	96.2	
14X	88	Horse Creek	15.99	59	3.2	63.5	4	1.15	6.24	6.10	97.9	
14Y	88	Horse Creek	12.78	59	3.2	63.5	4	1.15	5.64	5.51	97.6	
14Z	88	Horse Creek	15.54	59	3.2	63.5	4	1.15	7.48	7.30	97.6	
14AA	None	Horse Creek	1.83	58	3.2	Unburned		Unburned	2.86	2.86	100.1	
14BB	None	Horse Creek	9.45	58	3.2	Unburned		Unburned	11.90	11.90	100.0	
14CC	None	Horse Creek	6.43	58	3.2	Unburned		Unburned	6.36	6.36	100.0	

Table 3–4. Post-burn model parameters for South Platte River basins upstream and downstream from Cheesman Reservoir used in the manual calibration method.—Continued

[ID, identification number; BAER, Burned Area Emergency Rehabilitation; mi^2, square miles; %, percent; RCN, runoff curve number; IA, initial abstraction; LT, lag time; BOR, Bureau of Reclamation source; na, not applicable]

Model basin ID	Corresponding BAER basin(s)	Name of basin or drainage	Area (mi^2)	Unburned RCN	Medium and high burn %	Burned RCN	Change in RCN	Burned default IA	Unburned Taylor LT	Burned LT BOR	Percentage of unburned LT	Note
South Platte River basins and subbasins downstream from Cheesman Dam—Continued												
14DD	None	Horse Creek	9.00	58	3.2	Unburned		Unburned	5.48	5.48	100.0	
14EE	None	Horse Creek	13.32	58	3.2	Unburned		Unburned	7.47	7.47	100.0	
14FF	None	Horse Creek	8.88	58	3.2	Unburned		Unburned	8.27	8.27	100.0	
15	8	Lazy Gulch	1.23	57	39.1	90.1	34	0.22	2.21	1.70	77.0	
16	7	Brush Creek	2.33	58	59.3	92.2	34	0.17	3.66	2.60	71.0	
17	9	Unnamed drainage	1.16	57	0.0	57.2	0	1.50	2.67	2.67	99.9	
UB1	None	Unburned drainage 1bc	1.75	58	0.0	Unburned		Unburned	3.24	3.24	100.1	
18	4	Saloon Gulch	1.26	57	46.6	90.3	33	0.21	2.57	2.01	78.3	
UB2	None	Unburned drainage 2bc	1.07	57	0.0	Unburned		Unburned	2.36	2.36	99.8	
19A	1	Gunbarrel and Kelsey	0.69	57	2.0	63.3	6	1.16	2.33	2.25	96.5	
19B	1	Gunbarrel and Kelsey	4.72	57	2.0	63.3	6	1.16	4.23	4.13	97.6	
19C	1	Gunbarrel and Kelsey	4.79	57	2.0	63.3	6	1.16	4.07	3.97	97.5	
UB3	None	Unburned drainage 3bc	13.12	58	0.0	Unburned		Unburned	5.50	5.50	100.1	
M1	893	South Platte Reach 1	3.26	58	5.8	70.8	13	0.82	4.16	3.92	94.0	
M2	893	South Platte Reach 2	2.57	58	5.8	70.8	13	0.82	3.77	3.06	81.1	
M3	93, 893	South Platte Reach 3	2.98	58	9.1	74.1	16	0.70	4.19	2.98	71.2	
M4	93	South Platte Reach 4	4.19	58	12.3	78.9	21	0.53	4.60	2.94	63.9	

Table 3–5. Channel routing parameters used in the HEC-HMS model for South Platte River reaches upstream and downstream from Cheesman Reservoir used in the manual calibration method.

[ft, feet; ft/ft, foot per foot; ft^3/s, cubic feet per second; H:V, horizontal to vertical dimension in foot per foot; n, Manning's dimensionless roughness coefficent; U/S, upstream]

Routing method	Name of cross section	Reach length (ft)	Chanel slope (ft/ft)	Channel bottom width (ft)	Side slope (H:V)	Composite Manning's n	Note
	South Platte River reaches upstream from Cheesman Dam						
Muskingum-Cunge	U/S cross Section 1	26,700	0.006	173	2.0	0.054	Used average cross-section properties for entire reach
Muskingum-Cunge	U/S cross Section 2	52,800	0.006	173	2.0	0.054	
Muskingum-Cunge	U/S cross Section 3	4,000	0.006	173	2.0	0.054	
	South Platte River reaches downstream from Cheesman Dam						Routed peak outflow over spillway = 11.400 ft^3/s
Muskingum-Cunge	Cross section 1	16,770	0.002	160	1.5	0.066	Above Wigwam Creek confluence
Muskingum-Cunge	Cross section 2	12,010	0.003	150	4.0	0.063	Below Wigwam Creek confluence
Muskingum-Cunge	Cross section 3						Below Fourmile Creek confluence
Muskingum-Cunge	Cross section 4	12,340	0.004	110	2.5	0.060	Above Deckers and Horse Creek confluence
Muskingum-Cunge	Cross section 4.5						Trumbull stream gage
Muskingum-Cunge	Cross section 5						
Muskingum-Cunge	Cross section 6	19,140	0.003	210	20.0	0.058	Wide, flat flood plain through this reach
Muskingum-Cunge	Cross section 7						

Table 3–6. HEC-HMS model results for South Platte River basins and subbasins upstream and downstream from Cheesman Reservoir used in the manual calibration method.

[mi^2, square miles; ft^3/s, cubic feet per second; %, percent; PreQ, pre-burn discharge; RegrQ, regression-derived discharge; BulkQ, sediment-bulked discharge; na, not applicable]

Single basins (yellow) · Composite basins (pink) · Subbasins of composite basins (blue)

Model basin ID	Name of basin or drainage	Basin area (mi^2)	Percentage of medium-high burned area	Medium-high burned area (mi^2)	Regression derived discharge (ft^3/s)	Pre-burn discharge (ft^3/s)	Correlation between PreQ and RegrQ (%)	Post-burn discharge (ft^3/s)	Sediment bulked discharge (ft^3/s)	Ratio BulkQ to PreQ (BulkQ/PreQ)	Remarks
South Platte River basins and subbasins upstream from Cheesman Dam											
South Platte base flow								940			
0.1	Unnamed	0.60	19.6	0.119	9.4	9.2	98.4	77	81	8.8	
PA	South Platte Reach A	3.87	4.5	0.174	43.3	43.9	101.5	399	403	9.2	
UBB1	Unburned basin 1ac	19.82	0.0	0.000	166.0	164	98.8	Unburned	Unburned	Unburned	
UBB2	Unburned basin 2ac	8.70	0.0	0.000	84.3	84.4	100.1	Unburned	Unburned	Unburned	
1	Vermillion Creek	4.93	27.6	1.360	52.8	52.6	99.6	665	711	13.5	
UBB3	Unburned basin 3ac	1.20	0.0	0.000	16.5	16.3	98.7	Unburned	Unburned	Unburned	
2	Crystal Creek	5.27	29.1	1.531	55.8	55.5	99.5	663	711	12.8	
UBB4	Unburned basin 4ac	0.32	0.0	0.000	5.6	5.5	99.6	Unburned	Unburned	Unburned	
PB	South Platte Reach B	11.31	38.6	4.364	104.6	104	99.7	1,230	1,349	12.9	
3	Beaver Creek	3.54	33.7	1.194	40.2	40.3	100.1	531	576	14.3	
4	Hackett Gulch	6.56	33.2	2.177	66.8	66.4	99.5	954	1,033	15.6	
5	Mouth of Tarryall Creek	443	0.89	3.922	na	na	na	2,160	2,165	na	Total Q = Qreg + (Q_{100} for burned subbasins)
5A	Tarryall Creek	8.42	34.0	2.865	82.1	81.4	99.2	975	1,058	13.0	Pre-burn Q only for unregulated subbasins
5B	Tarryall Creek	3.11	34.0	1.057	36.1	35.9	99.4	477	518	14.4	Pre-burn Q only for unregulated subbasins
5C	Tarryall upstream	431	0.0	0.000	na	715	na	715	715	1.0	Unburned, regulated
6	Longwater Gulch	2.34	67.6	1.583	28.6	28.8	100.8	641	749	26.0	
7	Corral Creek	4.38	70.3	3.080	47.9	47.6	99.3	1,150	1,352	28.4	
7.1	Motberry Gulch	1.60	80.1	1.282	20.9	20.8	99.4	569	683	32.8	
	Cross Section UXS1	85.97	**24.2**	**20.784**				**9,210**	**9,667**		
7.2	Wildcat Creek	1.98	80.7	1.593	24.9	24.9	100.1	694	834	33.5	
8	Northrup Gulch	3.84	58.2	2.234	43.0	43.5	101.2	844	967	22.2	
	Cross Section UXS2	**91.78**	**26.8**	**24.611**				**9,710**	**10,361**		

Table 3–6. HEC-HMS model results for South Platte River basins and subbasins upstream and downstream from Cheesman Reservoir used in the manual calibration method.—Continued

[mi^2, square miles; ft^3/s, cubic feet per second; %, percent; PreQ, pre-burn discharge; RegrQ, regression-derived discharge; BulkQ, sediment-bulked discharge; na, not applicable]

Single basins — Composite basins — Subbasins of composite basins

Model basin ID	Name of basin or drainage	Basin area (mi^2)	Percentage of medium-high burned area	Medium-high burned area (mi^2)	Regression derived discharge (ft^3/s)	Pre-burn discharge (ft^3/s)	Correlation between PreQ and RegrQ (%)	Post-burn discharge (ft^3/s)	Sediment bulked discharge (ft^3/s)	Ratio BulkQ to PreQ (BulkQ/PreQ)	Remarks
South Platte River basins and subbasins upstream from Cheesman Dam—Continued											
8.1	Unnamed drainage A	1.03	78.0	0.803	14.6	14.6	100.3	470	562	38.5	**Peak discharge due to sediment bulking**
	Cross Section UXS3	**92.81**	**26.8**	**25.414**				**9,720**	**10,372**		**652**
8.2	Unnamed drainage B	0.72	81.7	0.591	10.9	10.8	98.9	391	471	43.7	**80**
PC	South Platte Reach C	6.49	61.4	3.987	66.2	66.4	100.2	1,230	1,419	21.4	**189**
9	Mouth of Turkey Creek	28.2	50.6	14.253	221.7	222	100.1	3,390	3,819	17.2	**429**
9A	Turkey Creek	0.61	98.7	0.599	9.4	10.1	na	330	411	40.7	
9B	Turkey Creek	1.99	94.9	1.889	25.0	25.2	na	766	948	37.5	
9C	Turkey Creek	8.09	44.4	3.588	79.4	72.3	na	975	1,083	15.0	
9D	Turkey Creek	0.99	98.7	0.980	14.1	13.8	na	406	506	36.7	
9E	Turkey Creek	0.97	100.0	0.968	13.8	13.9	na	370	463	33.3	
9F	Turkey Creek	1.57	90.9	1.425	20.6	21.3	na	584	717	33.7	
9G	Turkey Creek	6.44	37.3	2.400	65.8	55.8	na	631	690	12.4	
9H	Turkey Creek	2.16	20.2	0.435	26.7	27.4	na	333	350	12.8	
9I	Turkey Creek	0.27	23.5	0.063	4.8	4.6	na	68	72	15.8	
9J	Turkey Creek	0.40	3.7	0.015	6.7	6.4	na	42	43	6.7	
9K	Turkey Creek	0.48	6.8	0.032	7.7	7.6	na	74	75	9.9	
9L	Turkey Creek	0.88	42.1	0.369	12.7	12.2	na	184	203	16.6	
9M	Turkey Creek	2.97	44.7	1.327	34.8	35.1	na	544	605	17.2	
9N	Turkey Creek	0.37	44.4	0.164	6.3	7.9	na	129	143	18.2	
9.1	Unnamed drainage C	0.87	95.6	0.831	12.7	12.6	99.4	435	539	42.8	**103.9**
9.2	Sand Draw	0.67	96.3	0.641	10.2	10.2	100.6	294	365	35.7	**70.8**
9.3	Unnamed drainage D	0.75	93.0	0.698	11.2	11.3	100.4	300	370	32.8	**69.8**
10	Mouth of Goose Creek	95.2	15.1	14.335	603.9	607	100.5	4,120	4,275	7.0	**155**

Table 3–6. HEC-HMS model results for South Platte River basins and subbasins upstream and downstream from Cheesman Reservoir used in the manual calibration method.—Continued

[mi^2, square miles; ft^3/s, cubic feet per second; %, percent; PreQ, pre-burn discharge; RegrQ, regression-derived discharge; BulkQ, sediment-bulked discharge; na, not applicable]

Single basins (yellow) | Composite basins (pink) | Subbasins of composite basins (blue)

Model basin ID	Name of basin or drainage	Basin area (mi^2)	Percentage of medium-high burned area	Medium-high burned area (mi^2)	Regression derived discharge (ft^3/s)	Pre-burn discharge (ft^3/s)	Correlation between PreQ and RegrQ (%)	Post-burn discharge (ft^3/s)	Sediment bulked discharge (ft^3/s)	Ratio BulkQ to PreQ (BulkQ/PreQ)	Remarks
South Platte River basins and subbasins upstream from Cheesman Dam—Continued											
10A	Goose Creek	2.13	89.6	1.909	26.5	30.0	na	1,020	1,249	41.6	
10B	Goose Creek	4.67	89.6	4.181	50.5	56.4	na	1,860	2,277	40.4	
10C	Goose Creek	2.82	60.0	1.690	33.3	46.4	na	881	1,013	21.8	
10D	Goose Creek	7.38	63.4	4.677	73.6	78.7	na	1,470	1,703	21.6	
10E	Goose Creek	1.88	54.9	1.030	23.8	35.1	na	610	694	19.8	
10F	Goose Creek	6.27	8.7	0.544	64.4	81.2	na	278	284	3.5	
10G	Goose Creek	3.55	8.6	0.304	40.3	50.6	na	174	178	3.5	
10H	Goose Creek	7.64	0.0	0.000	75.8	80.8	na	Unburned	Unburned	Unburned	
10I	Goose Creek	4.69	0.0	0.000	50.7	63.1	na	Unburned	Unburned	Unburned	
10J	Goose Creek	5.48	0.0	0.000	57.7	73.3	na	Unburned	Unburned	Unburned	
10K	Goose Creek	10.95	0.0	0.000	101.8	129	na	Unburned	Unburned	Unburned	
10L	Goose Creek	12.16	0.0	0.000	111.1	98.8	na	Unburned	Unburned	Unburned	Peak sediment discharge (bulking) into Cheesman (ft^3/s)
10M	Goose Creek	13.86	0.0	0.000	123.7	97.9	na	Unburned	Unburned	Unburned	**1749**
10N	Goose Creek	11.70	0.0	0.000	107.6	79.8	na	Unburned	Unburned	Unburned	Total flood volume (bulked) into Cheesman (acre-feet)
South Platte River basins and subbasins downstream from Cheesman Dam											**19400**
11	Schoonover	1.71	85.4	1.461	22.1	22.0	99.5	607	737	33.5	
	Cross section DXS1		**33.2**	**1.649**				**11,952**	**12,943**		
12	Mouth of Sixmile and Wigwam	36.7	34.2	12.555	275.4	274	99.5	2,510	2,725	9.9	
12A	Sixmile and Wigwam	18.2	27.8	5.053	154.6	102	na	940	1,005	9.9	Mainly a stream reach
12B	Sixmile and Wigwam	5.222	42.5	2.219	55.4	80.6	na	709	784	9.7	
12C	Sixmile and Wigwam	3.425	51.9	1.778	39.1	48.2	na	552	624	12.9	Burn of 34.15% for composite basin

Table 3–6. HEC-HMS model results for South Platte River basins and subbasins upstream and downstream from Cheesman Reservoir used in the manual calibration method.—Continued

[mi², square miles; ft³/s, cubic feet per second; %, percent; PreQ, pre-burn discharge; RegrQ, regression-derived discharge; BulkQ, sediment-bulked discharge; na, not applicable]

Single basins | Composite basins | Subbasins of composite basins

Model basin ID	Name of basin or drainage	Basin area (mi²)	Percentage of medium-high burned area	Medium-high burned area (mi²)	Regression derived discharge (ft³/s)	Pre-burn discharge (ft³/s)	Correlation between PreQ and RegrQ (%)	Post-burn discharge (ft³/s)	Sediment bulked discharge (ft³/s)	Ratio BulkQ to PreQ (BulkQ/PreQ)	Remarks
South Platte River basins and subbasins downstream from Cheesman Dam—Continued											
12D	Sixmile and Wigwam	7.776	24.4	1.897	76.9	77.1	na	565	599	7.8	
12E	Sixmile and Wigwam	0.879	76.2	0.670	12.8	16.6	na	388	462	27.8	
12F	Sixmile and Wigwam	1.192	78.7	0.938	16.4	26.3	na	466	558	21.2	
	Cross section DXS2		**34.6**	**14.391**				**13,560**	**14,732**		
13	Fourmile Creek	8.22	59.7	4.906	80.4	80.8	100.5	958	1,101	13.6	
	Cross section DXS3		**37.1**	**19.445**				**14,449**	**15,789**		
	Cross section DXS4		**37.1**	**19.925**				**14,609**	**15,965**		
14	Mouth of Horse Creek	212	12.8	27.048	1,168	1,154	98.8	4,010	4,138	3.6	
14A	Horse Creek	3.576	20.7	0.738	40.6	39.9	na	358	376	9.4	Mainly a stream reach
14B	Horse Creek	1.356	75.3	1.021	18.3	36.6	na	507	602	16.5	Burn of 11.91% for composite basin
14C	Horse Creek	0.641	100.0	0.641	9.9	13.2	na	353	441	33.4	
14D	Horse Creek	0.633	45.8	0.290	9.8	20.4	na	209	233	11.4	
14E	Horse Creek	18.802	36.1	6.788	159.0	93.6	na	768	837	8.9	Mainly a stream reach
14F	Horse Creek	2.045	54.3	1.110	25.6	62.1	na	436	495	8.0	
14G	Horse Creek	0.547	29.9	0.164	8.6	21.2	na	128	138	6.5	
14H	Horse Creek	0.764	30.5	0.233	11.4	35.9	na	480	517	14.4	
14I	Horse Creek	1.155	44.1	0.509	16.0	36.6	na	353	392	10.7	
14J	Horse Creek	1.887	30.3	0.572	24.0	30.7	na	330	355	11.6	
14K	Horse Creek	15.536	41.0	6.370	135.9	65.7	na	1,120	1,235	18.8	Mainly a stream reach
14L	Horse Creek	1.193	41.4	0.494	16.4	30.0	na	323	356	11.9	
14M	Horse Creek	0.399	59.5	0.237	6.7	8.2	na	146	168	20.5	
14N	Horse Creek	0.653	87.2	0.569	10.0	15.2	na	337	410	27.0	
14O	Horse Creek	0.492	59.8	0.294	7.9	10.8	na	133	153	14.2	

Table 3–6. HEC-HMS model results for South Platte River basins and subbasins upstream and downstream from Cheesman Reservoir used in the manual calibration method.—Continued

[mi², square miles; ft³/s, cubic feet per second; %, percent; PreQ, pre-burn discharge; RegrQ, regression-derived discharge; BulkQ, sediment-bulked discharge; na, not applicable]

Single basins (yellow) | Composite basins (pink) | Subbasins of composite basins (blue)

Model basin ID	Name of basin or drainage	Basin area (mi²)	Percentage of medium-high burned area	Medium-high burned area (mi²)	Regression derived discharge (ft³/s)	Pre-burn discharge (ft³/s)	Correlation between PreQ and RegrQ (%)	Post-burn discharge (ft³/s)	Sediment bulked discharge (ft³/s)	Ratio BulkQ to PreQ (BulkQ/PreQ)	Remarks
South Platte River basins and subbasins downstream from Cheesman Dam—Continued											
14P	Horse Creek	0.582	22.7	0.132	9.1	20.4	na	148	156	7.7	Mainly a stream reach
14Q	Horse Creek	12.287	3.0	0.369	112.0	72.8	na	Unburned	Unburned	Unburned	Mainly a stream reach
14R	Horse Creek	12.753	0.0	0.000	115.5	70.0	na	Unburned	Unburned	Unburned	
14S	Horse Creek	17.419	4.8	0.831	149.3	181	na	362	366	2.0	Mainly a stream reach
14T	Horse Creek	8.854	4.8	0.422	85.5	79.0	na	159	161	2.0	Mainly a stream reach
14U	Horse Creek	7.391	4.8	0.353	73.7	86.3	na	171	173	2.0	
14V	Horse Creek	2.706	59.2	1.603	32.2	39.7	na	703	807	20.3	
14W	Horse Creek	7.199	4.8	0.343	72.1	80.9	na	161	163	2.0	
14X	Horse Creek	15.993	3.2	0.509	139.1	137	na	241	243	1.8	Mainly a stream reach
14Y	Horse Creek	12.778	3.2	0.406	115.7	134	na	225	227	1.7	Mainly a stream reach
14Z	Horse Creek	15.538	3.2	0.494	135.9	125	na	213	215	1.7	Mainly a stream reach
14AA	Horse Creek	1.83	3.2	0.058	23.4	28.6	na	Unburned	Unburned	Unburned	
14BB	Horse Creek	9.447	3.2	0.300	90.2	42.0	na	Unburned	Unburned	Unburned	
14CC	Horse Creek	6.426	3.2	0.204	65.7	52.1	na	Unburned	Unburned	Unburned	Mainly a stream reach
14DD	Horse Creek	8.996	3.2	0.286	86.7	83.5	na	Unburned	Unburned	Unburned	Mainly a stream reach
14EE	Horse Creek	13.315	3.2	0.423	119.7	92.9	na	Unburned	Unburned	Unburned	
14FF	Horse Creek	8.88	3.2	0.282	85.7	56.2	na	Unburned	Unburned	Unburned	
15	Lazy Gulch	1.23	39.1	0.480	16.8	17.0	101.0	309	339	20.0	
16	Brush Creek	2.33	59.3	1.380	28.5	28.7	100.8	507	582	20.3	
	Cross section DXS4.5		**18.0**	**48.352**				**17,828**	**18,632**		
	Cross section DXS5		**18.4**	**50.001**				**17,874**	**18,698**		
17	Unnamed drainage	1.16	0.0	0.000	16.1	15.8	98.6	Unburned	Unburned	Unburned	
	Cross section DXS6		**18.4**	**50.001**				18,056	**18,885**		
UB1	Unburned drainage 1bc	1.75	0.0	0.000	22.6	22.5	99.8	Unburned	Unburned	Unburned	
18	Saloon Gulch	1.26	46.6	0.588	17.2	17.2	99.9	290	324	18.9	

Table 3–6. HEC-HMS model results for South Platte River basins and subbasins upstream and downstream from Cheesman Reservoir used in the manual calibration method.—Continued

[mi^2, square miles; ft^3/s, cubic feet per second; %, percent; PreQ, pre-burn discharge; RegrQ, regression-derived discharge; BulkQ, sediment-bulked discharge; na, not applicable]

Single basins — Composite basins — Subbasins of composite basins

Model basin ID	Name of basin or drainage	Basin area (mi^2)	Percentage of medium-high burned area	Medium-high burned area (mi^2)	Regression derived discharge (ft^3/s)	Pre-burn discharge (ft^3/s)	Correlation between PreQ and RegrQ (%)	Post-burn discharge (ft^3/s)	Sediment bulked discharge (ft^3/s)	Ratio BulkQ to PreQ (BulkQ/PreQ)	Remarks
South Platte River basins and subbasins downstream from Cheesman Dam—Continued											
UB2	Unburned drainage 2bc	1.07	0.0	0.000	15.1		0.0	Unburned	Unburned	Unburned	
19	Mouth of Gunbarrel and Kelsey	10.2	2.0	0.204	96.1	96.8	100.8	220	221	2.3	
19A	Gunbarrel and Kelsey	0.686	2.0	0.014	10.4	10.2	97.9	22	22	2.1	Burn of 2% for composite basin
19B	Gunbarrel and Kelsey	4.719	2.0	0.094	51.0	45.4	89.1	103	104	2.3	
19C	Gunbarrel and Kelsey	4.791	2.0	0.096	51.6	47.6	92.3	108	109	2.3	
UB3	Unburned drainage 3bc	13.12	0.0	0.000	118.2	118	99.8	Unburned	Unburned	Unburned	
	Cross section DXS7		**16.9**	**51.309**				**18,163**	**18,930**		
M1	South Platte Reach 1	3.258	5.8	0.188	37.6	37.2	99.0	147	149	4.0	Mainly a stream reach
M2	South Platte Reach 2	2.568	5.8	0.148	30.9	31.0	100.4	135	137	4.4	Mainly a stream reach
M3	South Platte Reach 3	2.977	9.1	0.269	34.9	35.4	101.5	201	206	5.8	Mainly a stream reach
M4	South Platte Reach 4	4.187	12.3	0.516	46.2	46.0	99.6	395	407	8.9	Mainly a stream reach

Notes

Correlation percentages for subbasins are not meaningful, as subbasin discharge values were adjusted during calibration of the larger watershed to the regression equation by uniformly adjusting pre-burn runoff-curve number values for the individual basins to match the routed peak at the basin mouth. Therefore, the subbasin discharge values do not necessarily match the regression equation.

Table 3–7. Peak flows and recovered model parameters for South Platte River subbasins upstream and downstream from Cheesman Reservoir.

[mi², square miles; ft³/s, cubic feet per second; SCS, Soil Conservation Service]

HEC-HMS model basin identificatin number	Drainage area (mi²)	Peak-flow from 6-hour storm recurrence interval				Recovery SCS method watershed parameters		
		10-year storm peak flow (ft³/s)	50-year storm peak flow (ft³/s)	100-year storm peak flow (ft³/s)	500-year storm peak flow (ft³/s)	Runoff curve number	Initial abstraction (inches)	SCS lag time (minutes)
South Platte River basins upstream from Cheesman Dam								
9N	0.37	6	19	25	53	68.40	0.93	38
9C	8.09	97	281	358	626	69.70	0.87	210
9L	0.88	15	40	52	96	68.90	0.90	84
9M	2.97	41	119	151	272	68.60	0.92	127
9K	0.48	5	16	21	43	64.70	1.09	52
9J	0.40	3	11	15	30	62.80	1.18	53
9I	0.27	4	13	17	34	68.20	0.93	50
9H	2.16	25	78	101	191	66.50	1.01	89
9G	6.44	68	191	242	418	70.60	0.83	291
9F	1.57	41	109	141	255	72.60	0.76	62
9E	0.97	28	75	96	171	73.40	0.72	60
9D	0.99	28	75	97	174	73.10	0.74	57
9B	1.99	54	135	171	298	73.10	0.73	82
9A Turkey Creek	0.61	17	50	65	119	73.00	0.74	45
6 Longwater Gulch	2.34	43	115	147	267	70.00	0.86	92
3 Beaver	3.54	47	137	176	314	68.60	0.92	138
7 Corral	4.38	83	227	295	556	69.80	0.87	67
4 Hackett Gulch	6.56	69	224	290	536	66.50	1.01	115
1 Vermillion Creek	4.93	52	166	214	388	67.70	0.96	159
2 Crystal Creek	5.27	55	175	227	411	67.50	0.96	160
0.1	0.60	946	960	966	989	65.20	1.07	87
UBB1	19.82	16	114	164	353	61.60	1.25	592
UBB2	9.28	8	59	84	183	61.40	1.26	522
UBB3	0.31	4	13	16	31	67.40	0.97	72
UBB4 Unburned basin 4ac	0.32	0	4	6	13	56.10	1.56	63
PA	3.87	27	74	93	160	71.50	0.80	519
5B	3.11	36	111	144	265	66.90	0.99	111
5A Tarryall Creek	8.42	795	962	1034	1285	68.40	0.92	228
7.1 Motberry Creek	1.60	39	105	137	252	71.80	0.79	58
8 Northrup Gulch	3.84	72	189	238	413	70.90	0.82	125
7.2 Wildcat Creek	1.98	48	124	159	282	72.10	0.77	78
8.1 Unnamed drainage A	1.03	26	71	93	171	71.90	0.78	53
PB	11.31	106	273	341	572	72.60	0.75	450
8.2 Unnamed drainage B	0.72	18	57	77	149	71.80	0.79	32
10N Goose Creek	11.70	4	65	99	238	58.90	1.41	385
10M	13.86	3	74	115	279	58.50	1.43	374
10L	12.16	3	66	102	251	58.40	1.44	358
10K	10.95	0	48	88	258	55.10	1.66	187
10J	5.48	0	26	48	141	55.10	1.68	155
10I	4.69	0	23	42	123	55.10	1.68	150
10H	7.64	0	40	68	183	56.40	1.57	227

Table 3–7. Peak flows and recovered model parameters for South Platte River subbasins upstream and downstream from Cheesman Reservoir.—Continued

[mi², square miles; ft³/s, cubic feet per second; SCS, Soil Conservation Service]

HEC-HMS model basin identificatin number	Drainage area (mi²)	Peak-flow from 6-hour storm recurrence interval				Recovery SCS method watershed parameters		
		10-year storm peak flow (ft³/s)	50-year storm peak flow (ft³/s)	100-year storm peak flow (ft³/s)	500-year storm peak flow (ft³/s)	Runoff curve number	Initial abstraction (inches)	SCS lag time (minutes)
South Platte River basins upstream from Cheesman Dam—Continued								
10F	6.27	5	76	114	256	58.70	1.41	143
10G	3.55	3	49	72	159	58.50	1.42	106
10C	2.82	54	144	184	336	70.10	0.85	85
10E	1.88	34	92	120	227	69.20	0.89	68
10D	7.38	129	340	428	733	71.10	0.81	157
10B	4.67	111	269	333	553	73.60	0.72	147
10A Goose Creek	2.13	55	134	167	283	73.40	0.72	112
9.1 Unnamed drainage C	0.87	24	68	89	164	72.60	0.75	46
9.2 Sand Draw	0.67	19	54	70	129	72.90	0.74	45
9.3 Unnamed drainage D	0.75	21	57	73	131	72.90	0.74	57
PC South	6.49	92	240	299	504	72.30	0.77	262
Cheesman	225.34	1739	2814	3352	5535	--	--	--
Outlet (end of upper model reach)	225.34	1739	2814	3352	5535	--	--	--
South Platte River basins downstream from Cheesman Dam								
19C	4.79	1	42	66	161	57.20	1.50	159
19B	4.72	1	41	65	160	57.00	1.51	151
19A Gunbarrel and Kelsey	0.69	0	8	13	28	57.40	1.48	99
UB3	13.12	0	62	105	290	56.30	1.58	248
18 Saloon Gulch	1.26	22	60	78	149	68.90	0.90	68
UB1	1.75	0	10	18	51	55.30	1.69	119
14EE Horse Creek	13.31	7	87	131	304	59.30	1.37	361
14DD	9.00	2	62	96	236	58.00	1.45	262
14CC	6.43	2	47	72	171	58.60	1.42	274
14FF	8.88	7	62	91	204	60.30	1.32	395
14BB	9.45	9	65	94	202	61.40	1.26	477
14AA	1.83	0	16	26	64	55.70	1.59	100
14Z	15.54	7	101	154	362	59.00	1.39	340
14Y	12.78	3	86	134	329	58.00	1.45	268
14X	15.99	4	105	164	406	57.70	1.46	265
14W	7.20	4	63	95	222	58.90	1.40	237
14U	7.39	3	64	98	231	58.60	1.42	223
14V	2.71	54	139	176	309	71.00	0.82	109
14T	8.85	7	74	110	251	59.70	1.35	293
14R	12.75	4	70	106	253	59.10	1.40	403
14Q	12.29	8	81	119	270	60.00	1.33	407
14P	0.58	7	21	27	50	66.70	1.00	101
14O	0.49	8	24	32	66	68.20	0.93	42
14N	0.65	18	55	72	137	72.40	0.76	35
14M	0.40	8	25	34	69	70.30	0.85	36
14L	1.19	21	58	75	146	68.90	0.90	63
14K	15.54	132	364	460	789	71.10	0.81	404

Table 3–7. Peak flows and recovered model parameters for South Platte River subbasins upstream and downstream from Cheesman Reservoir.—Continued

[mi², square miles; ft³/s, cubic feet per second; SCS, Soil Conservation Service]

HEC-HMS model basin identificatin number	Drainage area (mi²)	Peak-flow from 6-hour storm recurrence interval				Recovery SCS method watershed parameters		
		10-year storm peak flow (ft³/s)	50-year storm peak flow (ft³/s)	100-year storm peak flow (ft³/s)	500-year storm peak flow (ft³/s)	Runoff curve number	Initial abstraction (inches)	SCS lag time (minutes)
South Platte River basins downstream from Cheesman Dam—Continued								
14J	1.89	25	73	94	169	68.00	0.94	121
14I	1.16	20	56	74	148	68.60	0.92	51
14H	0.76	9	27	36	76	65.40	1.06	47
14G	0.55	8	22	30	63	66.80	1.00	44
14F	2.05	23	72	94	179	66.00	1.03	83
14E	18.80	127	344	432	737	71.70	0.79	557
14S	17.42	11	132	197	452	59.50	1.36	318
14C	0.64	18	53	69	128	73.00	0.74	43
14B	1.36	30	85	112	211	71.00	0.82	52
14D	0.63	12	35	47	95	69.40	0.88	42
14A Horse Creek	3.58	23	78	101	186	67.40	0.97	294
17 Unnamed drainage	1.16	0	7	12	35	55.30	1.72	98
16 Brush Creek	2.33	44	117	149	269	70.20	0.85	92
15 Lazy Gulch	1.23	21	59	77	151	68.60	0.91	59
12B Sixmile and Wigwam	5.22	52	168	219	401	66.80	0.99	148
12C	3.43	44	132	169	305	68.10	0.94	125
12D	7.78	33	155	211	417	63.50	1.15	188
12E	0.88	22	62	82	155	71.70	0.79	45
12F	1.19	27	79	106	204	71.00	0.82	42
12A Sixmile and Wigwam	18.17	85	317	420	791	66.20	1.02	331
11 Schoonover	1.71	42	111	144	261	72.00	0.78	65
M1	3.26	5	49	70	151	59.60	1.36	127
Cheesman out (spillway)	--	1,739	2,814	3,352	4,867	--	--	--
Cheesman outlet gates	--	1,400	1,400	1,400	1,400	--	--	--
13 Fourmile Creek	8.22	105	288	364	625	70.80	0.82	240
M2 South Platte Reach 2	2.57	8	34	47	91	64.50	1.10	361
M3 South Platte Reach 3	2.98	12	48	64	123	65.70	1.05	335
M4 South Platte Reach 4	4.19	22	75	98	180	67.40	0.97	369
UB6	0.58	0	6	9	22	57.40	1.48	135
Outlet (end of model reach)	0.00	3,394	6,151	7,526	10,954	--	--	--

Table 3–8. South Platte River Basin rainfall distribution.

Minutes from beginning of storm	Percentage of total rainfall	Cumulative rainfall amount each minute of storm distribution			
		10-year, 6-hour storm (1.60-inch total)	50-year, 6-hour storm (2.20-inch total)	100-year, 6-hour storm (2.40-inch total)	500-year, 6-hour storm (3.00-inch total)
0005	0.010	0.016	0.022	0.024	0.030
0010	0.015	0.024	0.033	0.036	0.045
0015	0.020	0.032	0.044	0.048	0.060
0020	0.027	0.043	0.060	0.065	0.081
0025	0.032	0.051	0.071	0.077	0.096
0030	0.040	0.064	0.088	0.096	0.120
0035	0.046	0.073	0.101	0.110	0.138
0040	0.053	0.085	0.116	0.127	0.159
0045	0.060	0.096	0.132	0.144	0.180
0050	0.068	0.109	0.149	0.163	0.204
0055	0.077	0.123	0.170	0.185	0.231
0100	0.085	0.136	0.187	0.204	0.255
0105	0.093	0.149	0.204	0.223	0.279
0110	0.102	0.163	0.225	0.245	0.306
0115	0.112	0.179	0.247	0.269	0.336
0120	0.122	0.195	0.269	0.293	0.366
0125	0.132	0.211	0.291	0.317	0.396
0130	0.144	0.231	0.317	0.346	0.433
0135	0.157	0.251	0.346	0.377	0.471
0140	0.169	0.271	0.372	0.406	0.508
0145	0.188	0.301	0.413	0.451	0.564
0150	0.204	0.327	0.449	0.490	0.613
0155	0.240	0.384	0.528	0.576	0.720
0200	0.290	0.464	0.638	0.696	0.870
0205	0.360	0.576	0.792	0.864	1.080
0210	0.423	0.677	0.930	1.015	1.269
0215	0.490	0.784	1.078	1.176	1.470
0220	0.552	0.883	1.215	1.325	1.656
0225	0.606	0.969	1.333	1.454	1.818
0230	0.627	1.003	1.380	1.505	1.881
0235	0.648	1.037	1.425	1.555	1.944
0240	0.662	1.059	1.457	1.589	1.986
0245	0.680	1.088	1.496	1.632	2.040
0250	0.698	1.117	1.535	1.675	2.094
0255	0.710	1.136	1.562	1.704	2.130
0300	0.724	1.159	1.593	1.738	2.173
0305	0.738	1.181	1.623	1.771	2.214
0310	0.751	1.201	1.652	1.802	2.253
0315	0.761	1.217	1.674	1.826	2.283
0320	0.772	1.235	1.699	1.853	2.316
0325	0.783	1.253	1.722	1.879	2.349
0330	0.794	1.271	1.747	1.906	2.383
0335	0.805	1.288	1.771	1.932	2.415
0340	0.815	1.304	1.793	1.956	2.445
0345	0.823	1.317	1.810	1.975	2.469
0350	0.832	1.331	1.831	1.997	2.496

Table 3–8. South Platte River Basin rainfall distribution.—Continued

Minutes from beginning of storm	Percentage of total rainfall	Cumulative rainfall amount each minute of storm distribution			
		10-year, 6-hour storm (1.60-inch total)	50-year, 6-hour storm (2.20-inch total)	100-year, 6-hour storm (2.40-inch total)	500-year, 6-hour storm (3.00-inch total)
0355	0.841	1.345	1.850	2.018	2.523
0400	0.850	1.360	1.870	2.040	2.550
0405	0.860	1.376	1.892	2.064	2.580
0410	0.869	1.391	1.912	2.086	2.608
0415	0.878	1.405	1.931	2.107	2.634
0420	0.883	1.413	1.942	2.119	2.649
0425	0.892	1.427	1.963	2.141	2.676
0430	0.901	1.441	1.982	2.162	2.703
0435	0.907	1.451	1.996	2.177	2.721
0440	0.914	1.463	2.011	2.194	2.743
0445	0.920	1.472	2.024	2.208	2.760
0450	0.927	1.483	2.040	2.225	2.781
0455	0.934	1.495	2.055	2.242	2.803
0500	0.941	1.505	2.070	2.258	2.823
0505	0.948	1.517	2.085	2.275	2.844
0510	0.954	1.527	2.099	2.290	2.863
0515	0.960	1.536	2.112	2.304	2.880
0520	0.967	1.547	2.128	2.321	2.901
0525	0.973	1.557	2.140	2.335	2.919
0530	0.979	1.567	2.154	2.350	2.938
0535	0.985	1.576	2.167	2.364	2.955
0540	0.990	1.584	2.178	2.376	2.970
0545	0.994	1.591	2.187	2.386	2.983
0550	0.998	1.597	2.195	2.395	2.994
0555	1.000	1.600	2.200	2.400	3.000
0600	1.000	1.600	2.200	2.400	3.000
0605	1.000	1.600	2.200	2.400	3.000

Table 3–9. Flood peak flows through the Deckers-to-Trumbull reach, South Platte River.

[ft^3/s, cubic feet per second]

Cross section	River station	Recurrence interval discharges, 6-hour-storm			
		10-year (ft^3/s)	50-year (ft^3/s)	100-year (ft^3/s)	500-year (ft^3/s)
V	13	3,139	4,211	4,909	7,424
U	11	3,139	4,211	4,909	7,424
T	10	3,139	4,211	4,909	7,424
S	9.5	3,139	4,211	4,909	7,424
R	9	3,160	4,270	4,986	7,575
Q	8	3,160	4,270	4,986	7,575
P	7	3,160	4,270	4,986	7,575
O	6	3,486	5,860	7,212	12,244
N	5	3,486	5,860	7,212	12,244
M	4	3,486	5,860	7,212	12,244
L	3	3,486	5,860	7,212	12,244
K	2	3,486	5,867	7,225	12,279
J	1	3,490	5,883	7,246	12,320
I	0.5	3,538	6,016	7,417	12,630
H	0	3,538	6,016	7,417	12,630
G	–1	3,538	6,016	7,417	12,630
F	–2	3,538	6,016	7,417	12,630
E	–3	3,538	6,016	7,417	12,630
D	–4	3,538	6,016	7,417	12,630
C	–5	3,538	6,016	7,417	12,630
B	–6	3,538	6,016	7,417	12,630
A	–7	3,538	6,016	7,417	12,630

Table 3–10. Summary of Manning's n values for roughness and downstream reach lengths.

[Manning's n values are dimensionless; downstream reach lengths are the distance from the cross section downstream to the next cross section; ft, feet; *, interpolated in HEC-RAS]

Cross section	River station	Manning's n values			Downstream reach lengths		
		Left overbank	Channel	Right overbank	Left (ft)	Channel (ft)	Right (ft)
V	13	0.080	0.035	0.060	675	675	675
U	11.5	0.080	0.035	0.060	1,925	1,925	1,925
T	11	0.080	0.035	0.060	600	600	600
S	10	0.120	0.040	0.080	130	130	130
R	9.5	0.120	0.040	0.080	770	770	770
Q	9	0.120	0.040	0.080	830	830	830
P	8	0.120	0.040	0.080	27	27	27
	7.9*	0.120	0.040	0.080	27	27	27
	7.7*	0.120	0.040	0.080	27	27	27
O	7.6	0.120	0.040	0.080	208	208	208
	7.5	Bridge			Bridge		
N	7	0.070	0.045	0.080	332	332	332
M	5	0.070	0.045	0.100	350	350	350
L	4	0.070	0.045	0.080	654	654	654
K	3	0.100	0.045	0.080	196	196	196
	2.5	Bridge			Bridge		
J	2	0.100	0.045	0.080	800	800	800
I	1	0.100	0.045	0.080	2,120	2,120	2,120
H	0.5	0.100	0.045	0.080	1,160	1,160	1,160
G	0	0.054	0.038	0.054	525	525	525
F	–1	0.054	0.038	0.054	250	250	250
E	–2	0.054	0.038	0.054	525	525	525
D	–3	0.054	0.038	0.054	185	185	185
C	–4	0.054	0.038	0.054	200	200	200
	–5	Bridge			Bridge		
B	–6	0.054	0.038	0.054	2,380	2,380	2,380
A	–7	0.054	0.038	0.054	0	0	0

Table 3–11. Results of step-backwater computations using HEC-RAS program.

[ft^3/s, cubic feet per second; ft, feet; ft/s, feet per second; hr, hour; datum is National Geodetic Vertical Datum of 1929 in feet; -- no data]

Cross section	River station	Profile	Discharge total (ft^3/s)	Discharge left overbank (ft^3/s)	Discharge channel (ft^3/s)	Discharge right overbank (ft^3/s)	Water surface elevation (ft)	Critical water surface (ft)	Velocity channel (ft/s)	Flow area (ft^2)	Top width (ft)	Froude number channel
V	13	10-year, 6-hour storm	3,140	13	2,949	177	6,415.90	--	5.40	687	178	0.40
V	13	50-year, 6-hour storm	4,210	24	3,820	365	6,416.86	--	5.97	870	198	0.41
V	13	100-year, 6-hour storm	4,910	32	4,361	517	6,417.42	--	6.27	982	204	0.42
V	13	500-year, 6-hour storm	7,420	65	6,225	1,130	6,419.12	--	7.19	1,333	209	0.43
U	11.5	10-year, 6-hour storm	3,140	12	3,125	2	6,412.58	6,412.39	9.61	333	106	0.92
U	11.5	50-year, 6-hour storm	4,210	25	4,170	15	6,413.33	6,413.10	10.52	416	114	0.91
U	11.5	100-year, 6-hour storm	4,910	35	4,842	32	6,413.80	6,413.55	10.98	470	118	0.90
U	11.5	500-year, 6-hour storm	7,420	85	7,193	142	6,415.34	6,414.90	12.23	657	124	0.87
T	11	10-year, 6-hour storm	3,140	14	3,107	19	6,408.88	--	4.14	782	155	0.32
T	11	50-year, 6-hour storm	4,210	25	4,150	35	6,409.93	--	4.63	947	159	0.32
T	11	100-year, 6-hour storm	4,910	34	4,829	47	6,410.55	--	4.91	1,047	162	0.33
T	11	500-year, 6-hour storm	7,420	74	7,243	102	6,412.58	--	5.71	1,382	169	0.33
S	10	10-year, 6-hour storm	3,140	0	3,140	0	6,405.67	6,405.67	10.66	295	86	1.01
S	10	50-year, 6-hour storm	4,210	1	4,207	3	6,406.42	6,406.42	11.74	361	92	1.01
S	10	100-year, 6-hour storm	4,910	3	4,900	7	6,406.91	6,406.91	12.25	407	95	1.00
S	10	500-year, 6-hour storm	7,420	29	7,355	36	6,408.40	6,408.40	13.97	557	106	0.99
R	9.5	10-year, 6-hour storm	3,140	41	3,070	30	6,402.90	6,402.39	10.04	348	97	0.82
R	9.5	50-year, 6-hour storm	4,210	74	4,089	46	6,403.31	6,403.31	12.28	389	100	0.96
R	9.5	100-year, 6-hour storm	4,910	117	4,731	63	6,403.84	6,403.84	12.88	441	102	0.96
R	9.5	500-year, 6-hour storm	7,420	304	6,974	142	6,405.62	6,405.62	14.39	644	126	0.94
Q	9	10-year, 6-hour storm	3,160	50	3,082	28	6,398.12	--	7.14	485	130	0.61
Q	9	50-year, 6-hour storm	4,270	133	4,066	71	6,400.76	--	5.84	858	152	0.39
Q	9	100-year, 6-hour storm	4,990	178	4,717	95	6,401.57	--	6.07	985	159	0.38
Q	9	500-year, 6-hour storm	7,580	369	7,022	189	6,403.62	--	7.15	1,326	172	0.40
P	8	10-year, 6-hour storm	3,160	125	2,938	97	6,396.69	--	5.27	738	100	0.31
P	8	50-year, 6-hour storm	4,270	212	3,890	168	6,399.98	--	5.13	1,210	202	0.26
P	8	100-year, 6-hour storm	4,990	305	4,481	204	6,400.75	--	5.57	1,377	230	0.27
P	8	500-year, 6-hour storm	7,580	720	6,615	246	6,402.53	--	7.24	1,856	317	0.33

Table 3–11. Results of step-backwater computations using HEC-RAS program.—Continued

[ft^3/s, cubic feet per second; ft, feet; ft/s, feet per second; hr, hour; datum is National Geodetic Vertical Datum of 1929 in feet; -- no data]

Cross section	River station	Profile	Discharge total (ft^3/s)	Discharge left overbank (ft^3/s)	Discharge channel (ft^3/s)	Discharge right overbank (ft^3/s)	Water surface elevation (ft)	Critical water surface (ft)	Velocity channel (ft/s)	Flow area (ft^2)	Top width (ft)	Froude number channel
Interpolated	7.9*	10-year, 6-hour storm	3,160	65	2,966	129	6,396.70	--	4.93	787	134	0.29
Interpolated	7.9*	50-year, 6-hour storm	4,270	161	3,771	339	6,400.02	--	4.54	1,401	258	0.23
Interpolated	7.9*	100-year, 6-hour storm	4,990	246	4,310	434	6,400.81	--	4.87	1,619	294	0.24
Interpolated	7.9*	500-year, 6-hour storm	7,580	644	6,307	629	6,402.65	--	6.24	2,283	437	0.29
Interpolated	7.7*	10-year, 6-hour storm	3,490	12	3,466	12	6,396.52	--	5.59	667	142	0.35
Interpolated	7.7*	50-year, 6-hour storm	5,860	131	5,429	300	6,399.68	--	6.30	1,297	288	0.33
Interpolated	7.7*	100-year, 6-hour storm	7,210	228	6,526	456	6,400.34	--	7.16	1,501	329	0.36
Interpolated	7.7*	500-year, 6-hour storm	12,200	618	10,687	896	6,401.42	--	10.75	1,903	430	0.52
O	7.6	10-year, 6-hour storm	3,490		3,490		6,396.48	6,392.70	5.50	634	84	0.35
O	7.6	50-year, 6-hour storm	5,860	58	5,773	29	6,399.57	6,394.24	6.46	1,064	296	0.35
O	7.6	100-year, 6-hour storm	7,210	132	6,976	102	6,400.19	6,395.05	7.38	1,272	374	0.39
O	7.6	500-year, 6-hour storm	12,200	414	11,361	425	6,401.09	6,397.59	11.12	1,660	486	0.56
Upstream bridge	7.5	10-year, 6-hour storm	3,490	0	3,490	0	6,393.98	6,392.72	8.39	--	--	--
Upstream bridge	7.5	50-year, 6-hour storm	5,860	522	4,883	456	6,399.57	6,393.84	9.97	--	296	--
Upstream bridge	7.5	100-year, 6-hour storm	7,210	1,211	4,856	1,143	6,400.19	6,393.87	8.96	--	374	--
Upstream bridge	7.5	500-year, 6-hour storm	12,172	3,650	4,773	3,749	6,401.09	6,402.06	7.73	--	486	--
Downstream bridge	7.5	10-year, 6-hour storm	3,490	89	3,233	168	6,394.05	6,390.92	5.74	--	--	--
Downstream bridge	7.5	50-year, 6-hour storm	5,860	626	4,604	630	6,399.57	6,392.42	7.24	--	227	--
Downstream bridge	7.5	100-year, 6-hour storm	7,210	1,256	4,717	1,237	6,400.19	6,393.11	6.87	--	277	--
Downstream bridge	7.5	500-year, 6-hour storm	12,172	3,614	4,814	3,744	6,401.09	6,401.15	6.32	--	346	--
N	7	10-year, 6-hour storm	3,490	107	3,170	213	6,395.25	--	4.70	916	264	0.29
N	7	50-year, 6-hour storm	5,860	189	4,926	745	6,397.13	--	5.93	1,486	325	0.33
N	7	100-year, 6-hour storm	7,210	254	5,729	1,227	6,398.04	--	6.32	1,787	336	0.34
N	7	500-year, 6-hour storm	12,200	641	8,308	3,251	6,400.93	--	7.25	2,810	369	0.34
M	5	10-year, 6-hour storm	3,490	31	3,459	1	6,392.85	6,392.85	9.93	358	122	1.00
M	5	50-year, 6-hour storm	5,860	84	5,773	4	6,394.11	6,394.11	11.75	514	128	1.00
M	5	100-year, 6-hour storm	7,210	123	7,077	10	6,394.75	6,394.75	12.55	596	132	0.99
M	5	500-year, 6-hour storm	12,200	317	11,820	63	6,396.80	6,396.80	14.81	879	144	0.99

Table 3–11. Results of step-backwater computations using HEC-RAS program.—Continued

[ft^3/s, cubic feet per second; ft, feet; ft/s, feet per second; hr, hour; datum is National Geodetic Vertical Datum of 1929 in feet; -- no data]

Cross section	River station	Profile	Discharge total (ft^3/s)	Discharge left overbank (ft^3/s)	Discharge channel (ft^3/s)	Discharge right overbank (ft^3/s)	Water surface elevation (ft)	Critical water surface (ft)	Velocity channel (ft/s)	Flow area (ft^2)	Top width (ft)	Froude number channel
L	4	10-year, 6-hour storm	3,490	0	3,490	0	6,388.20	--	8.06	433	109	0.71
L	4	50-year, 6-hour storm	5,860	0	5,838	22	6,390.35	--	8.74	680	119	0.63
L	4	100-year, 6-hour storm	7,210	0	7,164	46	6,391.26	--	9.32	790	123	0.63
L	4	500-year, 6-hour storm	12,200	0	11,934	266	6,393.91	--	11.16	1,186	195	0.64
K	3	10-year, 6-hour storm	3,490	84	3,192	213	6,385.82	6,382.29	6.20	703	132	0.38
K	3	50-year, 6-hour storm	5,860	205	5,104	551	6,388.03	6,384.02	7.78	1,059	192	0.43
K	3	100-year, 6-hour storm	7,210	278	6,075	857	6,388.83	6,384.97	8.58	1,216	199	0.45
K	3	500-year, 6-hour storm	12,200	585	9,497	2,118	6,391.00	6,388.32	11.22	1,665	216	0.54
Upstream bridge	2.5	10-year, 6-hour storm	3,490	72	3,280	138	6,383.20	6,382.80	10.90	--	--	--
Upstream bridge	2.5	50-year, 6-hour storm	5,859	363	4,294	1,202	6,388.03	6,388.11	10.31	--	192	--
Upstream bridge	2.5	100-year, 6-hour storm	7,210	547	4,722	1,941	6,388.83	6,388.67	10.09	--	199	--
Upstream bridge	2.5	500-year, 6-hour storm	12,187	1,261	6,542	4,384	6,391.00	6,390.24	10.79	--	216	--
Downstream bridge	2.5	10-year, 6-hour storm	3,490	216	2,908	365	6,383.20	6,380.58	8.11	--	--	--
Downstream bridge	2.5	50-year, 6-hour storm	5,859	705	3,985	1,168	6,388.02	6,382.73	8.81	--	230	--
Downstream bridge	2.5	100-year, 6-hour storm	7,210	1,003	4,500	1,707	6,388.62	6,387.69	9.30	--	238	--
Downstream bridge	2.5	500-year, 6-hour storm	12,187	2,006	6,385	3,796	6,390.39	6,389.66	11.08	--	253	--
J	2	10-year, 6-hour storm	3,490	186	3,024	280	6,384.13	--	6.43	726	120	0.38
J	2	50-year, 6-hour storm	5,870	414	4,912	544	6,385.88	--	8.75	953	139	0.47
J	2	100-year, 6-hour storm	7,220	489	6,011	719	6,386.66	--	9.98	1,078	199	0.52
J	2	500-year, 6-hour storm	12,300	1,470	9,519	1,311	6,389.01	--	13.13	1,613	243	0.62
I	1	10-year, 6-hour storm	3,490	5	3,302	183	6,380.11	6,379.87	8.62	454	173	0.85
I	1	50-year, 6-hour storm	5,880	22	5,322	536	6,381.72	6,380.99	9.24	748	191	0.74
I	1	100-year, 6-hour storm	7,250	37	6,439	774	6,382.60	6,381.53	9.48	919	200	0.70
I	1	500-year, 6-hour storm	12,300	118	10,354	1,828	6,385.65		9.92	1,582	234	0.59
H	0.5	10-year, 6-hour storm	3,540	51	3,444	45	6,368.40	--	6.26	610	110	0.44
H	0.5	50-year, 6-hour storm	6,020	135	5,773	111	6,370.34	--	8.05	831	117	0.49
H	0.5	100-year, 6-hour storm	7,420	190	7,076	154	6,371.15	--	9.00	927	120	0.52
H	0.5	500-year, 6-hour storm	12,600	408	11,867	326	6,373.00	--	12.55	1,155	127	0.67

Table 3–11. Results of step-backwater computations using HEC-RAS program.—Continued

[ft^3/s, cubic feet per second; ft, feet; ft/s, feet per second; hr, hour; datum is National Geodetic Vertical Datum of 1929 in feet; -- no data]

Cross section	River station	Profile	Discharge total (ft^3/s)	Discharge left overbank (ft^3/s)	Discharge channel (ft^3/s)	Discharge right overbank (ft^3/s)	Water surface elevation (ft)	Critical water surface (ft)	Velocity channel (ft/s)	Flow area (ft^2)	Top width (ft)	Froude number channel
G	0	10-year, 6-hour storm	3,540	62	3,391	86	6,364.41	--	6.80	581	193	0.54
G	0	50-year, 6-hour storm	6,020	282	5,423	316	6,365.68	--	8.64	905	346	0.61
G	0	100-year, 6-hour storm	7,420	495	6,390	534	6,366.20	--	9.39	1,113	430	0.64
G	0	500-year, 6-hour storm	12,600	1,821	8,904	1,875	6,367.85	--	10.52	1,905	502	0.64
F	–1	10-year, 6-hour storm	3,540	85	3,146	308	6,362.96	--	5.44	805	314	0.45
F	–1	50-year, 6-hour storm	6,020	466	4,806	747	6,364.34	--	6.34	1,350	458	0.46
F	–1	100-year, 6-hour storm	7,420	707	5,525	1,188	6,364.98	--	6.58	1,645	476	0.46
F	–1	500-year, 6-hour storm	12,600	1,590	7,973	3,037	6,366.73	--	7.47	2,494	489	0.46
E	–2	10-year, 6-hour storm	3,540	0	2,596	944	6,362.60	--	4.64	1,103	342	0.34
E	–2	50-year, 6-hour storm	6,020	0	3,827	2,193	6,363.99	--	5.51	1,586	355	0.37
E	–2	100-year, 6-hour storm	7,420	0	4,506	2,914	6,364.58	--	5.98	1,800	363	0.38
E	–2	500-year, 6-hour storm	12,600	0	6,997	5,603	6,366.19	--	7.64	2,407	395	0.45
D	–3	10-year, 6-hour storm	3,540	486	3,024	30	6,361.42	--	5.84	762	259	0.45
D	–3	50-year, 6-hour storm	6,020	973	4,906	140	6,362.02	--	8.51	986	567	0.62
D	–3	100-year, 6-hour storm	7,420	1,246	5,769	405	6,362.33	--	9.52	1,162	571	0.67
D	–3	500-year, 6-hour storm	12,600	2,220	8,269	2,111	6,363.39	6,363.39	11.66	1,774	584	0.76
C	–4	10-year, 6-hour storm	3,540	290	2,854	396	6,361.11	6,359.04	5.19	1,153	877	0.39
C	–4	50-year, 6-hour storm	6,020	519	4,102	1,399	6,361.70	6,361.15	6.74	1,733	1,025	0.48
C	–4	100-year, 6-hour storm	7,420	661	4,310	2,449	6,362.23	6,361.62	6.51	2,278	1,036	0.45
C	–4	500-year, 6-hour storm	12,600	1,147	5,767	5,686	6,363.20	6,362.40	7.58	3,291	1,050	0.49
Upstream bridge	–5	10-year, 6-hour storm	3,518	0	1,854	1,664	6,361.11	6,361.52	6.30	--	528	--
Upstream bridge	–5	50-year, 6-hour storm	5,994	0	1,368	4,626	6,361.70	6,361.93	4.65	--	707	--
Upstream bridge	–5	100-year, 6-hour storm	7,405	72	839	6,493	6,362.23	6,362.04	2.57	--	963	--
Upstream bridge	–5	500-year, 6-hour storm	12,568	335	967	11,267	6,363.20	6,362.60	2.28	--	997	--
Downstream bridge	–5	10-year, 6-hour storm	3,518	23	2,016	1,479	6,361.11	6,358.44	6.18	--	528	--
Downstream bridge	–5	50-year, 6-hour storm	6,011	36	1,672	4,303	6,361.70	6,361.95	5.12	--	736	--
Downstream bridge	–5	100-year, 6-hour storm	7,405	80	1,033	6,291	6,362.22	6,362.22	2.99	--	950	--
Downstream bridge	–5	500-year, 6-hour storm	12,568	323	1,142	11,102	6,362.69	6,362.69	3.05	--	953	--

Table 3–11. Results of step-backwater computations using HEC-RAS program.—Continued

[ft^3/s, cubic feet per second; ft, feet; ft/s, feet per second; hr, hour; datum is National Geodetic Vertical Datum of 1929 in feet; -- no data]

Cross section	River station	Profile	Discharge total (ft^3/s)	Discharge left overbank (ft^3/s)	Discharge channel (ft^3/s)	Discharge right overbank (ft^3/s)	Water surface elevation (ft)	Critical water surface (ft)	Velocity channel (ft/s)	Flow area (ft^2)	Top width (ft)	Froude number channel
B	–6	10-year, 6-hour storm	3,540	26	3,283	231	6,358.52	6,358.52	10.26	426	187	0.80
B	–6	50-year, 6-hour storm	6,020	70	4,781	1,169	6,360.02	6,360.02	11.54	749	232	0.79
B	–6	100-year, 6-hour storm	7,420	101	5,119	2,200	6,361.08	6,361.08	10.64	1,210	773	0.68
B	-6	500-year, 6-hour storm	12,600	171	6,335	6,095	6,362.56	6,362.56	11.03	2,579	952	0.64
A	–7	10-year, 6-hour storm	3,540	2	3,513	26	6,347.58	6,345.89	4.59	806	365	0.44
A	–7	50-year, 6-hour storm	6,020	28	5,558	435	6,348.67	6,346.98	5.51	1,314	510	0.46
A	–7	100-year, 6-hour storm	7,420	55	6,612	754	6,349.16	6,347.50	5.90	1,572	550	0.47
A	–7	500-year, 6-hour storm	12,600	206	10,028	2,366	6,350.58	6,348.89	6.97	2,366	574	0.49

Table 3–12. Floodway data for the Deckers to Trumbull reach, South Platte River, computed in HEC-RAS.

[ft, feet; ft², square feet; ft/s, feet per second; NGVD ft, National Geodetic Vertical Datum of 1929 in feet; *, interpolated cross section in HEC-RAS; Cross section A is equivalent to cross section DXS5 in figure 9; u.s., upstream; d.s., downstream]

Flooding source			Floodway			100-year base flood water-surface elevation			
Cross section	River station	Distance above XS-A (ft)	Width (ft)	Section area (ft²)	Mean velocity (ft/s)	Regulatory (NGVD ft)	Without floodway (NGVD ft)	With floodway (NGVD ft)	Increase (NGVD ft)
V	13	14,895	100	714	6.87	6,417.42	6,417.42	6,417.61	0.19
U	11.5	14,220	95	476	10.32	6,413.80	6,413.80	6,414.16	0.37
T	11	12,295	140	1,002	4.90	6,410.55	6,410.55	6,410.68	0.13
S	10	11,695	85	400	12.28	6,406.91	6,406.91	6,406.91	0.00
R	9.5	11,565	66	366	13.43	6,403.84	6,403.84	6,403.81	–0.03
Q	9	10,795	120	1,000	4.99	6,401.57	6,401.57	6,402.53	0.96
P	8	9,965	75	1,016	4.91	6,400.75	6,400.75	6,401.63	0.88
	7.9*	9,938	86	1,099	4.54	6,400.81	6,400.81	6,401.67	0.85
	7.7*	9,912	76	967	7.45	6,400.34	6,400.34	6,401.12	0.78
O	7.6	9,885	153	1,198	6.02	6,400.19	6,400.19	6,401.19	1.00
	7.5 u.s. side of bridge	9,855	159	802	8.99	6,400.19	6,400.19	6,401.19	1.00
	7.5 d.s. side of bridge	9,807	140	843	8.56	6,400.19	6,400.19	6,400.98	0.79
N	7	9,677	83	944	7.64	6,398.04	6,398.04	6,398.49	0.45
M	5	9,345	114	573	12.58	6,394.75	6,394.75	6,394.83	0.08
L	4	8,995	125	911	7.91	6,391.26	6,391.26	6,392.24	0.97
K	3	8,341	97	884	8.16	6,388.83	6,388.83	6,389.31	0.48
	2.5 u.s. side of bridge	8,251	125	726	9.93	6,388.83	6,388.83	6,389.31	0.48
	2.5 d.s. side of bridge	8,225	174	951	7.58	6,388.62	6,388.62	6,388.72	0.10
J	2	8,145	53	632	11.43	6,386.66	6,386.66	6,387.05	0.39
I	1	7,345	154	835	8.68	6,382.60	6,382.60	6,382.69	0.10
H	0.5	5,225	95	930	7.98	6,371.15	6,371.15	6,372.08	0.93
G	0	4,065	101	780	9.51	6,366.20	6,366.20	6,367.20	0.99
F	–1	3,540	161	1,118	6.64	6,364.98	6,364.98	6,365.98	1.00
E	–2	3,290	136	998	7.43	6,364.58	6,364.58	6,365.08	0.49
D	–3	2,765	177	1,025	7.24	6,362.33	6,362.33	6,363.31	0.97
C	–4	2,580	256	1,061	7.00	6,362.23	6,362.23	6,362.49	0.26
	–5 u.s. side of bridge	2,480	454	834	8.90	6,362.23	6,362.23	6,362.49	0.26
	–5 d.s. side of bridge	2,455	443	876	8.47	6,362.22	6,362.22	6,362.49	0.27
B	–6	2,380	144	697	10.65	6,361.08	6,361.08	6,360.69	–0.39
A	–7	0	225	1,209	6.14	6,349.16	6,349.16	6,349.56	0.40

Table 3–13. Comparison of 1978 study 100-year flood elevations at selected cross sections to 2004 study 100-year flood elevations at the same cross sections.

[1978 data from Federal Emergency Management Agency (1978). All elevations in National Geodetic Vertical Datum of 1929, in feet]

Cross section		100-year flood elevation		Difference (2004 minus 1978)
1978	USGS 2004	1978	USGS 2004	
1	I	6,381	6,383	2
2	J	6,386	6,387	1
3	K	6,388	6,389	1
4	L	6,393	6,391	–2
5	M	6,395	6,395	0
6	N	6,398	6,398	0
7	O	6,400	6,400	0
8	P	6,403	6,401	–2
9	Q	6,405	6,402	–3
10	S	6,408	6,407	–1
11	T	6,410	6,414	4
13	V	6,417	6,417	0

Table 3–14. Pre- and post-burn model parameters for South Platte River subbasins upstream and downstream from Cheesman Reservoir used in the objective calibration method.

[ID, identification number; BAER, Burned Area Emergency Rehabilitation; mi^2, square miles; RCN, runoff curve number; IA, initial abstraction; LT, lag time; *, Tarryall basin 5C is regulated]

Model basin ID	Corresponding BAER Basin(s)	Name of basin or drainage	Drainage area (mi^2)	Percentage of medium-high burned area	Pre-burn RCN	Pre-burn IA	Pre-burn LT	Post-burn RCN	Post-burn IA	Post-burn LT	Recovered RCN	Recovered IA	Recovered LT
South Platte River subbasins upstream from Cheesman Dam													
0.1	84	Unnamed	0.60	19.6	55.7	1.59	110.84	82.4	0.43	53.17	65.2	1.07	87.09
PA	80, 77, 75	South Platte Reach A	3.87	4.5	64.3	1.11	627.79	84.2	0.38	353	71.5	0.80	518.8
UBB1	-	Unburned basin 1ac	19.82	0	60.3	1.32	529.45	60.3	1.32	529.45	–999	–2.20	–999
UBB2	-	Unburned basin 2ac	8.70	0	59.7	1.35	406.38	59.7	1.35	406.38	–999	–2.20	–999
1	78	Vermillion Creek	4.93	27.6	56.6	1.53	211.62	86.4	0.31	90.59	67.7	0.95	159.3
UBB3	-	Unburned basin 3ac	1.20	0	54	1.70	57.71	54.0	1.70	57.71	–999	–2.20	–999
2	76	Crystal Creek	5.27	29.1	56.5	1.54	212.3	86.3	0.32	91.02	67.5	0.96	160.26
UBB4	-	Unburned basin 4ac	0.32	0	56.7	1.53	40.45	56.7	1.53	40.45	–999	–2.20	–999
PB	891	South Platte Reach B	11.31	38.6	62.2	1.22	592.93	89.4	0.24	260.99	72.6	0.75	450.23
3	74	Beaver Creek	3.54	33.7	56.3	1.55	188.49	88.5	0.26	73.97	68.6	0.92	137.53
4	65	Hackett Gulch	6.56	33.2	54.9	1.64	153.55	86.0	0.33	63.72	66.4	1.01	114.54
5A	58	Tarryall Creek	8.42	34	57.8	1.46	299.64	86.5	0.31	131.56	68.4	0.92	227.99
5B	58, 72	Tarryall Creek	3.11	34	55.5	1.60	148.16	86.3	0.32	61.88	66.9	0.99	110.85
5C	-	Tarryall upstream	431.05										
6	63	Longwater Gulch	2.34	67.6	53.4	1.75	140.8	94.4	0.12	39.62	70	0.86	91.95
7	53	Corral Creek	4.38	70.3	54	1.70	101.2	93.5	0.14	30.16	69.8	0.87	67.34
7.1	57	Motberry Gulch	1.60	80.1	54.8	1.65	90.7	96.2	0.08	24.04	71.8	0.79	58.3
7.2	47	Wildcat Creek	1.98	80.7	55.3	1.62	119.99	96.2	0.08	32.21	72.1	0.77	77.48
8	51	Northrup Gulch	3.84	58.2	56.1	1.57	182.75	93.2	0.15	58.5	70.9	0.82	124.6
8.1	44	Unnamed drainage A	1.03	78	55.1	1.63	81.87	96.0	0.08	22.21	71.9	0.78	52.98
8.2	45	Unnamed drainage B	0.72	81.7	54.7	1.66	50.05	96.4	0.07	13.16	71.8	0.79	32.12
PC	892	South Platte Reach C	6.49	61.4	59.4	1.37	367.24	92.1	0.17	133.88	72.3	0.77	261.6
9A	37	Turkey Creek	0.61	98.7	55	1.64	71.58	98.1	0.04	17.12	73	0.74	44.74
9B	92	Turkey Creek	1.99	94.9	55.6	1.60	129.6	97.8	0.05	32.19	73.1	0.74	82.07
9C	46	Turkey Creek	8.09	44.4	57.6	1.47	286.48	89.2	0.24	113.15	69.7	0.87	209.72
9D	37	Turkey Creek	0.99	98.7	55.2	1.62	90.37	98.1	0.04	21.75	73.1	0.74	56.67
9E	40	Turkey Creek	0.97	100	55.5	1.60	95.04	98.3	0.03	22.86	73.4	0.72	59.62
9F	43	Turkey Creek	1.57	90.9	55	1.64	98.38	97.3	0.06	24.7	72.6	0.75	62.29
9G	91	Turkey Creek	6.44	37.3	59.7	1.35	385.56	88.3	0.27	165.81	70.6	0.83	290.33
9H	90	Turkey Creek	2.16	20.2	55.2	1.62	118.51	85.8	0.33	49.95	66.5	1.01	88.82
9I	54	Turkey Creek	0.27	23.5	56.7	1.53	67.09	87.3	0.29	27.77	68.2	0.93	49.95

Table 3–14. Pre- and post-burn model parameters for South Platte River subbasins upstream and downstream from Cheesman Reservoir used in the objective calibration method.—Continued

[ID, identification number; BAER, Burned Area Emergency Rehabilitation; mi^2, square miles; RCN, runoff curve number; IA, initial abstraction; LT, lag time; *, Tarryall basin 5C is regulated]

Model basin ID	Corresponding BAER Basin(s)	Name of basin or drainage	Drainage area (mi^2)	Percentage of medium-high burned area	Pre-burn RCN	Pre-burn IA	Pre-burn LT	Post-burn RCN	Post-burn IA	Post-burn LT	Recovered RCN	Recovered IA	Recovered LT
South Platte River subbasins upstream from Cheesman Dam—Continued													
9J	59	Turkey Creek	0.40	3.7	56.1	1.57	62.32	76.6	0.61	36.18	62.8	1.18	52.62
9K	62	Turkey Creek	0.48	6.8	55.6	1.60	65.9	81.6	0.45	32.4	64.7	1.09	52.24
9L	67	Turkey Creek	0.88	42.1	55.9	1.58	116.97	89.7	0.23	43.25	68.9	0.90	83.67
9M	73	Turkey Creek	2.97	44.7	56.3	1.55	174.29	88.6	0.26	68.07	68.6	0.92	127.11
9N	46 (partial)	Turkey Creek	0.37	44.4	55.6	1.60	52.96	89.0	0.25	20.04	68.4	0.92	38.16
9.1	33	Unnamed drainage C	0.87	95.6	54.7	1.66	72.58	97.8	0.05	17.58	72.6	0.75	45.54
9.2	34	Sand Draw	0.67	96.3	55.1	1.63	71.41	97.9	0.04	17.32	72.9	0.74	44.88
9.3	31	Unnamed drainage D	0.75	93	55.4	1.61	89.24	97.6	0.05	22.29	72.9	0.74	56.54
10A	26	Goose Creek	2.13	89.6	56.6	1.53	174.67	97.2	0.06	46	73.4	0.72	112.48
10B	26	Goose Creek	4.67	89.6	57	1.51	227.01	97.2	0.06	60.39	73.6	0.72	146.84
10C	25	Goose Creek	2.82	60	55	1.64	125.63	93.0	0.15	39.49	70.1	0.85	85.21
10D	87	Goose Creek	7.38	63.4	56.6	1.53	229.22	93.1	0.15	74.41	71.1	0.81	157.2
10E	30	Goose Creek	1.88	54.9	54.7	1.66	98.27	91.6	0.18	32.66	69.2	0.89	67.72
10F	39	Goose Creek	6.27	8.7	55	1.64	156.84	67.8	0.95	113.16	58.7	1.41	143.05
10G	32	Goose Creek	3.55	8.6	54.6	1.66	117.02	68.2	0.93	82.59	58.5	1.42	106.03
10H	-	Goose Creek	7.64	0	56.4	1.55	224.83	56.4	1.55	224.83	–999	-2.20	-999
10I	-	Goose Creek	4.69	0	55.1	1.63	147.39	55.1	1.63	147.39	–999	-2.20	-999
10J	-	Goose Creek	5.48	0	55.1	1.63	151.85	55.1	1.63	151.85	–999	-2.20	-999
10K	-	Goose Creek	10.95	0	55.1	1.63	184.17	55.1	1.63	184.17	–999	-2.20	-999
10L	-	Goose Creek	12.16	0	58.4	1.42	355.84	58.4	1.42	355.84	–999	-2.20	-999
10M	-	Goose Creek	13.86	0	58.5	1.42	372.64	58.5	1.42	372.64	–999	-2.20	-999
10N	-	Goose Creek	11.70	0	58.9	1.40	383.27	58.9	1.40	383.27	–999	-2.20	-999
South Platte River subbasins downstream Cheesman Dam													
11	28	Schoonover	1.71	85.4	55	1.64	100.72	96.5	0.07	26.5	72	0.78	64.72
12A	3	Sixmile and Wigwam	18.18	27.8	58.6	1.41	402	80.5	0.48	220.45	66.2	1.02	331.01
12B	2	Sixmile and Wigwam	5.22	42.5	56.2	1.56	194.2	85.2	0.35	85.58	66.8	0.99	147.94
12C	6	Sixmile and Wigwam	3.43	51.9	56	1.57	169.98	87.9	0.28	67.59	68.1	0.94	124.65
12D	5	Sixmile and Wigwam	7.78	24.4	56.4	1.55	224.89	77.7	0.57	127.16	63.5	1.15	187.84
12E	19	Sixmile and Wigwam	0.88	76.2	54.9	1.64	69.08	95.8	0.09	18.81	71.7	0.79	44.73
12F	22	Sixmile and Wigwam	1.19	78.7	54.4	1.68	64.1	95.3	0.10	17.75	71	0.82	41.78
13	21	Fourmile Creek	8.22	59.7	58.4	1.42	331.39	90.5	0.21	126.58	70.8	0.82	240.1
14A	11	Horse Creek	3.58	20.7	59.9	1.34	356	81.4	0.46	196.45	67.4	0.97	293.39

Table 3–14. Pre- and post-burn model parameters for South Platte River subbasins upstream and downstream from Cheesman Reservoir used in the objective calibration method.—Continued

[ID, identification number; BAER, Burned Area Emergency Rehabilitation; mi^2, square miles; RCN, runoff curve number; IA, initial abstraction; LT, lag time; *, Tarryall basin 5C is regulated]

Model basin ID	Corresponding BAER Basin(s)	Name of basin or drainage	Drainage area (mi^2)	Percentage of medium-high burned area	Pre-burn RCN	Pre-burn IA	Pre-burn LT	Post-burn RCN	Post-burn IA	Post-burn LT	Recovered RCN	Recovered IA	Recovered LT
South Platte River subbasins downstream Cheesman Dam—Continued													
14B	23	Horse Creek	1.36	75.3	54.6	1.66	78.91	94.9	0.11	22.31	71	0.82	51.68
14C	24	Horse Creek	0.64	100	54.9	1.64	68.69	98.3	0.03	16.26	73	0.74	42.88
14D	20	Horse Creek	0.63	45.8	55.2	1.62	59.73	91.4	0.19	20.28	69.4	0.88	41.5
14E	11, 50, 52, 55, 61,68,70	Horse Creek	18.80	36.1	63.2	1.16	696.8	86.1	0.32	356.52	71.7	0.79	556.53
14F	27	Horse Creek	2.05	54.3	52.4	1.82	117.44	88.4	0.26	41.85	66	1.03	83.05
14G	29	Horse Creek	0.55	29.9	55.4	1.61	58.37	86.2	0.32	24.43	66.8	0.99	43.62
14H	36	Horse Creek	0.76	30.5	54.8	1.65	61.67	84.3	0.37	27.14	65.4	1.06	47.04
14I	38	Horse Creek	1.16	44.1	54.6	1.66	73.56	90.6	0.21	25.35	68.6	0.92	51.38
14J	42	Horse Creek	1.89	30.3	56.5	1.54	162.34	87.2	0.29	67.12	68	0.94	120.78
14K	49	Horse Creek	15.54	41	60.7	1.29	531.8	88.2	0.27	234.98	71.1	0.81	404.46
14L	56	Horse Creek	1.19	41.4	54.9	1.64	89.81	90.7	0.21	31.08	68.9	0.90	62.74
14M	60	Horse Creek	0.40	59.5	55.7	1.59	52.04	92.6	0.16	16.91	70.3	0.85	35.65
14N	64	Horse Creek	0.65	87.2	55.1	1.63	54.28	97.0	0.06	13.92	72.4	0.76	34.62
14O	66	Horse Creek	0.49	59.8	55	1.64	58.86	89.4	0.24	21.54	68.2	0.93	41.93
14P	71	Horse Creek	0.58	22.7	56.7	1.53	131	84.4	0.37	60.34	66.7	1.00	101.45
14Q	none	Horse Creek	12.29	3	59.3	1.37	414.37	62.2	1.22	385.3	60	1.33	407.29
14R	none	Horse Creek	12.75	0	59.1	1.38	401.4	59.1	1.38	401.4	–999	–2.20	–999
14S	85	Horse Creek	17.42	4.8	57.6	1.47	333.76	64.6	1.10	279.07	59.5	1.36	318.19
14T	85	Horse Creek	8.85	4.8	57.9	1.45	306.87	64.8	1.09	257.28	59.7	1.35	292.92
14U	85	Horse Creek	7.39	4.8	56.6	1.53	234.13	64.0	1.13	194.17	58.6	1.41	222.77
14V	35	Horse Creek	2.71	59.2	55.9	1.58	161.2	93.5	0.14	50.49	71	0.82	109.14
14W	85	Horse Creek	7.20	4.8	57	1.51	248.77	64.2	1.12	207.23	58.9	1.40	237.18
14X	88	Horse Creek	15.99	3.2	56.6	1.53	272.27	61.2	1.27	242.29	57.7	1.47	264.75
14Y	88	Horse Creek	12.78	3.2	56.9	1.52	275.46	61.4	1.26	245.67	58	1.45	267.85
14Z	88	Horse Creek	15.54	3.2	58	1.45	348.88	62.2	1.22	313.28	59	1.39	340
14AA	none	Horse Creek	1.83	3.2	55	1.64	102.38	58.3	1.43	94.07	55.7	1.59	100.49
14BB	none	Horse Creek	9.45	3.2	60.7	1.29	485.37	63.5	1.15	452.08	61.4	1.26	476.55
14CC	none	Horse Creek	6.43	3.2	57.8	1.46	279.44	61.0	1.28	257.16	58.6	1.41	273.5
14DD	none	Horse Creek	9.00	3.2	57.1	1.50	267.98	60.5	1.31	245.89	58	1.45	262.16
14EE	none	Horse Creek	13.32	3.2	58.5	1.42	368.07	61.7	1.24	339.71	59.3	1.37	360.79
14FF	none	Horse Creek	8.88	3.2	59.5	1.36	403.1	62.5	1.20	373.46	60.3	1.32	395.3

Table 3–14. Pre- and post-burn model parameters for South Platte River subbasins upstream and downstream from Cheesman Reservoir used in the objective calibration method.—Continued

[ID, identification number; BAER, Burned Area Emergency Rehabilitation; mi^2, square miles; RCN, runoff curve number; IA, initial abstraction; LT, lag time; *, Tarryall basin 5C is regulated]

Model basin ID	Corresponding BAER Basin(s)	Name of basin or drainage	Drainage area (mi^2)	Percentage of medium-high burned area	Pre-burn RCN	Pre-burn IA	Pre-burn LT	Post-burn RCN	Post-burn IA	Post-burn LT	Recovered RCN	Recovered IA	Recovered LT
South Platte River subbasins downstream Cheesman Dam—Continued													
15	8	Lazy Gulch	1.23	39.1	54.9	1.64	84.19	90.4	0.21	29.51	68.6	0.92	59.18
16	7	Brush Creek	2.33	59.3	55.5	1.60	133.72	92.5	0.16	43.58	70.2	0.85	91.62
17	9	Unnamed drainage	1.16	0	55.3	1.62	94.16	55.3	1.62	94.16	–999	–2.20	–999
UB1	none	Unburned drainage 1bc	1.75	0	55.3	1.62	115.81	55.3	1.62	115.81	-999	-2.20	-999
18	4	Saloon Gulch	1.26	46.6	55.2	1.62	96.94	90.5	0.21	34.15	68.9	0.90	68.21
UB2	none	Unburned drainage 2bc	1.07	0	54.9	1.64	84.32	54.9	1.64	84.32	-999	-2.20	-999
19A	1	Gunbarrel and Kelsey	0.69	2	56	1.57	102.69	61.8	1.24	88.51	57.4	1.48	99.08
19B	1	Gunbarrel and Kelsey	4.72	2	55.4	1.61	157.11	62.0	1.23	132.87	57	1.51	150.79
19C	1	Gunbarrel and Kelsey	4.79	2	55.5	1.60	165.64	62.1	1.22	140.15	57.2	1.50	158.82
UB3	none	Unburned drainage 3bc	13.12	0	56.3	1.55	245.71	56.3	1.55	245.71	-999	-2.20	-999
M1	893	South Platte Reach 1	3.26	5.8	55.3	1.62	141.79	69.9	0.86	97.22	59.6	1.36	127.18
M2	893	South Platte Reach 2	2.57	5.8	61.1	1.27	393.83	72.1	0.77	294.51	64.5	1.10	360.94
M3	93, 893	South Platte Reach 3	2.98	9.1	60.7	1.29	380.89	76.1	0.63	251.64	65.7	1.04	334.7
M4	93	South Platte Reach 4	4.19	12.33	61.1	1.27	433.57	79.6	0.51	261.27	67.4	0.97	368.66

Explanation of Parameters

Pre-burn RCN = RCN determined from composite and individual BAER team basins (base RCN for natural forest min. 55)

Default IA = Initial Abstraction value determined by SCS method, $IA = 0.2 \times [(1{,}000/RCN) - 10]$.

Appendix 4. Appendix Tables 4–1—4–2

Table 4–1. Global Positioning System positions for South Platte River cross sections used in post-fire hazard analysis.

[All elevations are referenced to top of aluminum cap unless noted (GRD) or (HUB); UTM, Universal Transverse Mercator; NAD 83, North American Datum of 1983; NAVD 88, North American Vertical Datum of 1988; ft, feet; HUB, survey instrument hub; GRD, ground surface; LB, left bank; RB, right bank; Gage Sta., gaging station]

Cross-section identification	UTM Zone 13, NAD 83		NAVD 88 elevation (geoid 99) (ft)	Remarks
	X coordinate Easting (ft)	Y coordinate Northing (ft)		
DXS1(HUB)	477,986.253	4,343,306.038	6,500.44	
DXS1LB(GRD)	477,938.505	4,343,297.499	6,525.46	
DXS1RB(GRD)	478,068.958	4,343,322.911	6,497.37	Rebar 0.46 ft below hub
DXS2(HUB)	478,904.807	4,343,681.383	6,467.87	
DXS2LB	478,887.125	4,343,704.940	6,489.76	
DXS2RB(GRD)	478,969.329	4,343,606.025	6,480.57	
DXS3(HUB)	479,614.577	4,344,700.990	6,423.47	
DXS3LB	479,592.348	4,344,753.101	6,460.18	
DXS3RB(GRD)	479,636.612	4,344,645.984	6,442.45	
DXS4(HUB)	479,913.762	4,345,022.802	6,408.72	
DXS4LB	479,948.497	4,345,060.743	6,425.05	
DXS4RB	479,902.202	4,345,008.717	6,452.85	
DXS4.5(HUB)	480,857.763	4,345,702.909	6,387.97	
DXS4.5LB	480,864.862	4,345,728.710	6,409.11	
DXS4.5RB	480,843.438	4,345,650.779	6,393.04	
DXS5(HUB)	481,261.899	4,346,922.073	6,356.11	
DXS5LB	481,171.726	4,347,015.987	6,369.85	
DXS5RB	481,305.291	4,346,874.061	6,355.49	
DXS6(HUB)	481,791.463	4,348,552.495	6,351.87	
DXS6LB	481,676.268	4,348,610.702	6,346.67	
DXS6RB	481,932.866	4,348,484.984	6,395.21	
DXS7(HUB)	483,225.050	4,351,387.126	6,298.38	
DXS7LB	483,194.958	4,351,499.095	6,312.19	
DXS7RB	483,233.308	4,351,356.234	6,335.35	
DXS8(HUB)	484,023.989	4,352,730.141	6,292.42	
DXS8LB	483,818.698	4,352,792.488	6,305.49	Stake not found by GPS crew
DXS8RB	484,040.175	4,352,723.982	6,325.01	
DXS8.5(HUB)	484,215.700	4,353,651.673	6,266.91	
DXS8.5LB	484,171.349	4,353,594.817	6,284.64	
DXS8.5RB	484,233.498	4,353,674.483	6,282.33	
DXS9(HUB)	484,960.253	4,355,721.889	6,222.85	
DXS9LB	484,908.928	4,355,792.820	6,271.67	
DXS9RB	484,973.458	4,355,704.064	6,243.28	
DXS10(HUB)	485,623.612	4,357,974.849	6,199.08	
DXS10LB	485,547.168	4,358,007.244	6,200.66	
DXS10RB	485,658.706	4,357,959.868	6,200.75	
DXS11(HUB)	485,305.729	4,359,798.809	6,162.35	
DXS11LB	485,253.226	4,359,820.942	6,165.95	
DXS11RB	485,330.878	4,359,787.873	6,202.19	

Table 4–1. Global Positioning System positions for South Platte River cross sections used in post-fire hazard analysis.—Continued

[All elevations are referenced to top of aluminum cap unless noted (GRD) or (HUB); UTM, Universal Transverse Mercator; NAD 83, North American Datum of 1983; NAVD 88, North American Vertical Datum of 1988; ft, feet; HUB, survey instrument hub; GRD, ground surface; LB, left bank; RB, right bank; Gage Sta., gaging station]

Cross-section identification	UTM Zone 13, NAD 83		NAVD 88 elevation (geoid 99) (ft)	Remarks
	X coordinate Easting (ft)	Y coordinate Northing (ft)		
DXS12(HUB)	485,629.890	4,361,033.568	6,121.39	
DXS12LB	485,572.890	4,361,022.287	6,132.44	
DXS12RB	485,643.198	4,361,034.919	6,154.65	
DXS13(HUB)	485,521.902	4,362,167.728	6,091.85	
DXS13LB	485,526.388	4,362,181.144	6,100.79	
DXS13RB	485,508.874	4,362,128.641	6,093.91	
WXS2(HUB)	489,379.537	4,366,297.346	5,725.99	
WXS2LB	489,328.471	4,366,306.639	5,745.33	
WXS2RB	489,389.599	4,366,294.449	5,747.95	
WXS3(HUB)	489,371.572	4,367,199.807	5,691.57	
WXS3LB	489,324.709	4,367,196.454	5,690.53	
WXS3RB	489,401.623	4,367,201.744	5,721.33	
UXS1	471,751.252	4,330,513.623	7,131.68	
UXS1LB	471,629.409	4,330,498.789	7,135.40	
UXS1RB	471,813.445	4,330,521.141	7,144.99	
UXS2	472,771.431	4,333,173.589	6,962.48	
UXS2LB(HUB)	472,707.509	4,333,162.777	6,987.28	Stake not visited by GPS crew
UXS2RB	472,809.171	4,333,180.226	6,995.32	
BM6854(Gage Sta.)	473,201.828	4,334,857.208	6,857.12	Control Station for CDXS3
UXS3RB	473,235.792	4,334,798.047	6,872.54	
UXS3LB	473,149.827	4,334,839.811	6,873.94	
BM5671	489,072.657	4,367,617.932	5,679.74	Control Station for WDXS2 & WDXS3

Table 4–2. Global Positioning System positions for South Platte River cross sections used in detailed hydraulic analysis of recovered conditions.

[All elevations are referenced to ground surface; UTM, Universal Transverse Mercator; NAD 83, North American Datum of 1983; NAVD 88, North American Vertical Datum of 1988; RB, right bank; LB, left bank; na, not aplicable; approximate, endpoint digitized from Flood Insurance Rate Map (FEMA, 1978)]

Cross-section identification	UTM Zone 13 NAD 83 X coordinate Easting (ft)	UTM Zone 13 NAD 83 Y coordinate Northing (ft)	NAVD 88 elevation (geoid 99) (ft)	Remarks
A RB	481,171.726	4,347,015.987	6,369.85	
A LB	481,305.291	4,346,874.061	6,355.49	
B LB	481,189.538	4,346,127.056	6,379.89	
B RB	481,331.957	4,346,198.265	6,364.09	
C LB	481,262.507	4,346,098.412	6,366.91	
C RB	481,345.438	4,346,142.197	6,363.65	
D LB	481,279.612	4,346,076.716	6,368.82	
D RB	481,352.775	4,346,137.894	6,365.50	
E LB	481,331.203	4,345,959.541	6,368.47	
E RB	481,461.236	4,346,006.082	6,372.06	
F LB	481,340.532	4,345,871.064	6,376.14	
F RB	481,478.276	4,345,955.294	6,379.38	
G LB	481,322.815	4,345,821.092	6,375.17	
G RB	481,428.218	4,345,697.490	6,377.03	
H LB	480,864.862	4,345,728.710	6,409.11	
H RB	480,843.438	4,345,650.779	6,393.04	
I LB approximate	480,707.233	4,345,388.538	6,407.00	
I RB approximate	480,739.036	4,345,386.435	6,407.20	
J LB	480,699.912	4,344,993.783	6,393.07	
J RB	480,685.186	4,344,906.660	6,402.90	
K LB	480,654.322	4,344,981.835	6,386.56	
K RB	480,616.345	4,344,934.353	6,398.13	
L LB approximate	480,433.785	4,345,266.777	6,411.10	
L RB approximate	480,449.264	4,345,246.140	6,411.10	
M LB approximate	480,377.032	4,345,222.406	6,420.50	
M RB approximate	480,395.606	4,345,204.864	6,420.50	
N LB	480,322.515	4,344,930.170	6,415.51	
N RB	480,398.919	4,344,900.507	6,398.37	
O LB approximate	na	na		interpolated section
O RB approximate	na	na		
P LB	480,324.584	4,344,853.437	6,400.93	
P RB	480,331.913	4,344,810.617	6,413.36	

Table 4–2. Global Positioning System positions for South Platte River cross sections used in detailed hydraulic analysis of recovered conditions.—Continued

[All elevations are referenced to ground surface; UTM, Universal Transverse Mercator; NAD 83, North American Datum of 1983; NAVD 88, North American Vertical Datum of 1988; RB, right bank; LB, left bank; na, not aplicable; approximate, endpoint digitized from Flood Insurance Rate Map (FEMA, 1978)]

Cross-section identification	UTM Zone 13 NAD 83 X coordinate Easting (ft)	UTM Zone 13 NAD 83 Y coordinate Northing (ft)	NAVD 88 elevation (geoid 99) (ft)	Remarks
Q LB approximate	480,131.445	4,344,966.500	6,429.10	
Q RB approximate	480,131.445	4,344,946.895	6,430.00	
R LB	479,948.497	4,345,060.743	6,425.05	
R RB	479,902.202	4,345,008.717	6,452.85	
S LB approximate	479,905.465	4,345,072.783	6,431.10	
S RB approximate	479,892.050	4,345,057.306	6,431.80	
T approximate	479,746.555	4,345,129.538	6,441.40	
T approximate	479,772.352	4,345,103.740	6,430.90	
U LB	479,592.348	4,344,753.101	6,460.18	
U RB	479,636.612	4,344,645.984	6,442.45	
V LB approximate	479,473.108	4,344,606.375	6,444.00	
V RB approximate	479,493.745	4,344,601.216	6,447.60	

Appendix 5. Appendix Tables 5–1—5–4

Table 5–1. Mitchell Creek subbasin characteristics and pre-burn model parameters.

[mi², square miles; in, inches; ft, feet; ft/ft, foot per foot; min, minutes; hrs, hours; SCS, Soil Conservation Service]

Subbasin number	Subbasin name	Drainage area (mi²)	Pre-burn runoff curve number	Initial abstraction (in)	Subbasin length, L (ft)	Drainage-basin slope (ft/ft)	Storage	SCS lag time (min)	SCS lag time (hrs)
23	Storm King 1	0.201	72.5	0.759	6,708	0.535	3.80	14.9	0.248
24	Storm King 2	0.055	73.7	0.713	2,933	0.563	3.56	7.23	0.121
25	Mitchell E1	0.290	72.2	0.770	7,600	0.398	3.85	19.2	0.321
26	Mitchell E2	0.013	79.2	0.525	2,579	0.357	2.63	6.98	0.116
27	Mitchell E3	0.051	79.9	0.503	5,025	0.340	2.52	11.9	0.199
28	Mitchell E4	0.045	77.9	0.568	3,223	0.462	2.84	7.63	0.127
29	Mitchell W4-S	0.010	78.5	0.547	1,819	0.714	2.73	3.81	0.064
30	Mitchell W3	0.117	74.0	0.703	3,750	0.764	3.52	7.51	0.125
31	Mitchell W2	0.133	73.4	0.727	3,711	0.703	3.63	7.90	0.132
32	Mitchell W1	0.147	73.8	0.711	4,570	0.652	3.56	9.57	0.160
33	Mitchell W4-N	0.031	77.5	0.580	2,768	0.648	2.90	5.77	0.096
36	Upper Mitchell West	2.372	70.0	0.856	18,670	0.364	4.28	43.8	0.731
37	Upper Mitchell East	2.747	70.4	0.842	19,951	0.312	4.21	49.5	0.824
38	Fish hatchery	0.575	67.4	0.969	9,630	0.704	4.85	19.9	0.332
39	Donegan Bridge	4.418	69.5	0.879	29,604	0.412	4.39	60.4	1.007

Table 5–2. Mitchell Creek subbasin characteristics and post-burn model parameters.

[mi², square miles; in, inches; ft, feet; ft/ft, foot per foot; min, minutes; hrs, hours; SCS, Soil Conservation Service]

Subbasin number	Subbasin name	Drainage area (mi²)	Post-burn runoff curve number	Initial abstraction (in)	Subbasin length, L (ft)	Drainage-basin slope (ft/ft)	Storage	SCS lag time (min)	SCS lag time (hrs)
23	Storm King 1	0.201	94.7	0.111	6,708	0.535	0.557	6.78	0.113
24	Storm King 2	0.055	90.5	0.210	2,933	0.563	1.05	4.13	0.069
25	Mitchell E1	0.290	90.7	0.206	7,600	0.398	1.03	10.5	0.174
26	Mitchell E2	0.013	95.1	0.103	2,579	0.357	0.515	3.79	0.063
27	Mitchell E3	0.051	97.7	0.046	5,025	0.340	0.231	5.73	0.095
28	Mitchell E4	0.045	97.0	0.062	3,223	0.462	0.309	3.59	0.060
29	Mitchell W4-S	0.010	97.2	0.057	1,819	0.714	0.284	1.81	0.030
30	Mitchell W3	0.117	95.7	0.089	3,750	0.764	0.446	3.38	0.056
31	Mitchell W2	0.133	95.2	0.102	3,711	0.703	0.510	3.60	0.060
32	Mitchell W1	0.147	89.0	0.247	4,570	0.652	1.24	5.82	0.097
33	Mitchell W4-N	0.031	96.8	0.066	2,768	0.648	0.331	2.72	0.045
36	Upper Mitchell West	2.372	75.2	0.660	18,670	0.364	3.30	38.0	0.633
37	Upper Mitchell East	2.747	77.3	0.589	19,951	0.312	2.94	40.7	0.678
38	Fish hatchery	0.575	92.6	0.161	9,630	0.704	0.803	8.75	0.146
39	Donegan Bridge	4.418	74.4	0.688	29,604	0.412	3.44	52.7	0.879

Table 5–3. Results of rainfall-runoff modeling using recurrence intervals for the 1-hour storm in the Coal Seam burned area.

[mi^2, square miles; ft^3/s, cubic feet per second; SCS, Soil Conservation Service; CB, composite basin of several upstream subbasins]

Model basin number	HEC-HMS model basin identification	Drainage area (mi^2)	Flow peak from 1-hour storm recurrence interval				Recovery SCS method watershed parameters		
			10-year storm peak flow (ft^3/s)	50-year storm peak flow (ft^3/s)	100-year storm peak flow (ft^3/s)	500-year storm peak flow (ft^3/s)	Runoff curve number	Initial abstraction (inches)	SCS lag time (minutes)
23	CS23 Storm King 1	0.20	91	177	266	365	84.6	0.4	10
24	CS24 Storm King 2	0.06	24	51	89	115	82.6	0.4	6
25	CS25 Mitch E1	0.29	85	173	280	372	82.1	0.4	14
26	CS26 Mitch E2	0.01	12	22	34	43	87.9	0.3	5
27	CS27 Mitch E3	0.05	46	78	109	143	89.8	0.2	8
28	CS28 Mitch E4	0.05	44	80	110	153	88.5	0.3	5
29	CS29 Mitch W4-S	0.01	14	24	37	45	88.9	0.3	3
30	CS30 Mitch W3	0.12	83	162	258	334	85.9	0.3	5
31	CS31 Mitch W2	0.13	90	178	257	372	85.4	0.3	5
32	CS32 Mitch W1	0.15	51	110	194	248	81.8	0.5	8
33	CS33 Mitch W4-N	0.03	33	60	91	115	88.2	0.3	4
36	CS36 Upper Mitchell West	2.37	122	337	701	897	72.4	0.8	41
37	CS37 Upper Mitchell East	2.75	160	413	824	1,052	73.7	0.7	45
38	CS38 Fish Hatchery	0.58	154	323	516	718	81.0	0.5	13
CB	Fish Hatchery	6.23	355	746	1,517	1,937	--	--	--
39	CS39 Donegan Bridge	4.42	150	440	967	1,208	71.8	0.8	57
CB	Donegan Bridge	11.21	490	1,161	2,447	3,078	--	--	--

Table 5–4. Mitchell Creek rainfall distribution.

[in., inch]

Minutes from beginning of storm	Percentage of total rainfall	Cumulative rainfall amount each minute of storm distribution			
		10-year, 1-hour storm (1.35 in. total)	50-year, 1-hour storm (1.80 in. total)	100-year, 1-hour storm (2.40 in. total)	500-year, 1-hour storm (2.60 in. total)
0001	0.000	0.000	0.000	0.000	0.000
0002	0.008	0.011	0.014	0.019	0.021
0003	0.016	0.022	0.029	0.039	0.042
0004	0.025	0.033	0.044	0.059	0.064
0005	0.033	0.045	0.060	0.080	0.087
0006	0.043	0.057	0.077	0.102	0.111
0007	0.052	0.071	0.094	0.126	0.136
0008	0.063	0.085	0.113	0.151	0.164
0009	0.074	0.100	0.134	0.178	0.193
0010	0.086	0.117	0.155	0.207	0.224
0011	0.099	0.134	0.178	0.238	0.257
0012	0.112	0.152	0.202	0.270	0.292
0013	0.127	0.171	0.228	0.304	0.329
0014	0.142	0.192	0.256	0.341	0.369
0015	0.160	0.215	0.287	0.383	0.415
0016	0.180	0.243	0.324	0.432	0.468
0017	0.205	0.277	0.369	0.492	0.533
0018	0.255	0.344	0.459	0.612	0.663
0019	0.345	0.466	0.621	0.828	0.897
0020	0.437	0.590	0.787	1.049	1.136
0021	0.530	0.716	0.954	1.272	1.378
0022	0.603	0.814	1.085	1.447	1.568
0023	0.633	0.855	1.139	1.519	1.646
0024	0.660	0.891	1.188	1.584	1.716
0025	0.684	0.923	1.231	1.642	1.778
0026	0.705	0.952	1.269	1.692	1.833
0027	0.724	0.977	1.303	1.738	1.882
0028	0.742	1.002	1.336	1.781	1.929
0029	0.759	1.025	1.366	1.822	1.973
0030	0.775	1.046	1.395	1.860	2.015
0031	0.790	1.067	1.422	1.896	2.054
0032	0.804	1.086	1.448	1.930	2.091
0033	0.818	1.104	1.472	1.963	2.127
0034	0.831	1.122	1.496	1.995	2.161
0035	0.844	1.139	1.519	2.025	2.194
0036	0.856	1.156	1.541	2.055	2.226
0037	0.868	1.172	1.562	2.083	2.256
0038	0.879	1.187	1.582	2.110	2.285
0039	0.890	1.201	1.602	2.136	2.313
0040	0.900	1.215	1.620	2.160	2.341
0041	0.910	1.229	1.639	2.185	2.367
0042	0.920	1.242	1.656	2.208	2.392
0043	0.930	1.255	1.673	2.231	2.417

Table 5–4. Mitchell Creek rainfall distribution.—Continued

[in., inch]

Minutes from beginning of storm	Percentage of total rainfall	Cumulative rainfall amount each minute of storm distribution			
		10-year, 1-hour storm (1.35 in. total)	50-year, 1-hour storm (1.80 in. total)	100-year, 1-hour storm (2.40 in. total)	500-year, 1-hour storm (2.60 in. total)
0044	0.939	1.268	1.690	2.254	2.442
0045	0.948	1.280	1.707	2.276	2.466
0046	0.957	1.292	1.723	2.298	2.489
0047	0.966	1.304	1.739	2.319	2.512
0048	0.975	1.316	1.754	2.339	2.534
0049	0.983	1.327	1.770	2.360	2.556
0050	0.992	1.339	1.785	2.380	2.578
0051	1.000	1.350	1.800	2.400	2.600